

ABSTRACT

Title of Document: Hindcast Study: Predicting the distribution of *Vibrio vulnificus* in Chesapeake Bay.

Vinita Banakar, Master of Science, 2010.

Directed By: Dr. Rita Colwell, Distinguished Professor
Marine Estuarine Environmental Sciences
University of Maryland, College Park.

Vibrio vulnificus, is an ubiquitous bacterium which primarily causes seafood related gastroenteritis, primary septicemia, and wound infections worldwide. It occurs as part of the normal micro-flora in the coastal marine environment and has been frequently isolated from water, sediment and oysters. A hindcast prediction study was undertaken to determine the likelihood of occurrence of *V. vulnificus* in the surface waters of Chesapeake Bay. Hindcast predictions were achieved by forcing a multivariate habitat suitability model with simulated sea surface temperature and salinity in the Bay. Predictions of *V. vulnificus* occurrence were generated for the period between 1991 and 2005. Potential hotspots of occurrence of *V. vulnificus* in Chesapeake Bay were identified. The likelihood of *V. vulnificus* occurrence during wet and dry years was analyzed. Hindcast prediction can provide a better understanding of the environmental conditions optimal for occurrence of *V. vulnificus* in Chesapeake Bay.

**HINDCAST STUDY: PREDICTING THE DISTRIBUTION OF *VIBRIO*
VULNIFICUS IN CHESAPEAKE BAY.**

By
Vinita Banakar.

Thesis submitted to the Faculty of the Graduate School of the
University of Maryland, College Park, in partial fulfillment
Of the requirements for the degree of
Master of Science
2010

Advisory Committee:
Professor Rita Colwell, Chair.
Professor Anwar Huq.
Professor Raghu Murtugudde.

@ Copyright by

Vinita Banakar

2010

Acknowledgements

I would like to express sincere gratitude to the chair of my committee, Dr Rita Colwell. Thank you for your understanding, patience, and guidance throughout my time here.

I would like to thank my committee members: Dr. Raghu Murtugudde and Dr. Anwar Huq for their invaluable assistance during this project.

I would like to thank Dr. Guillaume Constantin de Magny for his immense help and guidance throughout my thesis project.

I would like to thank Dr. John Jacobs and Dr. Bob Wood from the Oxford Lab for providing the habitat model, without which this project would not have been possible.

I would like to thank my parents Virupaxa and Geeta Banakar, Sister Vijeta Poulekar and my fiance Sanket Bedare for their love and support.

Table of Contents

Acknowledgements.....	ii
Table of Contents.....	iii
List of Tables	iv
List of Figures	v
Chapter 1: Literature review	1
1.1 Introduction.....	1
1.2 Genotypes	3
1.3 Pathogenicity of <i>V. vulnificus</i>	4
1.4 Epidemiology	8
1.5 Ecology	9
1.5.1 Temperature and salinity.....	9
1.5.2 Aquatic wildlife and zooplankton.....	14
1.5.3 Bacteriophages.....	17
1.5.4 Viable but nonculturable state (VBNC).....	18
Chapter 2: Hindcast study: Predicting the distribution of <i>Vibrio vulnificus</i> in Chesapeake Bay	27
2.1 Ecological modeling for disease forecasting	31
2.2 Materials and Methods.....	39
2.2.1 <i>Vibrio vulnificus</i> empirical habitat suitability model:.....	39
2.2.2 Chesapeake Bay Regional Ocean Modeling System (ChesROMS):.....	40
2.2.3 Model retrospective predictions:.....	42
2.3 Results:.....	45
2.4 Discussion:.....	48
Appendix.....	71
References.....	105

List of Tables

Table 1. <i>V. vulnificus</i> abundance recorded by different studies.....	25
Table 2. <i>V. vulnificus</i> densities in water, sediment, oysters, crabs, and intestinal contents of fish collected during the months of April through October from Mobile Bay and the Mississippi Sound in Alabama.....	26

List of Figures

Figure 1. Relative rates of laboratory-confirmed infections with <i>Campylobacter</i> , STEC* O157, <i>Listeria</i> , <i>Salmonella</i> , and <i>Vibrio</i> compared with 1996 to 1998 rates, by year. Foodborne Diseases Active Surveillance Network (FoodNet), United States, 1996 to 2009.....	20
Figure 2. Effects of salinity and temperature on <i>V. vulnificus</i> concentration in oysters (per 100g) and low-tide water (per 100 ml) from rivers in the Great Bay estuary.	21
Figure 3. A) Effect of temperature on survival of <i>V. vulnificus</i> in 10 ppt sterile seawater. B) Effect of four temperatures (5, 12, 20 and 35oC) on the survival of <i>V. vulnificus</i> as recorded over 21 days. C) Effect of salinity on the survival of <i>V. vulnificus</i> in sterile seawater at 14°C.....	22
Figure 4. A) Relationship between numbers of CFU of <i>Vibrio</i> spp. and four of the environmental parameters measured at six estuarine sites. B) Relationship between average numbers of CFU of <i>V. vulnificus</i> (o) and water temperature (●). The arrows indicate culturability below the limit of detection.....	23
Figure 5. <i>V. vulnificus</i> abundance as a function of temperature and salinity. The sizes of the bubbles are proportional to the relative abundance of <i>V. vulnificus</i> , grouped into 9 categories: 1 to 50; 51 to 100; 101 to 250; 251 to 500; 501 to 750; 751 to 1,000; 1,001 to 2,500; 2,501 to 5,000 and >5,000 cells ml ⁻¹	24
Figure 6. <i>V. vulnificus</i> (VVAP) and total bacterial populations (total) enumerated in seawater samples.....	56
Figure 7. <i>V. vulnificus</i> and total bacteria enumerated in oysters.....	57
Figure 8. Graph showing the number of bacteria associated with >202 μm zooplankton per cubic meter of Chester River water. EUB, <i>Bacteria</i> ; GAM, γ-Proteobacterium; VIb/Pho, <i>Vibrio-Photobacterium</i> ; Vvul, <i>V. vulnificus</i> ; Vchol/mim, <i>V. cholerae-V. mimicus</i> ; Vcinc, <i>V. cincinnatiensis</i> . The shaded areas represent the number of cells per square millimeter of surface area and the bars represent the number of cells per zooplankter.....	58
Figure 9. : Bacterial cells associated with 64- to 202 μm zooplankton per cubic meter of Chester River water.....	59
Figure 10. <i>V. vulnificus</i> abundance plotted against surface salinity (A) and Water Temperature (B) over the study period in Chesapeake Bay.....	60

Figure 11. Predicted hindcast depicting the mean probability of <i>Vibrio vulnificus</i> during 1991. Color scale represents the probability of occurrence, with red=high (25%) and blue=low (0%).....	61
Figure 12. Hindcast depicting probability of occurrence of <i>V. vulnificus</i> in wet (1996) and dry years (1999). Color scale represents mean probability of occurrence with red high (25%) and blue low (0%).....	62
Figure 13. A) Specific locations where the annual sum of <i>V. vulnificus</i> probabilities in 1991 was recorded as maximum. B) Plot of mean probability of <i>V. vulnificus</i> over the Upper Bay. C) Mid Bay D) Western Estuaries. The Bold line represents the mean and the dotted line is the (+) standard deviation.....	63
Figure 14. Daily mean plots of simulated sea surface temperature and salinity from the hydrodynamic model (ROMS) for the Upper Bay (top panel), Mid Bay (middle), and West Estuaries (bottom panel) for the year 1991. Red horizontal line indicates the optimal salinity (11.5 ppt) as recorded by Jacobs <i>et al.</i>	64
Figure 15. Comparison between the annual mean probabilities of <i>V. vulnificus</i> for the wet year (1996) and dry year (1999). Arrows indicate high occurrence of <i>V. vulnificus</i> in 1996 and low occurrence of <i>V. vulnificus</i> in 1999 in the Mid Bay.	65
Figure 16. Daily mean simulated sea surface temperature and salinity from the hydrodynamic model (ROMS) for the Upper Bay (top panel), Mid Bay (middle), and West Estuaries (bottom panel) for the years from 1996 to 1999. Red Horizontal line represents the optimal salinity (11.5 ppt) as recorded by Jacobs <i>et al.</i>	66
Figure 17. Daily mean (solid bold line) and + standard deviation (line) of predicted <i>V. vulnificus</i> presence from 1991 to 2005 in the Upper Bay area (top panel), Mid-Bay area (middle) and West estuaries area of the Bay (bottom panel).....	67
Figure 18. Annual mean probabilities of <i>V. vulnificus</i> (1991) for the “Alternate Areas” i.e. Top of the Upper Bay and Bottom Bay area (lower panel).....	68
Figure 19. A) Inter-annual variability in the daily mean (solid line) and (+) standard deviation (line) of predicted <i>V. vulnificus</i> presence in the “Alternate Areas” from 1991 to 2005, i.e., top of the upper Bay (top panel) and bottom Bay (lower panel).B) Inter-annual variability in the simulated sea surface temperature and salinity by the hydrodynamic model (ROMS) for the Top of the Upper Bay and Bottom Bay from 1991 to 2005. The red horizontal line represents the optimal salinity (11.5 ppt) as recorded by Jacobs <i>et al.</i>	70

Chapter 1: Literature review

1.1 Introduction

Vibrio vulnificus, is an ubiquitous bacterium and comprises part of the normal microflora of the coastal marine environment worldwide. It has been isolated from water, sediment and a variety of seafood, such as shrimp, fish, oysters, and clams. *V. vulnificus* is known to be a natural inhabitant of the intestinal tract of oysters (*Crassostrea virginica*). The organism is a leading cause of seafood related infections and shellfish related deaths in the US. In the US, from 1981 to 1992, around 125 cases were reported with *V. vulnificus* infections. Approximately 44 (35%) of these infected individuals were reported as having died. Of the 40 deaths caused by septicemia, 35 (88%) were traced to raw oyster consumption and nine of these deaths occurred in 1992. The presence of *V. vulnificus* is strongly correlated with water temperature and *V. vulnificus* infections showed a seasonal variation with 91% of primary septicemias and 86% of wound infections occurring April through October, mostly due to the seasonality of *Vibrio vulnificus* and *Vibrio parahaemolyticus* in the environments (17).

A report by the FDA (459 US cases), between 1992 and 2007, recorded 51.6% of infected patients had died. Of 180 cases in 2002-2007 (available FDA data) 92.8% had consumed raw oysters prior to onset of symptoms, an indication that the infections were caused by *V. vulnificus* (35). Bivalves, such as oysters, clams, and mussels contain *V. vulnificus*, which can cause septicemia resulting in fever, chills, nausea, hypotensive shock and formation of secondary lesions. This form of *V. vulnificus* primary septicemia infection is the most lethal, with an average mortality rate exceeding 50% (29).

V. vulnificus can cause severe infection on exposure of open wounds to water harboring this bacterium (52). Surveillance for waterborne disease and outbreaks associated with recreational water, drinking water, and water not intended for drinking was conducted in the United States during 2003-2004. A total of 142 *Vibrio* cases associated with recreational waters were reported from 16 states. Among the patients for whom information was available, 70 (49.3%) of 142 were hospitalized and 9 (6.3%) died. The most frequently isolated *Vibrio* species was *Vibrio vulnificus*, which was isolated from 47 (33.1%) persons, of which 41 (87.2%) were hospitalized and six (12.8%) died. *V. parahaemolyticus* was isolated from 34 (23.9%) persons, of which 15 (44.1%) were hospitalized and none died. The most frequently reported location was the Gulf Coast (62.7%), Pacific coast states (19.7%), Atlantic coast states, excluding Florida (16.9%) and inland states (0.7%). Florida, Hawaii and Texas reported the highest number of cases, 51, 23 and 28, cases, respectively.

Most of the *Vibrio* illnesses were observed in the summer, especially in July and August (16). The US Food and Drug Administration has reported on an average, 34 cases of *V. vulnificus* infections (35). The CDC has reported that *Vibrio* infections increased by 78% between 1996 and 2006, and in 2005 around 121 cases of *V. vulnificus* were confirmed, suggesting that global climate change resulting in higher water temperatures perhaps causing an increase in the frequency of *V. vulnificus* and, thereby, influencing its global distribution (71). In the most recent report from the CDC for the year 2009 (71), the incidence per 100,000 population of *Vibrio* infections due to ingestion of contaminated food continued to increase and reached a total of 160 infections for an incidence rate of 0.35/100,000, compared to the number of cases reported in 2008 (131

infections or 0.29/100,000). Among 154 (96.3%) *Vibrio* isolates obtained in 2009, with species information included, 80 (52 %) were *V. parahaemolyticus*, 22 (14.3%) were *V. vulnificus* and 22 (14.3%) were *V. alginolyticus*. Figure 1 provides data showing the occurrence of *Vibrio* infections has been increasing since 2000 (CDC 2010).

V. vulnificus strains are classified into biotypes based on their biochemical properties. Seawater is a normal habitat of Biotype 1; this biotype is responsible for the majority of human infections. It behaves as an opportunistic pathogen and can cause fatal disease. On the other hand, biotype 2 is associated only with eels (1). In a study conducted by Biosca *et al.* (2) the biotype 2 strain expressed an LPS that was distinct from Biotype 1 and was indole positive. A recently found biotype 3, which possesses biochemical properties of biotype 1 and 2, was shown to cause human wound infections (3) . While biotype 3 does causes human infections, it has been limited to date to the location in Israel here it was isolated from persons handling tilapia fish (35).

1.2 Genotypes

A randomly amplified polymorphic DNA PCR, performed by Warner *et al.* (66) showed some differences between members of the genus *Vibrio* and isolates of *V. vulnificus*. Each *V. vulnificus* strain produced a unique band pattern, indicating members of this species are quite heterogeneous. *V. vulnificus* strains isolated from the clinical specimens produced an additional band that was only occasionally found in environmental samples. The presence of this band is correlated with its ability to produce infection in humans. By PCR analysis, *V. vulnificus* biotype 1 isolates (clinical & environmental) were identified. Strains possessing a sequence common to the clinical

isolates were designated as C type and strains having an environmental related sequence were designated as E type (61). Typing of the intergenic spacer region between the 16S and 23S rRNA revealed that clinical strains were highly similar, belonging to a single cluster that contained only the B type strain, whereas, the environmental isolates showed much more variability displaying the presence of A and B type 16S rRNA (20).

Genotyping studies have shown that 90% of isolates from human cases have the *vegC* sequence type, whereas 87% of the environmental strains have the *vegE* type. On examining the C and E genotypes in oysters and surrounding seawater, the researchers found that these genotypes were present in approximately equal proportions in water (46.9% E type versus 53.1% C type), but there is a greater percentage (84.4%) of the less virulent E type strain in oysters. It was seen that, as water temperatures increased, the levels of *vegC* strain from both sources (water and oysters) increased. Another study (65) showed that the E genotype possesses a selective advantage within oysters, whereas survival of C type genotype may be favored by water column temperature. In contrast to intergenic spacer typing results, a study conducted using the repetitive extragenic palindromic PCR (rep-PCR) technique, which demonstrated high diversity among clinical isolates while the environmental strains were quite similar to each other (5)

1.3 Pathogenicity of *V. vulnificus*

Some of the virulence factors exhibited by *V. vulnificus* include a polysaccharide capsule, extracellular enzymes, exotoxins, and iron acquisition. Evasion of the host defense is a mechanism used by microorganisms to survive inside the host and cause

disease. Surface expression of polysaccharide capsule by *V. vulnificus* helps it to evade the host immune response and acquire resistance to serum bactericidal action, an antiphagocytic action which results in high lethality for mice. Hence expression of CPS by *V. vulnificus* is absolutely necessary for pathogenicity. *V. vulnificus* can undergo phase variable expression of its capsule, i.e. a reversal between Opaque (Op encapsulated) to Translucent (Tr; reduced capsulation or non-encapsulated) colony morphologies. Increased phase conversion from Op to Tr type was seen in E-type strains, as compared to the C type strain, indicating that switching from Op to Tr might be due to environmental related factors (27). Grau *et al.* (22) demonstrated the presence of a rugose variant, which produces copious biofilm. The rugose isolate exhibits decreased motility, increased resistance to human serum, and increased biofilm formation. The role of rugosity in *V. vulnificus* pathogenicity is uncertain, as a study demonstrated increased resistance to Op-rugose but not to Tr-rugose. (35)

Infection with *V. vulnificus* infection is associated with elevated serum iron levels in individuals. Excess iron can increase growth rates of the pathogen and decrease neutrophil activity, leading to the conclusion that excess iron results in a compromised immune response (35). Transferrin is a glycoprotein in the human body which binds very tightly to iron. *V. vulnificus* has developed a multiple system for iron acquisition, one being scavenging iron from transferrin. *V. vulnificus* produces two types of siderophores, catechol and hydroxymate for iron acquisition. Vulnibactin, a catechol siderophore in *V. vulnificus* is important for iron acquisition for growth in iron limited media. This siderophore is required for scavenging iron from transferrin and holotransferrin, as shown by mutational analysis of the genes involved in vulnibactin synthesis and transport.

Mutation of vulnibactin associated genes (*vvsA*, *vvsB*, *vvsU*) resulted in decreased virulence as compared to wild type strains (35).

The gene *vvhA* is an extracellular hemolysin, which contributes to iron release via hemolytic activity. The hemolysin toxin is known to cause acute cellulitis, fluid accumulation, intestinal irregularities, partial paralysis, and lethality (23), (35). Inactivation of hemolysin by *vvhA* mutation did not show a difference in the LD₅₀ from that of cytolysin positive strains when injected into an iron loaded mouse, indicating that the hemolysin is not solely responsible for infection (70). *VvpE*, is an extracellular protease enzyme which is known to be involved in *V. vulnificus* infection. The *vvpE* protease produced by *V. vulnificus* causes tissue necrosis and cutaneous lesions, as well as increased vascular permeability. Mutational analysis of *VvpE* showed that it is not absolutely required for virulence (35).

Another gene which is the most important in infection caused by *V. vulnificus*, is the *rtxA1*. The amino acid sequence of the RtxA1 toxin of *V. vulnificus* has a high homology to the *rtxA* sequence of *V. cholerae*. This toxin causes rearrangement of the cytoskeletal structure, bleb formation, and aggregation of actin, which leads to cellular necrosis. The RtxA1 toxin plays an important role in the development of systemic disease, demonstrated by Gulig *et al.* (24) who showed the *rtxA* mutant had reduced systemic infection to the liver. RtxA toxin expression was greatly enhanced when *V. vulnificus* was incubated with host cells, indicating that cell to cell contact is important for cytotoxicity. An operon similar to the *rtxBDE* operon of *V. cholerae* is found in *V. vulnificus*. *HlyU* is a transcriptional regulator which binds upstream to the *rtxA* operon and

regulates the expression of *rtxA1*. Mutational analysis of *hlyU* resulted in decreased *rtxA1* expression.

Endotoxic shock is a characteristic of *V. vulnificus* disease, a symptom due to the presence of lipopolysachharide. Injection of LPS into mice showed a drop in mean arterial pressure and rapid death of the animal, indicating that LPS is responsible for lethality. Agents such as LDL, cholesterol, and estrogen have been shown to mitigate the effects of LPS. An increase in the mouse survival rate was seen when LDL was administered prior to injecting the mouse with LPS. Results generated by Merkel *et al.* (46) concluded that estrogen provides protection against *V. vulnificus* LPS induced endotoxic shock

Other factors important for *V. vulnificus* infection include pili, outer membrane proteins, and flagella. As previously mentioned, cell to cell contact is required for cytotoxicity. Gram negative bacteria use pili for adherence to host cells. *V.vulnificus* mutants were generated which possess a mutation in *pilA* and *pilD*. Paranjpye *et al.* (54) demonstrated a *pilD* mutant exhibited reduced adherence to HEp-2 cells and decreased virulence. Inactivation of *pilA* reduced the ability to form biofilms and significantly decreased adherence to HEp-2 cells. OmpU is an outer membrane protein which binds to fibronectin. Mutational studies carried out by Goo *et al.* (21) showed that OmpU is an important virulence factor and is required for adherence. IlpA is another outer membrane protein which is important for production of interferon- γ in human peripheral mononuclear cells. IlpA mutants demonstrated reduced mortality in mice, compared to the wild type. Flagellum based motility is required for biofilm formation and pathogenesis. The role of flagella in *V. vulnificus* pathogenesis was studied by carrying

out mutation in flagellar proteins. Loss of flagellar structural components encoded by *flgC* and *flgE* resulted in a significant decrease in motility, cellular adhesion, and cytotoxicity (35). Thus, the above studies indicate that cell attachment is required for *V. vulnificus* toxin secretion and pathogenicity.

1.4 Epidemiology

The three major clinical manifestations of *Vibrios* include wound infection, primary septicemia, and gastroenteritis. Wound infections are defined as those where a patient incurred a wound infection before or during exposure to seawater or contaminated seafood drippings and where *V. vulnificus* was cultured from that wound, blood, or any normal sterile site. Primary septicemia was defined as a systemic illness with fever and shock, where *V. vulnificus* was isolated from blood or sterile site from an individual with a history of raw shellfish consumption (63). Most of the *V. vulnificus* infections in the US occur in the southeastern and Gulf coast regions. *Vibrios* proliferate in the warm waters and most of the infections occur in the warmer months, when the numbers of *V. vulnificus* are highest. In the US, the onset of systemic and wound infections occurs primarily between the months of April and September. A study of the epidemiology of *V. vulnificus* infections was conducted by Shapiro *et al.* (62). The study included data from 22 states. From the analysis, of 422 infections from 1988 to 1996, 45% were wound infections, 43% primary septicemia, 5% were gastroenteritis cases, and the remaining 7% were undetermined exposure. The cases of primary septicemia and gastroenteritis were preceded by consumption of raw shellfish. Of the 181 cases of primary septicemia, 173 patients reported eating raw oysters at least 7 days prior to the onset of symptoms the

majority of gastroenteritis cases were due to consumption of raw oysters. About 89% of the harvested oysters were from water with temperatures greater than 22°C. Contact with water or shellfish in such areas or during the season of high *V. vulnificus* prevalence was reported in the majority of cases of wound infections. Many wound infections are due to occupational exposure among oyster shuckers and commercial fisherman. In the above survey, cases of gastroenteritis, where *V. vulnificus* was isolated from the stool sample, made up 11% of the total ingestion-associated infections and was mainly due to consumption of raw shellfish (62).

1.5 Ecology

Vibrio vulnificus, a halophilic bacterium, was first described by Hollis *et al.* (31) in 1976 and shown to be associated with serious human infections. *V. vulnificus* and *V. parahaemolyticus* have been isolated from various sites all around the US, including the Great Bay of Maine (51) and Alaska (45). Lower densities of *V. vulnificus* were isolated from Pacific, Canadian, and North Atlantic waters where the temperature are usually low throughout the year and higher densities present in warmer waters of the Mid-Atlantic, the Chesapeake Bay, and the Gulf of Mexico (38, 37, 51, 12, 10, 69, 48).

1.5.1 Temperature and salinity

A study carried out by Kelly (1982) show seasonal variation in the occurrence of *V. vulnificus* and suggested that the growth is favored by relatively high temperatures and low salinity. The study was done on the surface waters of the Gulf Coast, where water temperatures varied widely throughout the year, ranging from a low of 12.5°C in

December to a high of 31°C in August. Peak incidence of *V. vulnificus* was discovered when the water temperature had been above 25°C for several months, i.e. in September following the summer warmth. The salinity cut off point was 16‰ (parts per thousand), where a statistically significant difference in the rate of recovery of the organism was observed between the different sites, i.e., with salinity <16‰ and salinity >16‰. Kelly (1982) comments that the organisms may grow in selected environments where conditions are optimal and may be disseminated to other environments by tidal flow or freshwater runoff. In addition to surface water, *V. vulnificus* is known to have been isolated from sediment, plankton, and marine organisms where the sea surface temperature (SST) is 25.6°C and salinity 29.9‰ (53). Kaysner *et al.* (37) conducted a study in west coast estuaries and found a low frequency of occurrence in the estuaries of Washington, Oregon, and California. *V. vulnificus* was isolated from just 31 of the 529 samples analyzed. Most of the water samples from which *V. vulnificus* has been isolated were in temperatures >15°C and salinities of 15 to 30‰. A study done by O'Neil *et al.* (51) in the Great Bay estuary of New Hampshire and Maine demonstrated that levels of *V. vulnificus* increased dramatically from an initial low concentration in July, after temperature and salinity levels in the water at low tide had increased to >20°C and >10.0‰ respectively. From Figure 2, the seasonal relationship between incidence of *V. vulnificus* in oysters and the temperature and salinity levels is shown for the Great Bay estuary. *V. vulnificus* was not detected after October, when temperatures and low tide salinities were <10.0°C and <5‰, respectively. Statistical analysis showed that temperature and salinity taken together revealed a significant relationship ($r = 0.85$) with presence of the pathogen. While warm temperatures and low salinities in the tidal rivers

of the Great Bay estuary provided a suitable environment for growth of *V. vulnificus* throughout the summer months, to the contrary, *V. vulnificus* was not isolated from Great Bay, indicating that the concentrations of *V. vulnificus* were lower in the Great Bay than in the surrounding waters. Kasper *et al.* (36) showed that *V. vulnificus* was optimal at temperatures between 13 and 22°C. Figure 3 A shows on day 2, the numbers of *V. vulnificus* had increased when the temperature ranged from 13 to 30°C, but on day 6, the greatest numbers were found when the temperature ranged between 13 to 22°C. When *V. vulnificus* was inoculated in sterile seawater and incubated at 5, 12, 20 and 35°C, the most rapid decrease in numbers of *V. vulnificus* occurred in samples incubated at 5 and 35°C, as shown in Figure 3 B. Their research also demonstrated the effect of salinity on survival of *V. vulnificus*, salinities between 5 and 25 ppt, *V. vulnificus* levels increased but when salinities were 30, 35, and 38 ppt, *V. vulnificus* decreased by 58, 88 and 83%, respectively. This trend can be observed in Figure 3 C. Lipp *et al.* (41) tested water and sediment samples from Charlotte Harbor, Florida, for *V. vulnificus*. The number of *V. vulnificus* in the water column ranged between 58 CFU/100 ml and 1.21×10^3 CFU/100ml, whereas *V. vulnificus* in sediment was two orders greater than in the water column. The influence of salinity was greater on the *V. vulnificus* variability compared to temperature. The optimal salinity at the site was 15 ppt. which resulted in highest concentrations of the pathogen. There was an overall positive correlation at salinities below 15 ppt ($r=0.481$; $P<0.001$) and a negative correlation ≥ 15 ppt ($r= -0.433$; $P<0.001$), suggesting that salinity strongly controls the geographical and seasonal distribution of the pathogen between the water column and sediment.

Pfeffer *et al.* (58) conducted a multiyear study of the ecology of *V. vulnificus* in estuarine waters of the eastern United States. Isolation of *Vibrio* spp. was positively correlated with water temperature (r_s Spearman's rank correlation coefficient = 0.81845; $P < 0.01$), turbidity, presence of estuarine bacteria, and levels of total coliforms and negatively correlated with dissolved oxygen levels, as seen in Figure 4. *V. vulnificus* accounted for an average of 7.7% of the *Vibrio* spp., with average monthly levels ranging from < 0.01 to 23 CFU/ml. Highest concentrations were detected in the warm-weather months, i.e. *V. vulnificus* isolation was most prevalent when the average water temperature ranged from 15 to 27°C and average salinity between 8 and 14 psu. *V. vulnificus* was not isolated between the months of December and March, when the water temperature were $< 13^\circ\text{C}$. (see Figure 4). There was no significant relationship between salinity and *V. vulnificus* isolation, as the salinity in the study area (estuaries of eastern North Carolina) was always between 5 and 20 ppt., which is the optimal range for growth of *V. vulnificus*, suggesting that salinity was not a limiting factor for the growth of the bacterium. As seen from the above studies, the size of *V. vulnificus* populations is strongly correlated with temperature, although the general trend is for *V. vulnificus* abundance to be inversely correlated with salinity, a relationship that depends on the salinity. Usually high abundances are found when the salinity ranges from 5 to 10ppt. the optimal salinity range. But at 20 to 25ppt, *V. vulnificus* abundance showed positive correlation with salinity.

Results of Randa *et al.* (60) showed that *V. vulnificus* was positively correlated with water temperature, total bacterial abundance, chlorophyll concentration and salinity. Water temperature explained nearly 60% of the variability in *V. vulnificus* abundance.

During the summer, when the temperature did not vary much, salinity was positively correlated with *V. vulnificus* and accounted for 36% of the fluctuation in abundance. When an analysis combining temperature and salinity effects on *V. vulnificus* abundance was done (Table 1), it showed that, on the whole, *V. vulnificus* abundance was positively correlated to temperature and negatively correlated to salinity. The researchers commented that this trend is not followed when the salinity levels are different (Figure 5). In the range of 5 to 10 ppt, *V. vulnificus* abundance is not correlated with temperature and high abundances are observed in this salinity range, irrespective of temperature (10 to 32°C). On the other hand, at 20 to 25 ppt., *V. vulnificus* abundance was positive correlated with salinity. Another study Hsieh *et al.* (32) showed a similar positive correlation between *Vibrio* concentration and salinity. The regression equation that they generated, using salinity as a coefficient, was $\ln(\text{VIB}) = 0.29\text{SAL} + 3.88$ ($r^2=0.62$), where VIB indicates *Vibrio* concentration, SAL is the salinity. But when salinity and POC (particulate organic carbon) were both included, the governing equation was $\ln(\text{VIB}) = 0.25\text{SAL} + 0.97\text{POC} + 2.88$ ($r^2 = 0.69$). Temperature dependence was difficult to discern as the range measured during the summer was small ($27.0^\circ\text{C} \pm 2.6^\circ\text{C}$). The authors argue that the reason for different relationships between *Vibrio* and salinity is the hydrology of the estuaries and resultant relationships between nutrients, organic matter, and salinity. The site chosen for their study (NRE –Neuse River Estuary) is a lagoonal estuary, bounded by Pamlico Sound and barrier islands, which was similar to the study area (Barnegat Bay) of Randa *et al.* (60). On the other hand, the salt wedge in the tidal estuaries demarks a boundary between the nutrient and organic rich freshwater and oligotrophic marine water. They concluded that the lagoonal estuary exhibits more

gradual gradients along the salt wedge and has a longer water residence time, allowing bacterioplankton to proliferate at the higher salinities.

1.5.2 Aquatic wildlife and zooplankton

Marine biota, such as oysters, finfish, crustaceans, mollusks and plankton can provide environments where *V. vulnificus* can reproduce. *V. vulnificus* is a persistent component of the microbial flora of oysters and makes the oyster unamenable to traditional methods of controlled purification, such as UV light depuration. *V. vulnificus* has been enumerated in seawater, oyster shell biofilms, homogenates of oyster meats, and tissues containing hemolymph, digestive region, gills, and adductor muscle. Depuration systems conducted at temperatures greater than 23°C cause *V. vulnificus* counts to increase in oysters, especially in the hemolymph, adductor muscle, and mantle. At elevated seawater temperatures, i.e., at >21°C, *V. vulnificus* multiplies markedly in oyster tissues and large numbers are released into the surrounding seawater at rates exceeding bactericidal activities of UV light. At low temperatures, such as 15°C, *V. vulnificus* was not detected in the seawater samples and the counts in oyster meats were low. In contrast, at high temperatures of 23°C, *V. vulnificus* counts in oyster meats increased 100,000 fold (64). Similarly, in another study, *V. vulnificus* was found more frequently and at a higher concentration in oysters than in water (51). DePaola *et al.* (12) found significant densities of *Vibrio vulnificus* in the intestines of fish from the US Gulf Coast. *V. vulnificus* is abundant in a variety of estuarine fish species that commonly inhabit oyster reefs of the US Gulf Coast. *V. vulnificus* densities found in the intestines of some fish were higher than those in the surrounding water and sediment or in nearby crabs and oysters. Densities

were highest in spring and summer. *V. vulnificus* densities in sheephead fish intestines were generally 2 to 4 logs greater than in oysters and sediment and approximately 5 logs higher than in seawater.

Table 2 lists the mean densities of *V. vulnificus* in the intestinal contents of various fish and environmental specimens collected from inshore estuarine water during spring and summer. Highest densities of *V. vulnificus* were found in benthic fish, such as sheephead, pigfish, black drum, sea catfish, pinfish, spot, Atlantic croaker, and Gulf toadfish. In offshore sites of the Gulf of Mexico, *V. vulnificus* was found only in two fish that were collected. These offshore sites were generally more saline (32 to 35‰ NaCl) than inshore sites (5 to 28‰ NaCl) where *V. vulnificus* was more prevalent. Wright *et al.* (69) were able to isolate *V. vulnificus* from Chesapeake Bay oysters, when water temperatures were 7.6°C, at concentrations ranging from 1.0×10^3 to 4.7×10^4 /g. A national survey was conducted by Cook *et al.* (11) from June, 1998 to July, 1999, of oysters harvested from the Gulf (49%), Pacific (14%), Mid-Atlantic (18%), and North Atlantic (11%) coasts of the US and Canada (8%). Densities of both *V. vulnificus* and *V. parahaemolyticus* in market oysters followed a seasonal distribution, with highest densities in the summer. The oysters harvested from the Gulf Coast showed highest densities of both organisms, which often exceeded 10,000 MPN/g. The majority of the oysters harvested along the North Atlantic, Pacific and Canadian Coasts had *V. vulnificus* densities below detectable levels. Oysters collected from the Gulf Coast sites had a seasonal distribution of *V. vulnificus*, i.e. a large number (median concentration, 2300 organisms [MPN] per gram of oyster meat) were found from May through October. During the months of November through December, there was a gradual reduction (to \leq

10 per g). This trend continued from January to March, with a sharp increase in late March and April to summer levels (48). This study found that *V. vulnificus* numbers increased with water temperature, up to 26°C. Higher concentrations ($> 10^3$ per g) were typically found in oysters from intermediate salinities (5 to 25 psu) and smaller *V. vulnificus* numbers ($< 10^2$ per g) at salinities above 28 ppt.

Vibrio spp. comprise a significant portion of the natural bacterial flora of zooplankton, especially zooplankton with chitinous exoskeletons (25). Huq *et al.* (33) found a large number of vibrios associated with zooplankton in the surrounding water column, suggesting that *Vibrio* spp have a competitive advantage in the chitinous exoskeleton micro-environment of zooplankton. Heidelberg *et al.* (25) showed that there was a large population of bacteria associated with both large and small size classes of zooplankton. A taxonomically diverse group of bacteria was associated with zooplankton and a larger proportion was found in and on zooplankton during the cooler months of the year. *V. vulnificus* was one of the *Vibrio-Photobacterium* species associated with large and small zooplankton.

1.5.3 Bacteriophages

Bacteriophages pathogenic for *Vibrio spp.* are abundant in the marine environment. Moebus and Nattkemper (47) isolated 366 phages from the Atlantic, 362 of which initiated infection in bacteria belonging to the *Vibrionaceae* family (15). Pelon *et al.* (57) isolated nine phages infecting *V. vulnificus* from estuarine water samples collected in Louisiana. Of 60 *V. vulnificus* tested, 87% were susceptible to one or more phages. Similarly DePaola *et al.* (13) isolated phages lytic to *V. vulnificus* from estuarine water, sediment, plankton, crustaceans, molluscan shellfish, and the intestines of finfish of the US Gulf Coast. The phage densities were higher (2 to 4 \log_{10}) in molluscan shellfish than in the other samples. Other bacterial species were also isolated from oysters and tested for susceptibility to *V. vulnificus* phages, but none were lysed by the *V. vulnificus* phages. It was found that, in spite of the low occurrence of *V. vulnificus*, the number of phages present was high, indicating long term persistence of phages during the winter. The close association of phages with various oyster tissues and fluids most likely reduces their elimination by excretion and is consistent with long-term retention. A similar study done by DePaola *et al.* (14), enumerated phages ($>10^4$ phages per g of oyster tissue⁻¹) infecting *V. vulnificus*. The phages were found throughout the year in oysters collected from estuaries adjacent to the Gulf of Mexico. The isolates belonged to three families of double stranded DNA phages, i.e. *Podoviridae*, *Styloviridae*, and *Myoviridae*. Results from the above studies indicate that there exists a morphologically

diverse group of phages infecting *V. vulnificus*, which is abundant and widely distributed in oysters.

1.5.4 Viable but nonculturable state (VBNC)

A bacterial cell in the VBNC state may be defined as one which fails to grow on routine bacteriological media, but would otherwise grow and develop into a colony under normal environmental conditions. Investigation into the temporal distribution of *V. vulnificus* demonstrated that the number of culturable *V. vulnificus* in the water column, sediment, and oyster tissue declined in the cooler months, which led to the hypothesis that *V. vulnificus* was not absent from the marine system during the cooler months, but rather developed into a non-platable, or nonculturable form, i.e. a VBNC form (40). *V. vulnificus* cells entering into the VBNC state have distinct morphological characteristics. The first includes reduction in size. *V. vulnificus* cells in the log phase of growth are rod shaped and 3µm long, whereas those in the VBNC state are coccoid, typically 0.6 µm in diameter. During this process, significant changes in membrane structure, protein composition, ribosomal content, and DNA arrangements occur. Researchers have found a dramatic decrease in the levels of synthesis of DNA, RNA, and protein when these cells were exposed to temperatures of 5°C. During this state, there is a dramatic increase in the amount of unsaturated fatty acid, and decrease in nutrient transport, and respirations rates. Entry into the VBNC state by *V. vulnificus* is induced by low (<10 °C) temperature incubation. The ability of VBNC cells to be able to exit this dormant state and return to a metabolically active, culturable state is termed resuscitation, which is triggered by removal of stresses (low temperatures and salinities). In *V. vulnificus*, exit from the low

temperature-induced VBNC state could be achieved by upshift in temperature. It was seen that, during this shift, culturable cells rapidly began to appear and population levels approximately equaled the original levels within 12-24 hr. Hence, the VBNC state is a mechanism to survive adverse conditions in the environment. Enumeration of colony forming units (CFU) in artificial seawater indicated that *V. vulnificus* enters the VBNC state within 4 days at 5-10°C (68). However in some studies (69), *V. vulnificus* was isolated from water and oysters at 8 to 7.6° C, but in an other study done in the Gulf Coast (38). *V. vulnificus* could not be detected at temperatures <12.5°C. The difference in the results of these different studies most primarily reflects the sensitivity of the methods used to detect the VBNC cells.

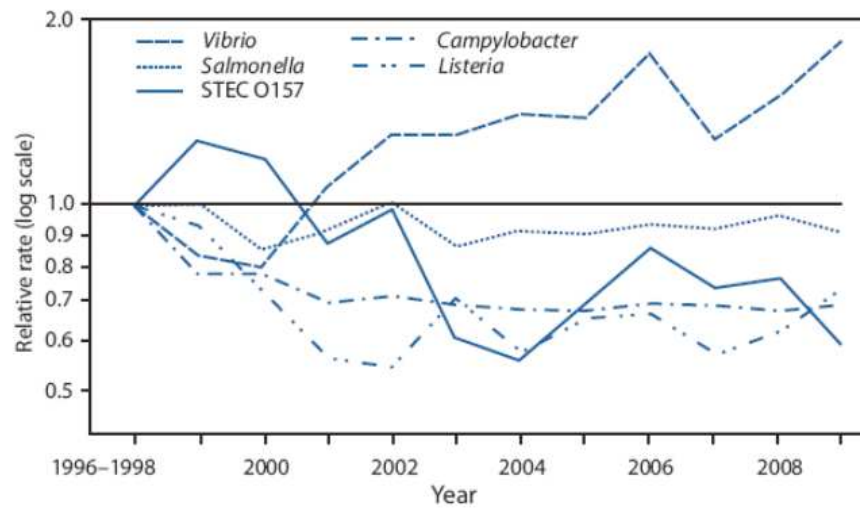


Figure 1: Relative rates of laboratory-confirmed infections with *Campylobacter*, STEC* O157, *Listeria*, *Salmonella*, and *Vibrio* compared with 1996 to 1998 rates, by year. Foodborne Diseases Active Surveillance Network (FoodNet), United States, 1996 to 2009

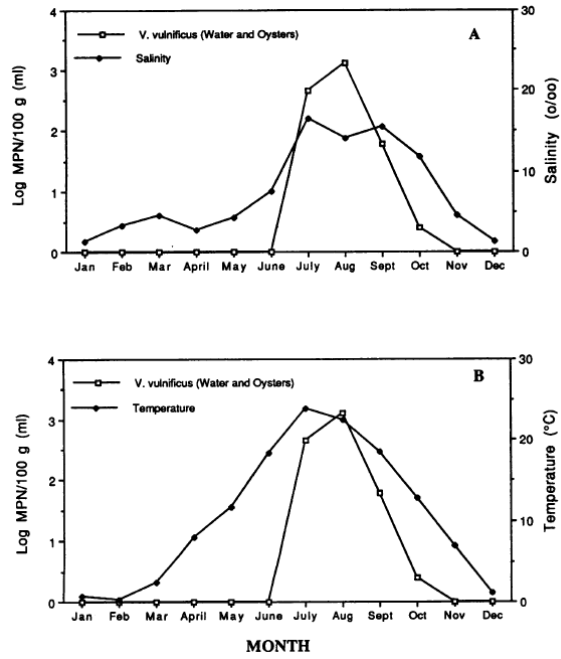


Figure 2: Effects of salinity and temperature on *V. vulnificus* concentration in oysters (per 100g) and low-tide water (per 100 ml) from rivers in the Great Bay estuary (51).

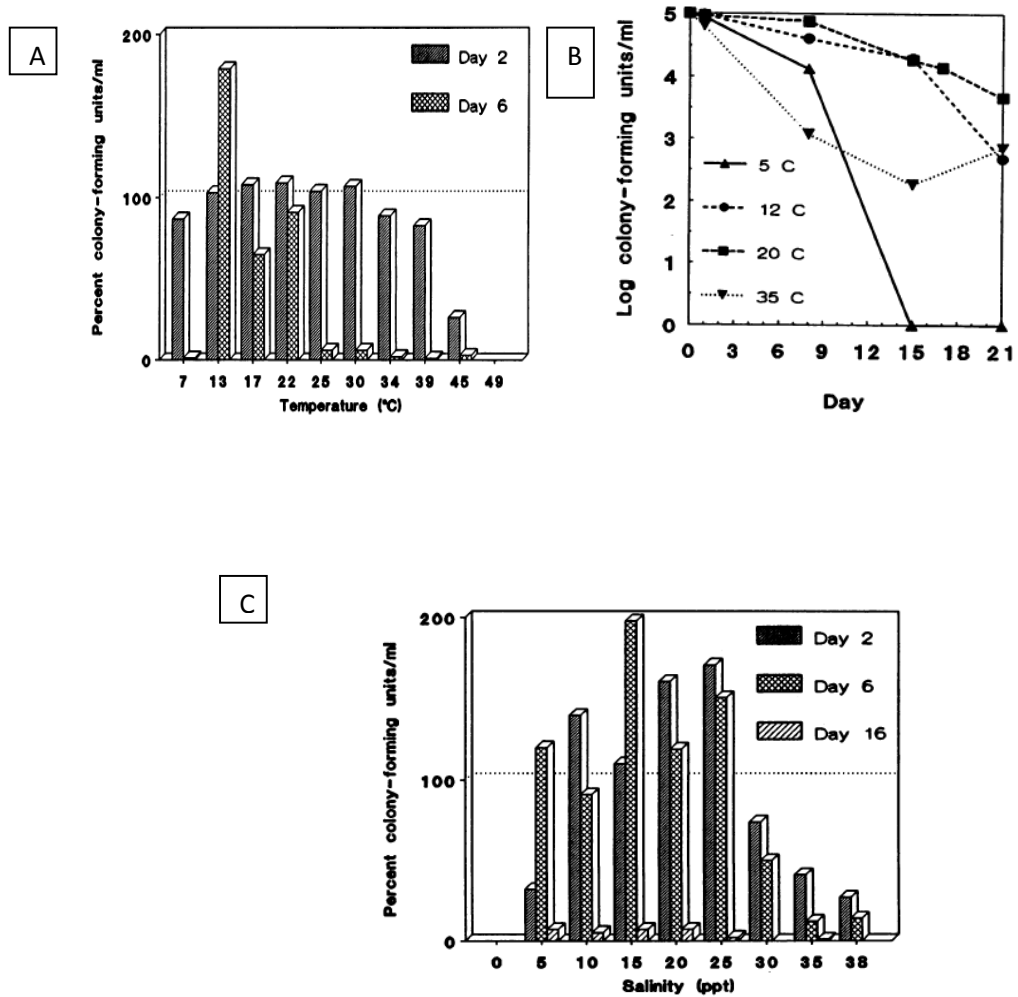
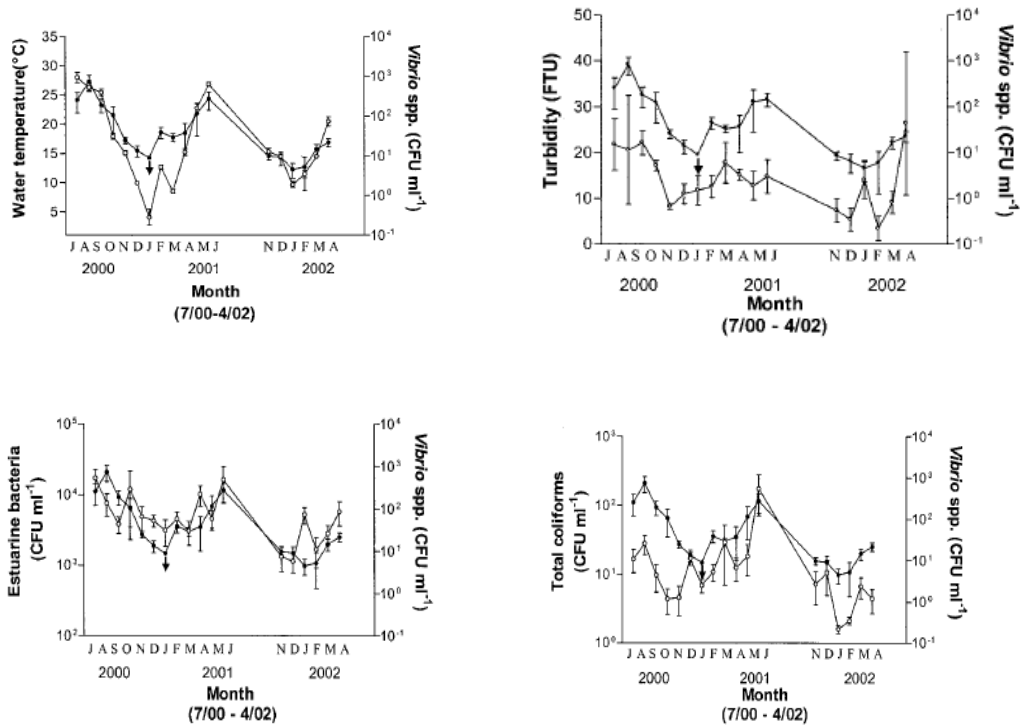


Figure 3: A) Effect of temperature on survival of *V. vulnificus* in 10 ppt sterile seawater. B) Effect of four temperatures (5, 12, 20 and 35°C) on the survival of *V. vulnificus* as recorded over 21 days. C) Effect of salinity on the survival of *V. vulnificus* in sterile seawater at 14°C (36).

A



B

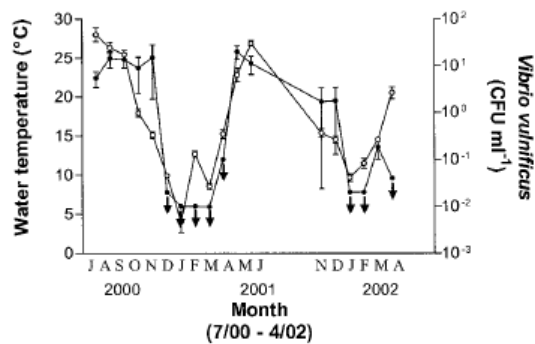


Figure 4: A) Relationship between numbers of CFU of *Vibrio* spp. and four of the environmental parameters measured at six estuarine sites. B) Relationship between average numbers of CFU of *V. vulnificus* (o) and water temperature (●). The arrows indicate culturability below the limit of detection (58).

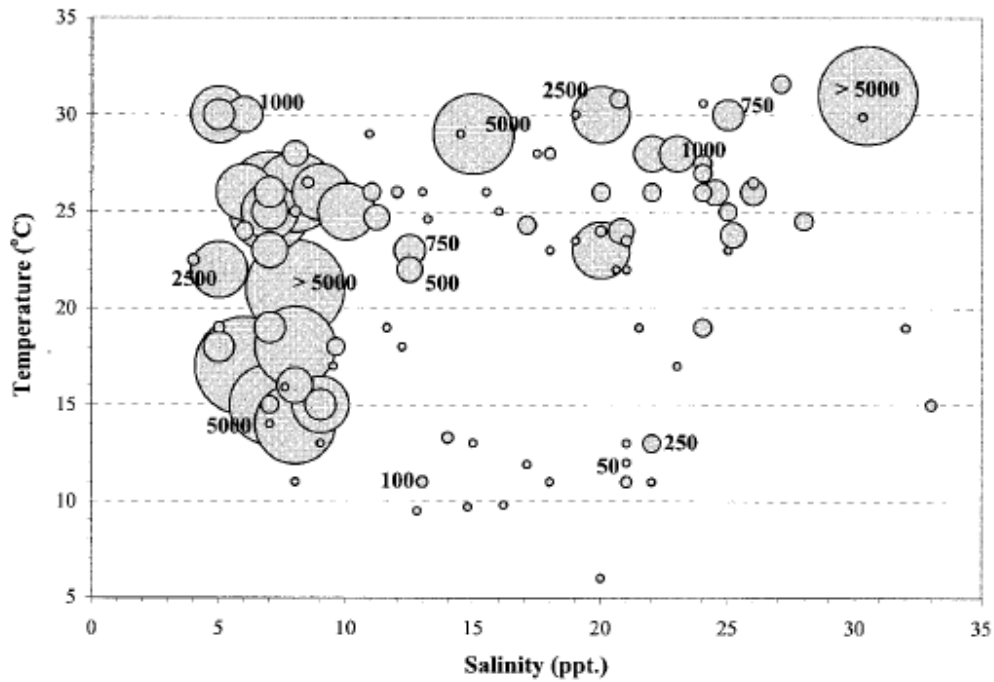


Figure 5: *V. vulnificus* abundance as a function of temperature and salinity. The sizes of the bubbles are proportional to the relative abundance of *V. vulnificus*, grouped into 9 categories: 1 to 50; 51 to 100; 101 to 250; 251 to 500; 501 to 750; 751 to 1,000; 1,001 to 2,500; 2,501 to 5,000 and >5,000 cells ml⁻¹ (60).

Sampling site(s)	Year of study	Method of identification and enumeration ^a	<i>V. vulnificus</i> abundance (cells ml ⁻¹)	Reference
Chesapeake Bay, Del.	2002	Fluorescent oligonucleotide probe direct counting procedure	2–10,000	Heidelberg et al. (15)
Charlotte Harbor, Fla.	2001	Membrane filtration followed by identification and enumeration on CPC agar	50–3,000	Lipp et al. (30)
Mobile, Ala.	1997	Most-probable-number assay with immunoassay identification	0–251	DePaola et al. (13)
Chesapeake Bay, Del.	1996	Plating with oligonucleotide probe identification and enumeration	0–200	Wright et al. (50)
Mobile Bay and Mississippi Sound, Ala.	1994	Most-probable-number assay with CPC agar identification	32–2,511	DePaola et al. (11)
Apalachicola Bay, Fla.	1982	Most-probable-number assay with TCBS agar plates and API identification kit	0–7,000	Tamplin et al. (43)

^a CPC, colistin-polymyxin B-cellobiose; TCBS, thiosulfate-citrate-bile salt-sucrose.

Table 1 *V. vulnificus* abundances recorded by different studies (60)

Sample type	No. of samples	Mean <i>V. vulnificus</i> MPN/100 g or ml (log ₁₀)	SD
Water	9	2.9	0.7
Sediment	8	5.6	0.8
Oyster (<i>Crassostrea virginica</i>)	7	5.2	1.3
Blue crab (<i>Callinectes sapidus</i>)	3	4.8	0.4
Mud crab (<i>Panopeus</i> spp.)	4	5.0	1.2
Atlantic croaker (<i>Micropogonias undulatus</i>)	3	7.8	0.6
Atlantic spadefish (<i>Chaetodipterus faber</i>)	1	3.4	
Atlantic stingray (<i>Dasyatis sabina</i>)	1	4.6	
Black drum (<i>Pogonias cromis</i>)	8	8.5	0.7
Crevalle jack (<i>Caranx hippos</i>)	5	4.5	2.6
Gafftopsail catfish (<i>Bagre marinus</i>)	1	>1.5	
Gulf menhaden (<i>Brevoortia patronus</i>)	4	5.4	1.8
Gulf toadfish (<i>Opsanus beta</i>)	1	8.4	
Pigfish (<i>Orthopristis chrysoptera</i>)	8	8.8	1.1
Pinfish (<i>Lagodon rhomboides</i>)	3	8.5	0.3
Red drum (<i>Sciaenops ocellatus</i>)	3	2.5	1.4
Scaled sardine (<i>Harengula jaguana</i>)	1	5.4	
Sea catfish (<i>Arius felis</i>)	8	8.8	1.3
Sheepshead (<i>Archosargus probatocephalus</i>)	11	8.2	1.0
Southern kingfish (<i>Menticirrhus littoralis</i>)	1	5.4	
Spanish mackerel (<i>Scomberomerus maculatus</i>)	3	5.5	1.0
Striped mullet (<i>Mugil curema</i>)	5	4.8	2.7

Table 2: *V. vulnificus* densities in water, sediment, oysters, and crabs and intestinal contents of fish collected during the months of April through October from Mobile Bay and the Mississippi Sound in Alabama (12).

Chapter 2: Hindcast study: Predicting the distribution of *Vibrio vulnificus* in Chesapeake Bay

Vibrio vulnificus is a natural inhabitant of warm estuarine waters all over the world and can infect humans via wound infections and seafood consumption (38, 37, 53, 51, 69, 11, 58, 26, 18, 56, 55). *V. vulnificus* can invade through the intestinal barrier, causing primary septicemia. Nearly all the systemic infections (95%) have occurred in persons with underlying chronic diseases, including liver disease, hemochromatosis, or conditions which lead to immunosuppression. *V. vulnificus* causes a mild to severe gastrointestinal illness, which might progress to septicemia, with a significant mortality in a susceptible population.

The Chesapeake Bay is the largest estuary in the United States. It lies off the Atlantic Ocean, surrounded by Maryland and Virginia. The Chesapeake Bay's drainage basin covers 64,299 square miles (166,534 km²) in the District of Columbia and parts of six states: New York, Pennsylvania, Delaware, Maryland, Virginia, and West Virginia. More than 150 rivers and streams drain into the Bay. The Chesapeake Bay is approximately 200 miles (300 km) long, from the Susquehanna River in the north to the Atlantic Ocean in the south. At its narrowest point between Kent County's Plum Point (near Newtown) and the Harford County shore near Romney Creek, the Bay is 2.8 miles (4.5 km) wide. At its widest point, just south of the mouth of the Potomac River, it is 30 miles (50 km) wide. Total shoreline for the Bay and its tributaries is 11,684 miles (18,804 km) and the surface area of the bay and its major tributaries is 4,479 square miles

(11,601 km²). Average depth of the bay is 46 feet (14 m) and the maximum depth is 208 feet (63 m) (http://en.wikipedia.org/wiki/Chesapeake_Bay).

The Chesapeake Bay watershed is home to thousands of species of plants and animals. From the fish that swim in the Bay's waters to the deer that live in the watershed's upper reaches, each species fills a distinct role in the overall functioning of the ecosystem. Some of the better-known inhabitants of the Bay watershed include blue crabs, oysters, striped bass and bald eagles. The Chesapeake region is also home to a multitude of other animals, including frogs, beavers, ducks, clams and jellyfish. The entire lower food web, i.e. both the benthic and planktonic communities are important indicators of the health of the Chesapeake Bay. Phytoplankton, or algae, are primary producers, which means they form the base of the Chesapeake Bay food web. Benthos and zooplankton are vulnerable to unhealthy water conditions, such as chemical contaminants, excess nutrients and sediment, and low oxygen levels. Algae respond directly to nutrient pollution that is, when there are too many nutrients in the water, large algae blooms can form and harm aquatic life (<http://www.chesapeakebay.net/>). Hence the Chesapeake Bay is one of the most diverse ecosystems in the world. In order to gain an improved understanding of *V. vulnificus*, we examined the distribution of *V. vulnificus* using a hindcast study over the Chesapeake Bay.

A study was conducted for a period of 15 years by researchers (30) in the Chesapeake Bay community to analyze clinical and epidemiological features of *Vibrio* infections. During the time period (1974 to 1988) of the study, 40 different *Vibrio* isolates (8 species) from 32 patients were indentified. *V. vulnificus* was frequently isolated from

wound (7 isolates), sputum (1 isolate) and bone (2 isolates). Epidemiologic exposure histories identified salt water contact, seafood, or travel. The first study to elucidate the distribution of *V. vulnificus* in the Chesapeake Bay was conducted by Wright *et al.* (69). They used a DNA oligonucleotide probe and enumerated *V. vulnificus* populations in the water column, plankton, oysters and sediment. The results demonstrated that the number of *V. vulnificus* in surface water ranged from 3.0×10^1 to 2.1×10^2 /ml, averaging between 0.6 to 17.4 % of the total bacterial population (Figure 6). Over the period between May and December, 1992, the mean number of *V. vulnificus* for the entire set of Chesapeake Bay water samples tested was found to be 8.0% of total culturable bacteria. For bottom water samples, at all stations during warm months (May, June, September, and December), the mean number of *V. vulnificus* was 5.3×10^2 organisms per ml. When the stations in the Upper Bay and Lower Bay were compared, during the warmer months *V. vulnificus* was more frequently isolated from all water samples collected from the Upper Bay and less frequently from the Lower Bay. Samples were collected from oyster beds located in the Severn River and Patuxent River. *V. vulnificus* was not detected in oysters collected during February and March, 1992. At other times of the year, *V. vulnificus* was always present in oysters at both locations and in numbers ranging from 1.0×10^4 to 4.7×10^4 per g of oyster (Figure 7). *V. vulnificus* was isolated from plankton samples at all locations, but only from four of nine sediment samples. *V. vulnificus* was consistently isolated from sediment collected at locations of oyster beds or immediately downstream from an oyster bed. Hence *V. vulnificus* was detected in all the samples e.g. surface and bottom waters, oyster tissues, sediment and plankton at almost all of the study sites in Chesapeake Bay. Usually high detections was achieved in summer months and low

detection in winter months. It was concluded, using a multiple regression analysis, that increased *V. vulnificus* concentration was correlated with lower salinities and with isolation from samples closer to the bottom. A study done by Heidelberg *et al.* (25) characterized the γ -Subclass Proteobacteria associated with Zooplankton in the Chesapeake Bay. It was observed that large populations of bacteria are associated with both large and small zooplankton. The number of bacteria associated with large zooplankton ranged from 1.0×10^8 to 3.8×10^9 cells per m^3 of CRW (Choptank River Water), of which the total number of *V. vulnificus* was between 2.4×10^5 and 1.3×10^7 cells/ m^3 . Maximum number of *V. vulnificus* populations associated with large zooplankton was recorded in early spring and summer. The number of *V. vulnificus* per individual zooplankter of $>202\mu m$ size class ranged from 3.6×10^1 to 1.0×10^4 (Figure 8). *Vibrio-Photobacterium* spp. comprised 1 to 26% of the total large zooplankton-associated Bacteria, of which *V. vulnificus* comprised 1 to 57% of the total *Vibrio-Photobacterium* population. As for taxa associated with the small size zooplankton (64 to $202 \mu m$), the total number of *V. vulnificus* was 3×10^5 to 2.9×10^7 cells/ m^3 (Figure 9). *V. vulnificus* constituted 0.5 to 51% of the total *Vibrio-Photobacterium* population associated with small zooplankton. The total number of bacteria per square millimeter of surface area was significantly smaller than found on the large zooplankton.

2.1 Ecological modeling for disease forecasting

The science of ecological forecasting is beginning to emerge as a new discipline, which could have an expanding role in policy formulation and management. Ecological forecasting can provide an important tool for the public by providing sciences based sound estimates of what is likely to occur and allow consideration of preventive action. The spatial extent of ecological forecasting ranges from small plots to regions to continents to the globe. Ecosystem forecasting involves different systems, such as forecasting of extreme climate events, biomass, agriculture, public health, and marine ecosystems. Some projects of ecological forecasting include The Chesapeake Bay Forecast System (CBFS), Great Lakes Coastal Forecasting System (GLCFS), EcoCast, Coastal Louisiana Ecosystem Assessment and Restoration (CLEAR), NOAA Harmful Algal Bloom Operational Forecast System (HAB-OFS).

Human disease forecasting can be used as an important tool in understanding disease dynamics in water and on land and climatic factors controlling these dynamics. Skillful disease forecasting requires extensive spatial and temporal data. For instance, cholera predictions require climate data, which determine growth and/or spread of the pathogen and vectors. Satellite data can be used to analyze global scenarios of disease spreading in response to environmental degradation and climate change (6). Forecasting on a large scale and for predicting long term ecosystem changes will require expert judgement, analysis and assessment, in addition to numerical simulation and prediction. On a large scale, remotely sensed data by a series of Earth-observing satellites and field data can be combined to develop and test relationships between satellite based

observations, the field data and earth system processes, which will make possible ecosystem analysis. A large part of ecological forecasting includes mathematical modeling. Stochastic errors in the initial conditions can greatly affect model predictions as they will include large errors. Recently, the dynamics of infectious disease and epidemics are being studied by integrating information from laboratory experiments and field studies with mathematical models.

For example, the SEIR (S-fraction of susceptible individuals, E-fraction of exposed individuals, I-fraction of infective individuals, and R-fraction of recovered individuals) modeling framework is important in many models of infectious disease transmission dynamics. The SEIR modeling framework depicts the different states of the progression of the disease through a population. SEIR is a part of a larger modeling framework that is needed to fully represent the dynamic relationships among climate, the ecosystem and infectious diseases. The different types of modeling approaches used are classified as mechanistic models and empirical/statistic models. A mechanistic model makes use of theoretical knowledge of the underlying mechanism, i.e., mathematical equations are used to represent a process that can be universally applied to similar systems in different environments. A mechanistic model is considered to be dynamic because it includes quantitative interactions among multiple variables and feedback processes and allows for non-stationary and evolutionary behaviors. However, most of the present day process-based models do not consider the various kinds of adaptations or evolution in the factors that determine transmission or host response. Empirical/statistic models are based on observational studies; these models are based on relationships between the climate and disease-related variables. Empirical based studies on the past

patterns of variations will be used to project how the studied variables may change in the future. Empirical models can make use of simple indices of risk (e.g. identifying minimum temperature threshold for malaria transmission) up to multivariate models that make use of many environmental parameters affecting risk. Empirical models can be less data demanding than mechanistic models.

Models included in the studies of climate and infectious diseases must have the following features: 1) small number of parameters; 2) well understood dynamic behavior; 3) proper consideration of temporal and spatial scales; 4) incorporation of experimental data and expert opinion; and 5) demonstrable skill at prediction. Proper validation is critical for infectious disease models as they are complex and behave non-linearly. A cross validation procedure provides one means to test the goodness of prediction. Risk assessment studies also are an important part of infectious disease ecology. Risk assessment includes hazard identification, dose response, exposure assessment and quantitative risk characterization. Epidemiological surveillance must be employed to relate changes in disease incidence to environmental changes. Remote sensing devices can be used to monitor a wide variety of environmental parameters which are relevant to disease risk. Early warning systems are critical to mitigate potential harm and provide an opportunity to prevent hazardous events from occurring. Early warning systems for infectious disease can provide public health officials and the general public an advanced notice about the likelihood of disease outbreak in a particular location. Climate forecasts and ecological observations can be used to predict the appearance of the pathogen and allow opportunities to minimize the transmission. Even though epidemic based forecasts might not be that accurate, the information can be used to issue alerts to the public that

the environmental conditions are likely to lead to a disease outbreak, which can then induce intensive surveillance efforts of the area in question (72).

Ocean-Atmosphere models have evolved, based on the development of other Earth System component models. Earth system models consider the essential feedbacks between the physical climate system and the terrestrial and marine biogeochemistry and ecosystems. An Earth-System prediction must focus on quantitative forecasts for decision making. It is important that short term Earth-System predictions must focus on finer spatial scales as the faster time scale Earth System interactions and human responses occur. On the other hand longer time scale projections must consider a range of options for the integration of humans and their actions. Earth- System prediction frameworks must consist of linkages from climate to human health which include intermediate steps of microhabitat selection by the relevant microbes, transmission dynamics, hydrology, socioeconomics, and the need for research and adaptation measures. An example of Regional Earth System prediction is being carried out by researchers at the Earth System Science Interdisciplinary Center (<http://cbfs.umd.edu>) of the University of Maryland where dynamically downscaled seasonal to interannual climate forecasts and IPCC projections for the Chesapeake watershed with a regional atmosphere, watershed, and a regional ocean model are being generated. The projections (seasonal and interannual and decadal) include pathogens, harmful algal blooms, sea nettles, water and air quality, fisheries, dissolved oxygen, inundation, and storm surge. Using computational resources, models can be run at a scale of a few hundred meters and further downscaling can be accomplished down to a few meters which will lead to information which can be used for

human health, agriculture, transportation, energy, land use, air and water quality management and sustainable use of the Earth system (49).

A study done by Lobitz *et al.* (43) monitored remotely sensed data including ocean parameters which could provide early warning of conditions associated with cholera outbreaks. The remote sensed data included sea surface temperature (SST) and sea surface height (SSH) which was analyzed with the Cholera case data obtained in Bangladesh. The researchers discovered that the SST shows an annual cycle similar to the cholera case data. The SSH was correlated with cholera case data, as it is an indicator of incursion of plankton laden water inland. The SST data was acquired from the Advanced Very High Resolution Radiometer (AVHRR) sensor. The SSH measurements were derived from sea surface anomalies, which were derived from the difference between correlated altimeter measurements and three year mean ocean surface. The phytoplankton concentration was estimated from chlorophyll concentration which was generated by the Sea-Viewing Wide Field of View Sensor (SeaWiFS). Besides *Vibrio cholerae*, remotely sensed parameters were used for the prediction of *Vibrio parahaemolyticus* in the Gulf Coast oysters (59). The study archived remotely sensed measurements (SST, chlorophyll, turbidity) with data published on *V. parahemolyticus* in Alabama oysters. They found the predictions based on in situ data and satellite data agreed well with each other. The observed *V. parahemolyticus* densities were slightly higher than either of the predictions (in situ and remote sensed). Also the observed *V. parahaemolyticus* densities were more variable than the model predictions because only water temperature was used in the model predictions. Multiple regression analysis of $\log V_{para/g}$ against remote sensed SST and salinity showed both were significant. Effect of the salinity was seen to be

quadratic [Mean (log Vp/g) = -1.904 + 0.084 x RS_{SST} + 0.248 x Salinity – 0.006 x Salinity². The residuals (observed – predicted) observations were then used to analyze the effect of chlorophyll and turbidity. No significant correlation was seen between the residuals with RS (turbidity), but there was a significant correlation between residuals and RS (chlorophyll). Constantin de Magny *et al.* (9) carried out an analysis with the aim of developing a predictive model for cholera. Cholera outbreaks during 1998-2006 in Kolkata, India and Matlab, Bangladesh were recorded. Positive relationships were observed between the number of cholera cases and CHL anomaly (CHL_{ano}) and rainfall anomaly (PRE_{ano}). A quasi-Poisson model was generated for Kolkata and Matlab.

$$1) Y|\eta \sim P_o(\mu, \sigma^2)$$

$$2) \text{Log}(\mu) = \eta = \beta_0 + \beta_1 I_{MAM} + \beta_2 I_{JJA} + \beta_3 I_{SON} + \beta_4 \log(1+\text{chol}_{t-1}) + \beta_5 \text{CHL}_t + \beta_6 \text{CHL}_{t-1} + \beta_7 \text{CHL}_{t-2} + \beta_8 \text{SST}_t + \beta_9 \text{SST}_{t-1} + \beta_{10} \text{Rain}_t + \beta_{11} \text{Rain}_{t-1}.$$

In this equation, y is the observed counts, η is the fitted model, P_o represents the Poisson distribution, the β_j are the model parameters, and I_{MAM} I_{JJA} I_{SON} represents the quarterly mean of cholera case index for March-April-May, June-July-August, and September-October-November. Cross validation predictions were made in order to evaluate the models. The predicted cholera cases were generated using the fitted model and the cross validation model. When comparing the observed and predicted cases, the cross validation model underestimated the highest values of cholera cases than the fitted model. The environmental factors (SST, CHL and rainfall data) were statistically significant in the two geographical locations. The authors discuss that the high values of CHL_{ano} were due to phytoplankton blooms, which fueled the zooplankton populations

(carrier of *V. cholerae*). Heavy precipitation (high PRE_{ano}) could influence cholera transmission by feeding surface runoff into streams and rivers flood the water supply or cause increased river flow carrying rich nutrients which will then result in plankton blooms. The spatial resolutions of satellite datasets and finer temporal resolution is important to predict cholera outbreaks.

Constantin de Magny *et al.* (8) constructed a system which could predict the likelihood of the presence of *V. cholerae* in the surface water of the Chesapeake Bay. The system generated forecasts of the occurrence of the pathogenic *Vibrio* spp. The prediction was developed by using a multivariate empirical habitat model (see Equation 5 in Table 7 of Louis *et al.*, 2003), which estimated the probability of *V. cholerae* within a range of temperatures and salinities in the Bay. A study was conducted by Jacobs *et al.* (34) to predict the distribution of *V. vulnificus* in the Chesapeake Bay. The surface water samples were collected from the mainstem Chesapeake Bay during the months of July and October, 2007, and April, July, and October of 2008. The researchers found majority of the positive observations were at water temperatures >25°C and within a relative narrow salinity range (i.e. at 8.6 and 20 ppt.) (see Figures 10 A and B). The authors used the median salinity (SAL_{opt}) which was 11.5 ppt. The model generated R² values for temperature and salinity to be 0.70 and 0.94, respectively. The final regression model generated an equation which related the Logit (*Vvulnificus*) to temperature and SAL_{opt}, the interaction between temperature and salinity was not being significant. Hence this study generated an empirical model and predicted the distribution of *V. vulnificus* in the Chesapeake Bay. The model was able to classify *V. vulnificus* presence 93% of the time when only temperature and distance from optimal salinity was used. Hence as discussed

above, modeling and forecasting approaches will be of great assistance in meeting the challenges of identifying and predicting the impacts of pathogens on human health. Linking sources to human health requires the ability to predict the concentrations and pathogenicity, identify appropriate space and time scales over which to measure and model, and integrate model predictions with assessment of human health risk and management strategies.

The objective of my thesis was to develop daily hindcasts (1991 to 2005) of the probability of *V. vulnificus* occurrence in the Chesapeake Bay. Based on the results of the hindcasts, we will be able to find where in the Bay is the maximum likelihood of occurrence of *V. vulnificus*. Furthermore the hindcast study will help us to categorize the presence of *V. vulnificus* to temperature and salinity. The system that was developed in this study generates predictions of the likelihood of *V. vulnificus* in the Chesapeake Bay by exploiting environmental parameters that govern the distribution of *V. vulnificus*. Using this prediction system, geographic locations in the Chesapeake Bay where environmental conditions coincide with the preferred physical habitat of *V. vulnificus* were identified (34). This approach was used previously to predict the likelihood of *V. cholerae* in the Chesapeake Bay (8).

2.2 Materials and Methods

2.2.1 *Vibrio vulnificus* empirical habitat suitability model:

The logistic regression equation used for this study was taken from a previous study done by Jacobs *et al.* (34), who used surface water samples (2007 -2008) from the Chesapeake Bay mainstream. Since the Chesapeake Bay Ecological Prediction System generates only temperature and salinity, just these two variables were evaluated for the development of the empirical model. The logit model for *V. vulnificus* was derived from data gathered using Quantitative PCR (qPCR). The logistic regression used temperature, salinity, and interaction terms. The authors reported that since the prevalence data was not normally distributed (Kolmogorov-smirnov, D=0.187, p<0.01), the median salinity, 11.5 ppt was used as optimum salinity. The SALopt was calculated as the absolute value of (salinity-11.5). The empirical model used in our study is as follows:

$$\text{Log } it \text{ (Vvulni)} = -7.867 + 0.316 \times T - 0.342 \times \text{SALopt}$$

The probability of *V. vulnificus* presence from the model was estimated using $p = \frac{\text{elogit}}{1 + \text{elogit}}$, where log *it* refers to the Log *it* used in the model. Jacob *et al.* (2010) reported that the logistic regression resulted in a concordance of 94.2% (n=235). Since the interaction term between temperature and salinity was not significant (p>0.05), this term was excluded from the model. ChesROMS (Chesapeake Bay Regional Ocean Modeling System; Constantin de Magny *et al.*, 2009) was used to force the simulated SST and sea surface salinity into the habitat suitability model.

2.2.2 Chesapeake Bay Regional Ocean Modeling System (ChesROMS):

ChesROMS is an ocean modeling system for the Chesapeake Bay region which was developed by scientists at NOAA, the University of Maryland, Chesapeake Research Consortium (CRC), and Maryland Department of Natural Resources (MD-DNR) supported by the NOAA Monitoring and Event Response for Harmful Algal Blooms (MERHAB) program. The model was developed based on the Rutgers Regional Ocean Modeling System (ROMS, <http://www.myroms.org/>). The model was developed to provide a community modeling system for nowcasts and forecasts of 3D hydrodynamic circulation, temperature and salinity, sediment transport, biogeochemical and ecosystem states with applications to the ecosystem and human health in the Bay. ChesROMS model has been tested using historical data inputs and has found to accurately simulate the actual conditions from 1991 to 2005.

ChesROMS (v1.2) consists of a 150 x 100 cell horizontal grid and 20 layers vertically, which yields a spatial resolution in the horizontal that ranges from 500 m to 5 km and in the vertical ranging from 0.2 to 1.5 m.

(<http://ches.communitymodeling.org/models/ChesROMS/index.php>).

ChesROMS, the prediction system comprises a suite of Unix Shell scripts, Perl scripts, Fortran and C Programs, NCL programs, MATLAB scripts, and GIS shape files that automatically perform the tasks of compiling the model input files from

observations, running the model, processing the model output, and displaying the graphical products on a dynamic, interactive website (8).

2.2.3 Model retrospective predictions:

The prediction system used MATLAB scripts (see Appendix) to generate daily hindcasts of *V. vulnificus* probability (Vvulni) for a 15-year period from 1991 to 2005. Script 1 (Appendix) was used to calculate the *V. vulnificus* probability based on the Jacobs *et al.* (34) model. The script generates a data set (matlab file) which consists of the *V. vulnificus* (1991-2005) probability. Using the data set generated from Script 1, we used Script 2 which generates a plot of the yearly mean of *V. vulnificus* in the Bay. To further evaluate the influence of SST and surface salinity on the distribution of *V. vulnificus*, we used Script 3, which generates the sum of probability and the mean probability (individual year) of *V. vulnificus*, the SST, and salinity for the entire bay. This script can be used to analyze individual years, as well as multiple years, which helps examine seasonal and interannual variability of the likely presence of *V. vulnificus* in the Bay and compare with the SST and salinity prediction.

For each year, Script 3 takes the average of the three most likely locations where *V. vulnificus* probability is high in order to produce a time series for that area. The difference between the individual cells within the area and the area average is saved as a set of random variables to calculate the variance and standard deviation, which is a measure of the variability within the area. The plot generated contains the curve for average time series, with standard deviation as the upper and lower bound envelopes. The Script 3 then puts together the area average and standard deviation of *V. vulnificus* probability, SST, and salinity for each year, coming up with a long time series. We then

used the results generated from Script 3 and pinpointed the hotspots of predicted *V. vulnificus* presence in the Chesapeake Bay. Script 4 was written to generate mean probability (individual and multi year) of *V. vulnificus* for the hotspots. Script 4 was executed to generate plots of seasonal and interannual variability of SST and salinity over the selected hotspots. Furthermore, we went to select areas which showed low probability of *V. vulnificus*, i.e. areas other than the hotspots.

Script 5 was used to generate plots of seasonal and interannual variability of the mean probability of *V. vulnificus* and the variability in the SST and salinity over the “Alternate Areas”. Nine tidal constituents from the Advanced Circulation Model for the Coastal Hydrodynamics (ADCIRC) model and non-tidal water levels were combined to provide boundary sea surface height change to the model. The non-tidal water level data were retrieved from the NOAA National Ocean Service webpage which contains the non-tidal water level data. The webpage provides historical and real-time data observed by monitoring stations located at Wachapreague, Virginia, and Duck, North Carolina. The Chapman condition for surface elevation and the Flather condition for barotropic velocity were applied to the barotropic component (depth-averaged, fast propagating surface wave mode) at the open-ocean boundary. For the baroclinic component, radiation condition was used for velocity and radiation condition with nudging for temperature and salinity. The United States Geological Survey (USGS) stream water monitoring website provides the daily freshwater discharge data for the nine tributaries. Monthly climatological temperature and salinity from the World Ocean Atlas (WOA, 2001) database were used, with a nudging technique to prescribe temperature and salinity changes at the mouth of the Chesapeake Bay. Atmospheric forcing, including 3-hourly winds, net shortwave and

downward longwave radiation, air temperature, relative humidity, and atmospheric pressure were obtained from the North American Regional Reanalysis (NARR) produced at NCEP (8).

2.3 Results:

Daily Hindcasts, using the Jacob *et al.* (34) model, of the likelihood of *V. vulnificus* from 1991 to 2005 over the Chesapeake Bay were generated. Figure 11 shows the *V. vulnificus* mean probability for the year 1991. The color scale represents the probabilities which recorded as highest (0.25;Red) and lowest (0;Blue). Figure 12 shows the mean probability during transition between 1996 (wet year) to 1999 (dry year). During the dry year of 1999, *V. vulnificus* probabilities were located mostly northwards i.e. upper bay and west estuaries which that would increase the chances of human contact with the pathogen. Whereas for 1996, a wet year the *V. vulnificus* probabilities shifted southwards. Based on the plot of *V. vulnificus* mean probability for 1991 (Figure 11), the three hotspots (Figure 13 A) which showed the highest probabilities were identified as the Upper Bay (color Magenta), (Chester River, Choptank River), Mid Bay, (color Red) and the West Estuaries (color Green) (Potomac, Rappahanock, York, and James River).

In Figure 13, it can be seen that high probabilities occur in the three hotspots between May and October. There is a gradual increase in the mean probabilities of *V. vulnificus* during the beginning of summer, peaking in July and August and decreasing after October. The maximum mean probability of *V. vulnificus* in 1991 is at 0.2. In all three hotspots the pattern of mean probabilities of *V. vulnificus* was similar between July and October. Dramatic differences in the patterns were not observed between the three regions because the hotspots selected included a broader area, i.e., the whole of the upper bay, mid bay and west estuaries and not specific sites. From Figure 13, a lot of variance can be seen in the data (as the standard deviation is very high), which might be due to the

hotspots we selected which were spread over a broader area. The patterns of the predicted *V. vulnificus* probability observed in 1991 is due to the variations of Sea Surface Temperature (SST) and Salinity.

The pattern of SST and salinity for the year 1991 at the three hotspots are presented in Figure 14. The patterns of SST are similar among all the three regions, with a minimum observed in February, a progressive and regular increase through the summer months of July and August, followed by a decrease in September. Mean predicted salinity also followed a similar pattern in all the three regions, gradually increasing from a low in April to high in October. The maximum salinities recorded in the three regions, i.e., the Upper Bay, Mid-Bay and Western Estuaries were ca. 17 ppt, 20 ppt and 15 ppt respectively. Differences in patterns of salinity around the optimal salinity were observed in the three regions. In the upper bay area, the salinity was around the optimal salinity of 11.5 psu, as recorded by Jacobs *et al.* (34) during the months of July and August, which coincided with maximum mean probabilities of *V. vulnificus* in that region. In the mid-Bay area the salinity was slightly higher than the optimal salinity, whereas in the western estuaries the salinity followed a similar pattern as in the upper bay area. In summary, the predicted likelihood of *V. vulnificus* follows closely the patterns of SST but is significantly influenced by the optimal salinity in the three “hotspots” during July and August. On considering the Upper Bay, during January to April, the salinity anomalies were close to optimal salinity (11.5) and the SST was lower than 10°C, in spite of the salinities being close to optimal salinity during this time no probabilities of *V. vulnificus* were observed in the Upper Bay (Figure 13 B).

The transition of the probabilities of *V. vulnificus* from the wet year (1996) to a dry year (1999) is shown in Figure 15. The presence of high mean probabilities is obvious over the three hotspots during a wet year (1996), compared to a dry year (1999). Compared with wet (1996) and dry (1999) years (Figure 16), the salinity in 1996 was close to the SALopt in the Mid-Bay region and during 1999 the salinity was close to the SALopt in the Upper Bay. Hence we see the southward shift during 1996 and northward shift during 1999. The SST however, during 1996 and 1999 followed the same pattern at the three hotspots. The freshwater discharge from the Susquehanna River is an important driver in the dynamics of *V. vulnificus* during 1996 and 1999. Figure 17 shows the inter-annual variability in the hindcasts of daily area mean *V. vulnificus* likelihood between 1991 & 2005 for the three hotspots. The Mid-Bay region experienced large swings in average *V. vulnificus* probabilities between wet and dry years, i.e., the wet years showed higher probabilities than the dry years.

The “Alternate Areas” were selected as the top of the upper Bay and the bottom Bay. Figure 18 depicts inter-annual variability in the likelihood of *V. vulnificus* occurrence over the “Alternate Areas” for the year 1991. From Figure 19 A and B It can be seen that the low average probabilities of *V. vulnificus* (A) from 1991 to 2005 was due to the very low (<11.5 ppt) and very high (>11.5 ppt) salinities in the areas at the top of the upper Bay and bottom Bay respectively (B).

2.4 Discussion:

Daily hindcasts of *V. vulnificus* from 1991 to 2005 demonstrated a very interesting distribution of the pathogen over the Bay. *V. vulnificus* was found to be concentrated in the regions of the Mid-Bay, Upper Bay and West Estuaries. From the Figures 13 and 14, it can be seen that the reason for high probabilities at the three hotspots was due to the salinity and SST i.e. the maximum probabilities of *V. vulnificus* was only when the salinity was close to SALopt (11.5) and SST ($>20^{\circ}\text{C}$). At the three hotspots *V. vulnificus* was observed only between May to October. We conclude that the spatial patterns of *V. vulnificus* in the Chesapeake Bay are controlled by the salinity and the temporal pattern of *V. vulnificus* is controlled by SST.

Furthermore, when we compared wet (1996) and dry years (1999), it was found that during 1996 high probabilities of *V. vulnificus* were observed over the Mid-Bay, while in 1999 the region of high probabilities of *V. vulnificus* shifted northwards and was located mostly in the Upper Bay. Referring to Figure 16, during 1996 the Mid-Bay exhibited salinity close to SALopt and therefore had a high likelihood of occurrence in the Mid-Bay region. On the contrary, during 1999 the salinity levels were close to SALopt in the Upper Bay and upper parts of the Western Estuaries. Hence, we conclude that a strong association exists between *V. vulnificus* and the salinity profiles during wet and dry years.

A study by Kimmel *et al.* (39) found that salinity in the Upper Bay during 1996 was 5.89 psu and during 1999 it was 11.0 psu. In the Mid-Bay during 1996 the salinity was 13.77 psu and during 1999 it was 18.21 psu. Our study supports their observations of the conditions

in 1996 and 1999. The salinity distribution in the Bay during 1996 was characterized by high fresh water input in January and an above average freshwater input during July. The result was low salinity and temperature in the Upper and Mid-Bay during 1996 into April of 1997. A drought period was observed during 1999, where below average freshwater input was observed, as expected. Hence, salinity and temperature during the dry period were much higher in the Bay. Referring to Figure 17 (inter-annual variability of mean probabilities of *V. vulnificus*), most of the variability among different years is observed in the Mid-Bay. Figures 18 and 19 show there is further support for the conclusion that salinity is important in determining the mean probabilities of *V. vulnificus*. The “Alternate Areas” at the top of the Upper Bay and Bottom Bay exhibited salinities distant from the SALopt, i.e., at the top of the Upper Bay, it was very low and at the bottom of the Bay it was very high, with the result that the mean probabilities of *V. vulnificus* over these areas was very low.

Constantin de Magny *et al.* (8) found that the probability of *V. cholerae* was mostly located at the outflow of the Susquehanna River and in the upper reaches of the Potomac, Rappahanock, York, and James rivers on the west side of the Bay and the Choptank River in the east side. They observed variance in the predicted salinities were much larger than SST in all regions. In the study, which results confirm, they found differences in the salinity profiles at the three “hotspots” (Susquehanna, West Estuaries and Choptank). The “hotspots” were different from those in this study because of the differences in empirical habitat models. Constantin de Magny *et al.* (8) used a significant interaction term (temperature x salinity) but Jacob *et al.* (34) found this interaction term to be insignificant. Also, instead of using the salinity directly, Jacob *et al.* used the SALopt, an absolute value calculated as salinity -11.5.

In a previous study in the Chesapeake Bay carried out by Wright *et al.* (69), *V. vulnificus* was not detected in any samples during February and March, when the water temperature was <8°C. Their results are in accordance with ours, where we found *V. vulnificus* probabilities to be too low from November to March, when the temperature was <10°C. Lipp *et al.* (41) in a Charlotte Harbor study found a positive correlation with salinities <15 ppt and negative correlation with salinities >15 ppt. Similarly in this study an increase in *V. vulnificus* probability was found only when the salinity was close to 11.5 ppt (May to October) and low probabilities were observed when salinities were significantly above the optimal salinity after November, thereby indicating a negative correlation. In conclusion, the results of our study demonstrate the probability of occurrence of *V. vulnificus* at the three “Hotspots” suggest the spatial patterns of *V. vulnificus* is governed by salinity and the temporal patterns of *V. vulnificus* is governed by sea surface temperature. Hence, by using the empirical model of Jacob *et al.* and the ChesROMS hydrodynamic model, we were able to predict the likelihood of *V. vulnificus* in the Chesapeake Bay.

How can Climate Change influence be linked to the distribution of *V. vulnificus* in the Chesapeake Bay? It is known that, the likelihood of *V. vulnificus* with temperature and salinity is particularly important in the context of climate change. As reported by Boesch (4), observations of Chesapeake Bay water temperatures from the 1940’s show an increasing trend of 0.4°F per decade, of which much of the increase has occurred during the past 30 years. Najjar *et al.* (50) reported water temperatures in the Bay during the 1990’s were ca. 1°C warmer than during the 1960’s. Studies have predicted a positive correlation between water temperature in the Bay and regional atmospheric and oceanic temperature. The six scenarios (A1B, A1T, A1F1, A2, B1, B2) considered by Najjar *et al.* (50) indicate that a 3 to

6°C warming is likely to occur by 2070 to 2099. A report by US Climate Change Science Program (Boesch, 2008) concluded that extreme precipitation episodes have become more frequent and intense in recent decades over most parts of North America. Heavy rainfall, intense tropical storms, and hurricanes will directly influence the probability of contact between pathogenic bacterial populations in the Bay and human populations. Most of the inter-annual variability in the streamflow into the Bay is driven by precipitation and seasonality of stream-flow to the Chesapeake Bay is important since it helps in regulating the timing of spring phytoplankton blooms, which in turn, dictates zooplankton dynamics. As demonstrated in previous studies in the Chesapeake Bay *Vibrio spp.* are associated with zooplankton with respect to spring and winter precipitation, the consensus among different models indicates an increase in the January-May outflow of the Susquehanna River Flow an increased Susquehanna River discharge will further dictate salinity profiles of the mainstem of the Bay. Gibson and Najjar (19) estimated a 10% change in the annual Susquehanna River flow would result in a change in annual mean salinity of ~ 1, 4 and 7% in the lower, middle and upper mainstem Bay. They predicted the highest flow scenario (32% increase) would result in isohalines of the Bay receding by approximately 6.3 km near the mouth of the Susquehanna River and to as much as 55 km near the middle of the Bay. The maximum change would occur in the central Bay, ~-0.6 for 10% increased flow. By the end of the 21st century, projected flow changes of -40 to +30% will result in an annual mean salinity in the Central Bay changed by as much as 2 in either direction. Decreased salinities can, thereby, increase the dissolved oxygen concentration which could influence bacterial presence in the surface water. Salinity patterns in the main-stem of the Bay and the April-September average stratification in the mid Bay are strongly correlated with the January-May average

Susquehanna River flow. A likely increase in Susquehanna River flow in the future will increase summer stratification.

While the Global mean sea surface height has increased at a rate of 1.8 ± 0.3 mm/ yr over the second half of the 20th century, in the Chesapeake the rates range from 2.7 to 4.5 mm/ yr (50). The projected rise throughout the Bay has been estimated to be approximately 10 inches by 2030 and up to 25 inches by 2100 (Najjar *et al.*, 2009). The Intergovernmental Panel on Climate Change (IPCC), has projected a global sea level rise of 7 to 15 inches under the low emission scenario and 9 to 20 inches under high emissions (4). Hilton *et al.* (28) attempted to test if the sea level rise over the second half of the 20th century caused a detectable increase in the salinity of the Chesapeake Bay and found the residual salinity between 1949 and 2006 exhibited a statistically significant linear trend. The salinity change estimated over the period varied from -2.0 to 2.2. The mean salinity change in the mainstem Bay was ca. 0.8, which, according to the model simulations, was explained by the sea level rise. The Chesapeake has a large salinity gradient, oligohaline in the upper estuary, mesohaline in the mid bay, and polyhaline in the lower bay. Sea level rise will cause a salt water intrusion, thereby shifting the salinity gradient upward, i.e., the upper bay may begin to exhibit mesohaline conditions. This would affect the probability of *Vibrio* pathogens reaching the Upper Bay since increased river flow and the increase in sea level would have a significant effect on the temperature and salinity patterns.

Besides its effect on salinity, temperature, river flow, sea level rise and precipitation, climate change has the potential to alter Bay phytoplankton species composition with changes in precipitation patterns and intensity of storms. An increase in winter and spring precipitation will result in nutrient loading which, in turn, will cause an increase in

phytoplankton production. Increased storms overland will result in discharge of nutrients, resulting in short term stratification and increased occurrence of algal blooms. Hsieh *et al.* (32) found that the number of *Vibrios* attached to phytoplankton increased with phytoplankton concentration. Therefore, climate induced increases in harmful algal blooms may increase the human health threat, either directly or by fueling pathogen (*Vibrio spp.*) growth with the bloom-derived organic matter (50).

Climate events like the El-Niño Southern Oscillation (ENSO), the North Atlantic Oscillation (NAO) and the Pacific Decadal Oscillation (PDO) have been shown to be associated with the occurrence of major outbreaks of *Vibrio* infections. The persistent ENSO event in the tropical Pacific from 1990 to June 1995 was coincidental to the Cholera Outbreak in Peru (7). A *V. parahaemolyticus* epidemic in 1997 in South America was shown to be linked to the 1997-98 ENSO episode (44). Cholera outbreaks in Bangladesh are related to the ENSO which occurs on an interannual frequency (42). In general the *Vibrio* diseases in the US have been increasing since the 1997-98 ENSO. (71).

Extreme events are also associated with the increased occurrence of *Vibrio vulnificus* infections. Hurricane Katrina, which made landfall on August 29, 2005, had a major impact on the US Gulf Coast. Surveillance data identified 22 new cases of *Vibrio* illnesses caused by *V. vulnificus*, *V. parahaemolyticus*, and non-toxigenic *V. cholerae*. Among the 22 cases reported, 18 were wound associated *Vibrio* infections. Of these 18 cases, 14 (82%) were caused by *V. vulnificus* and 3 (18%) by *V. parahaemolyticus*. Five patients (28%) with wound associated *Vibrio* infections died. The results indicate that the *Vibrio* related wound infections can result from post-hurricane exposure of wounds to the flood waters (71). A major outbreak of systemic *V. vulnificus* infections which occurred in 1996 among Israeli

fish market workers was linked to climate change by Paz *et al.* (56) who found the summers of 1996 to 1998 to be the hottest in the previous 40 years. They analyzed a time series of monthly minimum, maximum, and mean temperature which showed significant increase in summer temperatures during the 18 year period, with highest mean temperature in the summer of 1996. Lag correlation analysis revealed significant correlations between temperature values and hospitalization dates. Wetz *et al.* (67) conducted a study which included measurement of concentrations of *V. vulnificus* during extreme weather events that occurred in North Carolina during Hurricane Ophelia and Tropical Storm Ernesto. The total *Vibrio spp.* and *V. vulnificus* concentrations were an order of magnitude higher during the Tropical Storm Ernesto than Hurricane Ophelia, with Tropical Storm Ernesto preceded by Southerly Winds, after which mixing due to Storm-induced northeasterly winds introduced sediment, resulting in a more pronounced change in *Vibrio spp.* concentration during the Tropical Storm.

Future work will be to develop forecasts (days to seasons) by applying the habitat suitability model with forecasted SST and salinity generated by CBFS (<http://cbfs.umd.edu>). By developing models and forecasts of the occurrence of a pathogen in a particular location, a valuable means to test our understanding of the linkages between climate, ecosystems and infectious diseases will be provided. Long term forecasts of *V. vulnificus* will be useful for monitoring the potential impacts of climate change events on *V. vulnificus* populations, which will assist public health officials in taking precautionary measures against the threat of *V. vulnificus*. However, validation of the forecasts will be required for public health application and is, therefore, the next and most important step in developing a forecast system. Since the model in this study used surface water, in the future it would be interesting

to develop models using middle and bottom water, sediments and oyster samples, since previous studies indicated a strong association of *V. vulnificus* with sediment and oyster. Most *V. vulnificus* infections in the Chesapeake Bay are wound infections or gastroenteritis from consumption of raw contaminated seafood. Hence prediction systems based on the probability of occurrence of *V. vulnificus* in sediment and oysters will be very useful. An additional implication of this study and those done by Constantin de Magny *et al.* (2009) and Jacob *et al.* (2010), is the ability to develop a prediction system for *V. parahaemolyticus*. *V. parahaemolyticus* can cause wound infections and gastroenteritis from ingestion of raw or undercooked seafood contaminated with this pathogen. Hence application of this type of prediction system to different geographical locations, given sufficient relevant data for the area of interest, will be highly useful to the local population.

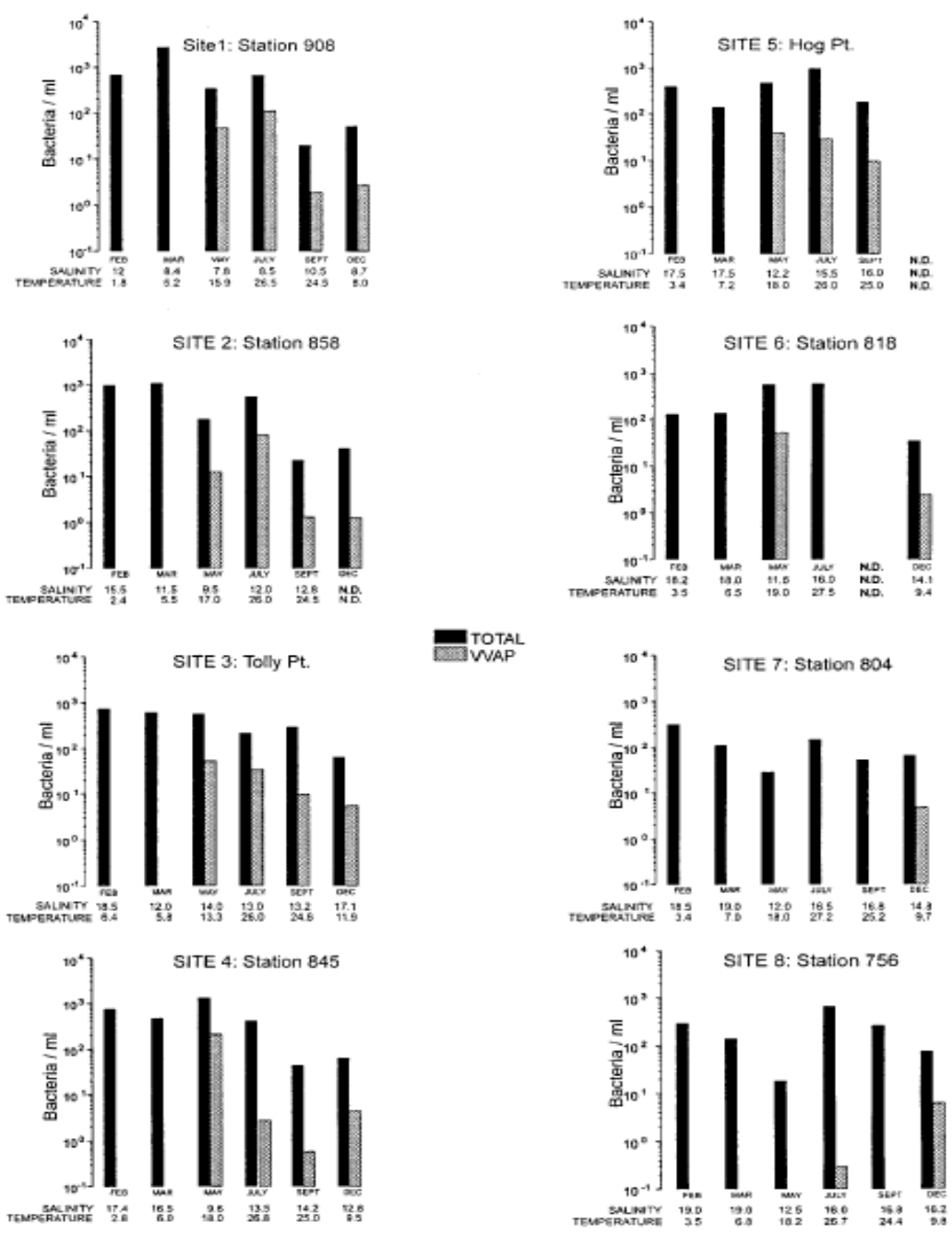


Figure 6: *V. vulnificus* (VVAP) and total bacterial populations (total) enumerated in seawater samples (69).

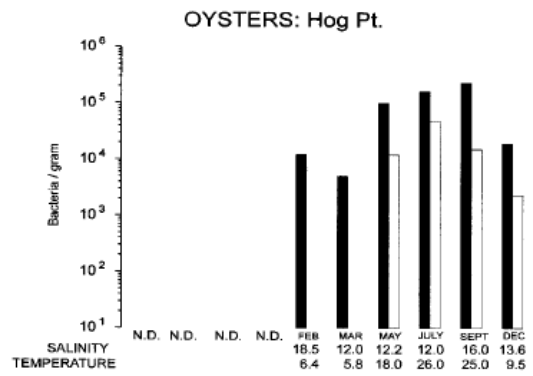
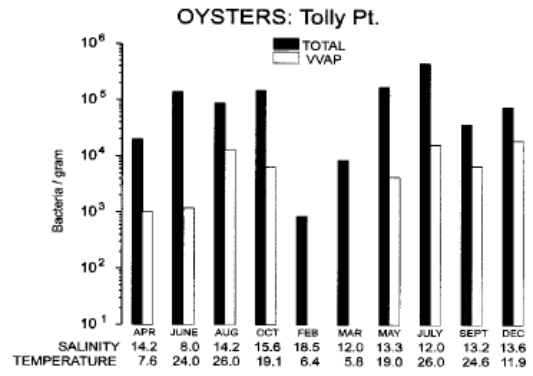


Figure 7: *V. vulnificus* and total bacteria enumerated in oysters (69).

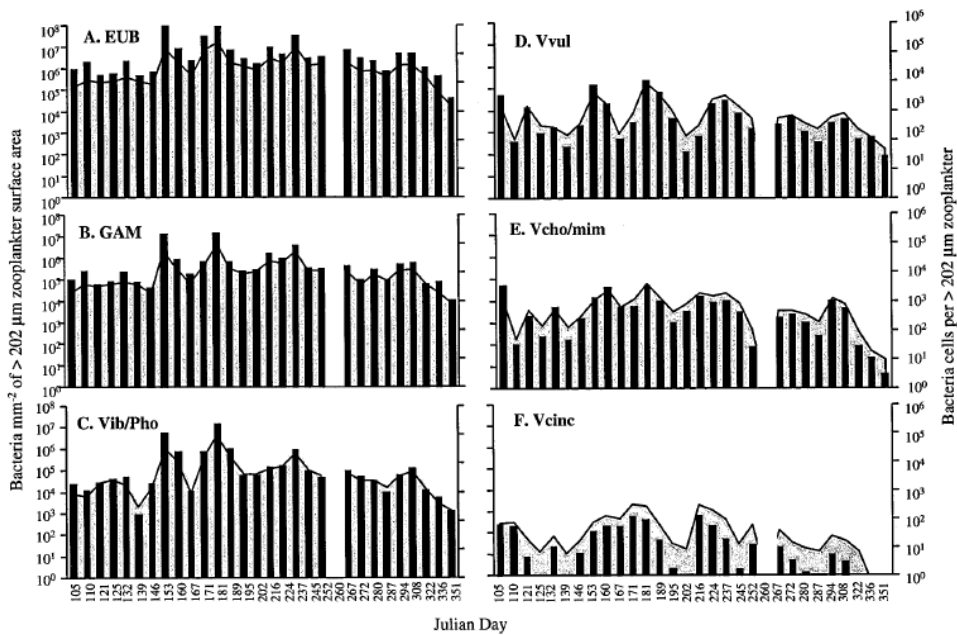


Figure 8: Graph showing the number of bacteria associated with >202 μm zooplankton per cubic meter of Chester River Water. EUB, *Bacteria*; GAM, *γ-Proteobacterium*; Vib/Pho, *Vibrio-Photobacterium*; Vvul, *V. vulnificus*; Vchol/mim, *V. cholerae-V. mimicus*; Vcinc, *V. cincinnatiensis*. The shaded areas represent the number of cells per square millimeter of surface area and the bars represent the number of cells per zooplankter (25).

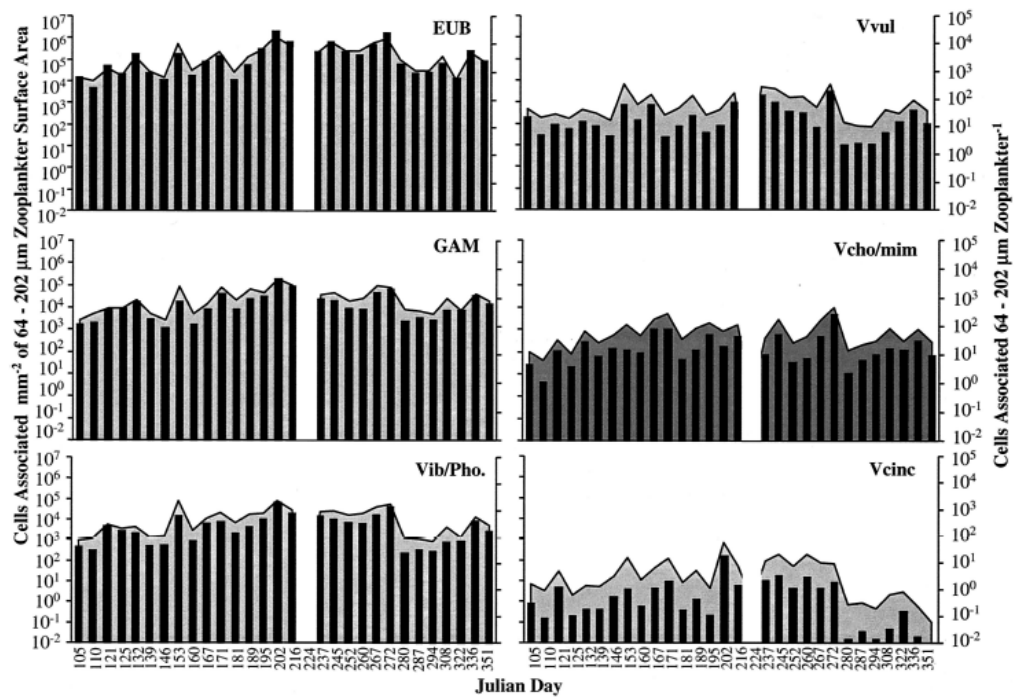


Figure 9: Bacterial cells associated with 64- to 202 μm zooplankton per cubic meter of Chester River water (25).

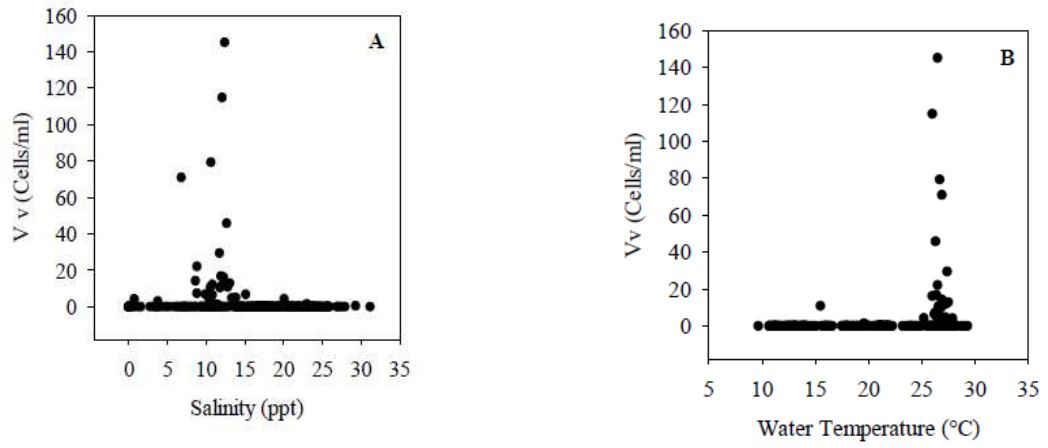


Figure 10: *V. vulnificus* abundance plotted against surface salinity (A) and Water Temperature (B) over the study period in Chesapeake Bay (34).

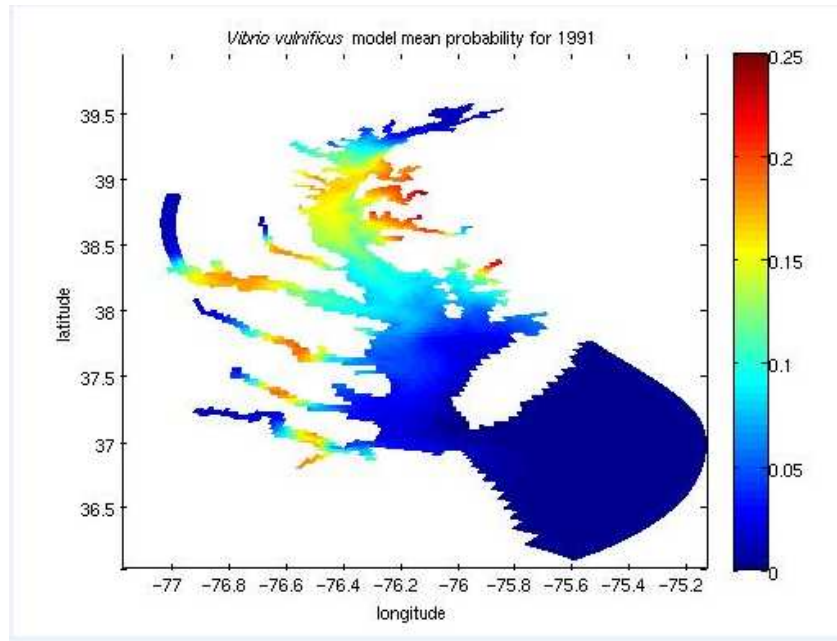


Figure 11: Predicted hindcast depicting the mean probability of *Vibrio vulnificus* during 1991. Color scale represents the probability of occurrence, with red=high (25%) and blue=low (0%).

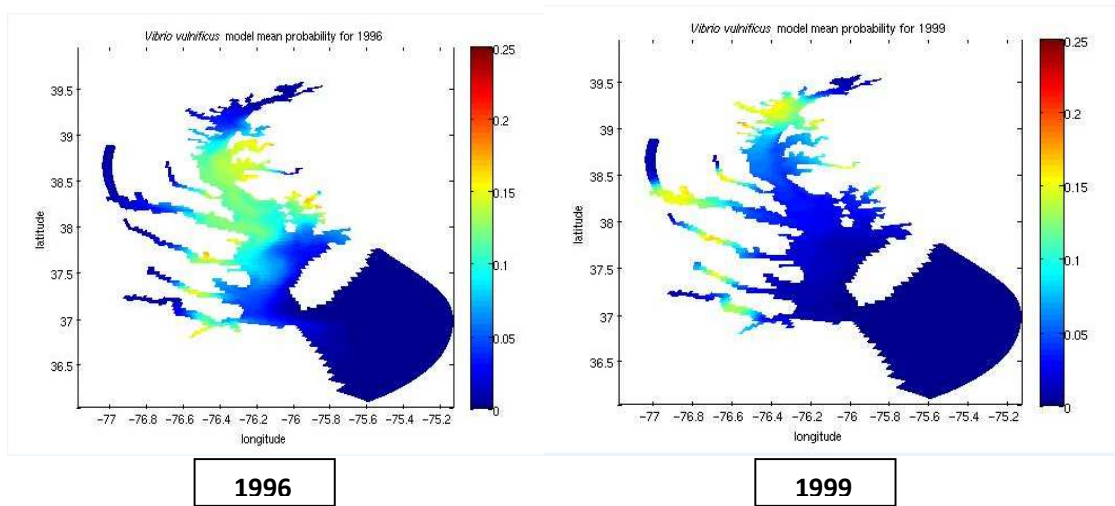


Figure 12: Hindcast depicting probability of occurrence of *V. vulnificus* in wet (1996) and dry years (1999). Color scale represents mean probability of occurrence with red high (25%) and blue low (0%).

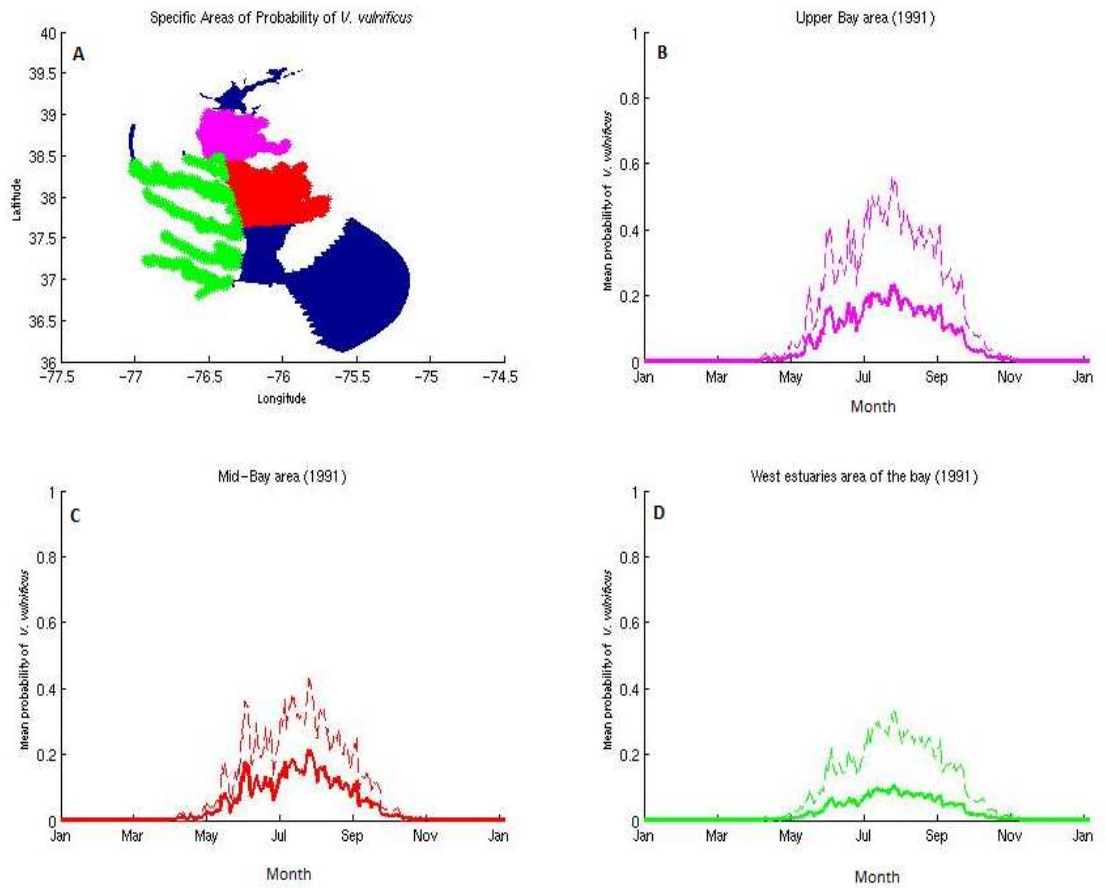


Figure 13: A) Specific Locations where the annual sum of *V. vulnificus* probabilities in 1991 was recorded as maximum. B) Plot of mean probability of *V. vulnificus* over the Upper Bay. C) Mid Bay D) Western Estuaries. The Bold line represents the mean and the dotted line is the (+) standard deviation.

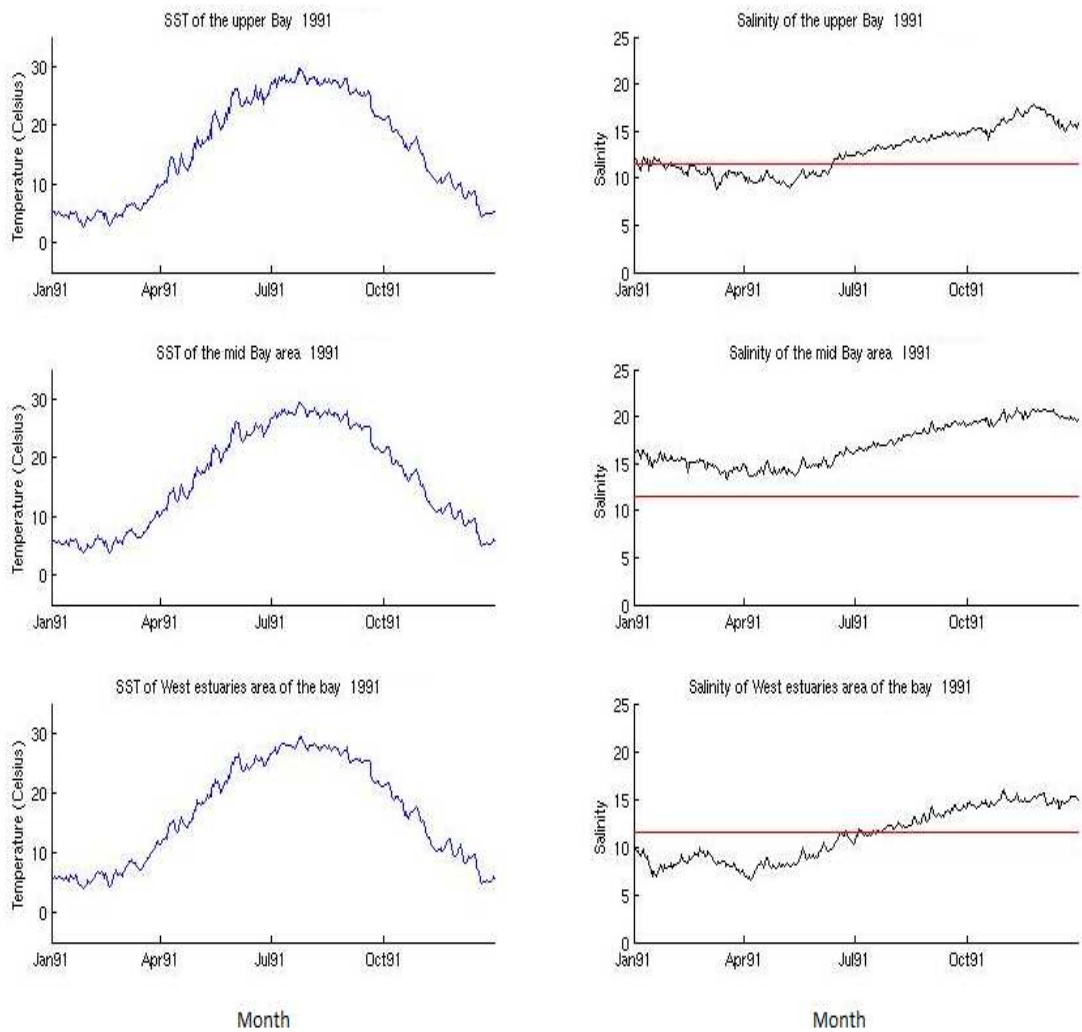


Figure 14: Daily mean plots of simulated sea surface temperature and salinity from the hydrodynamic model (ROMS) for the Upper Bay (top panel), Mid Bay (middle), and West Estuaries (bottom panel) for the year 1991. Red horizontal line indicates the optimal salinity (11.5 ppt) as recorded by Jacobs *et al.*

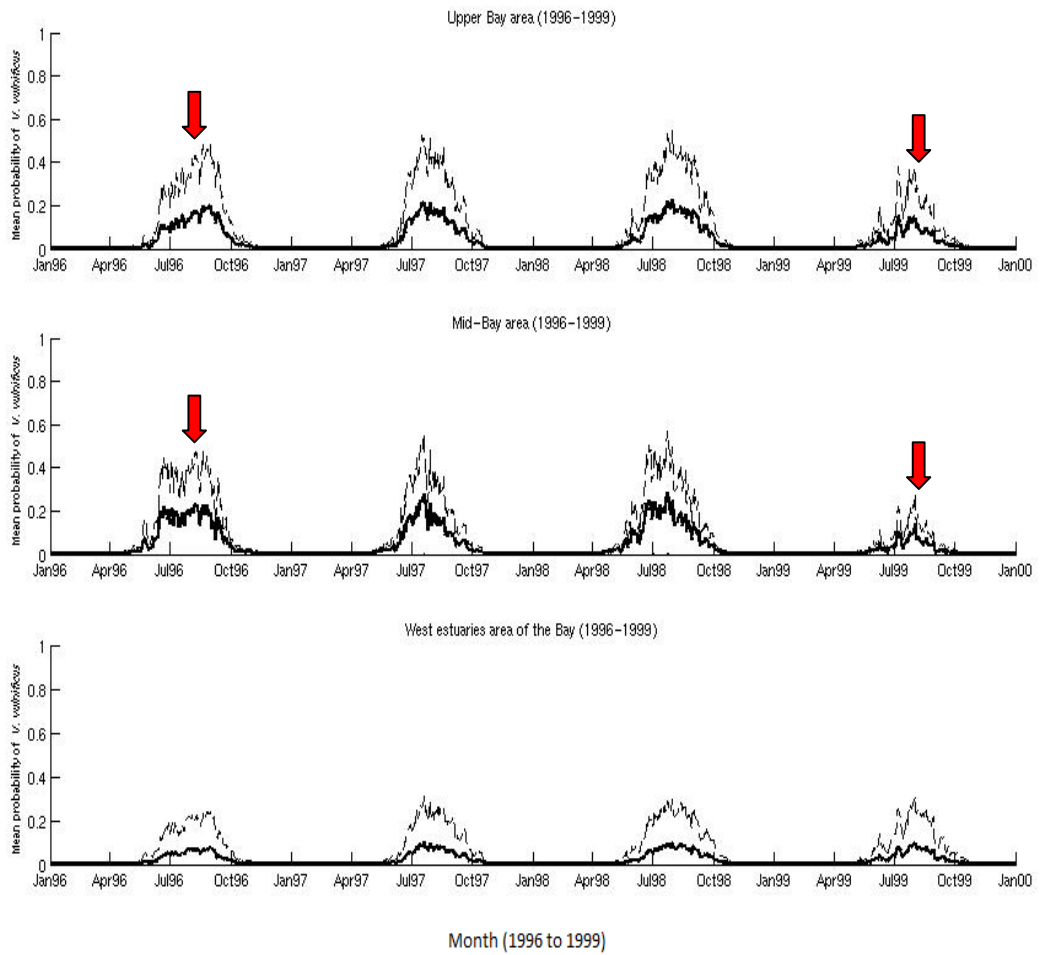


Figure 15: Comparison between the annual mean probabilities of *V. vulnificus* for the wet year (1996) and dry year (1999). Arrows indicate high occurrence of *V. vulnificus* in 1996 and low occurrence of *V. vulnificus* in 1999 in the Mid Bay.

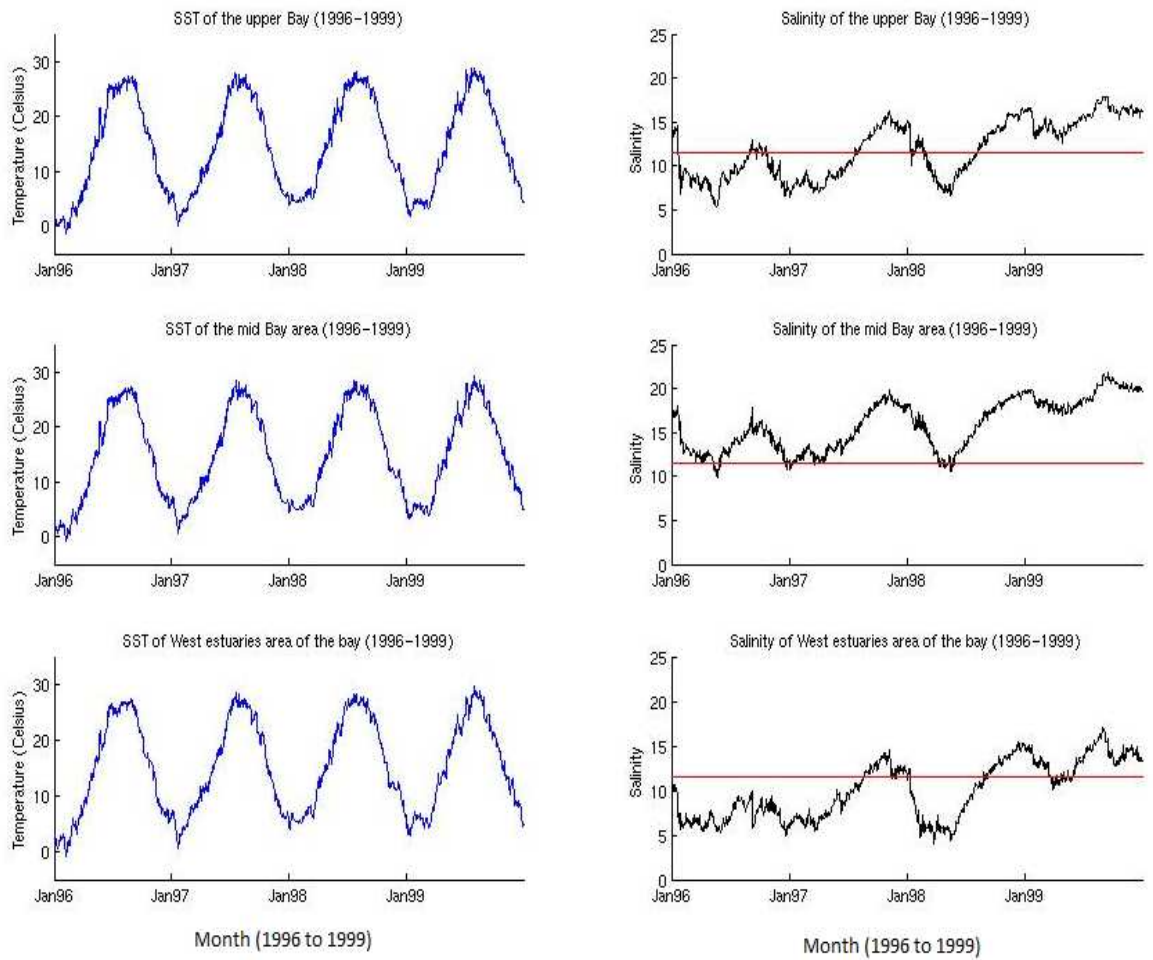


Figure 16 Daily mean simulated sea surface temperature and salinity from the hydrodynamic model (ROMS) for the Upper Bay (top panel), Mid Bay (middle), and West Estuaries (bottom panel) for the years from 1996 to 1999. Red Horizontal line represents the optimal salinity (11.5 ppt) as recorded by Jacobs *et al.* (2010).

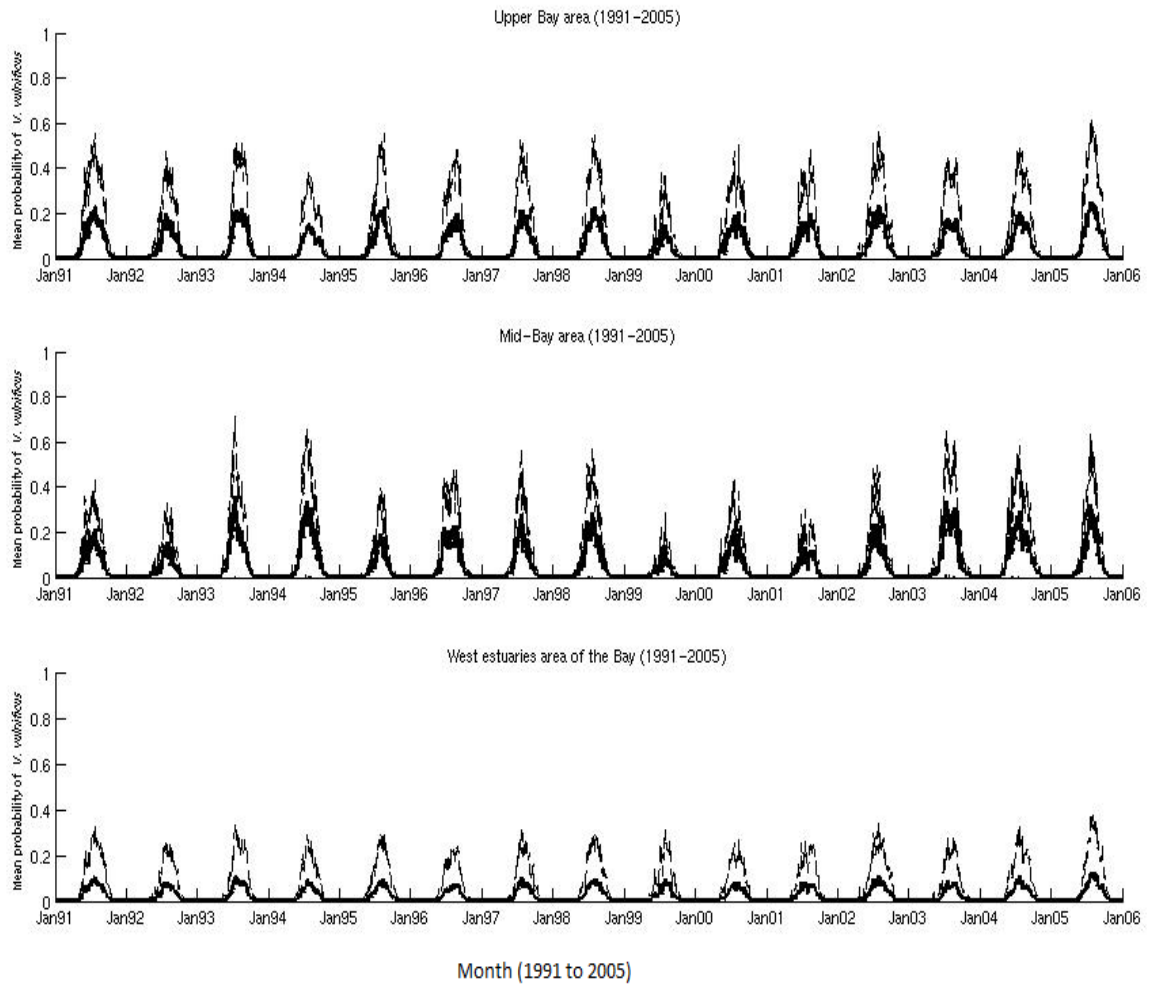


Figure 17: Daily mean (solid bold line) and + standard deviation (line) of predicted *V. vulnificus* presence from 1991 to 2005 in the Upper Bay area (top panel), Mid-Bay area (middle) and West estuaries area of the Bay (bottom panel).

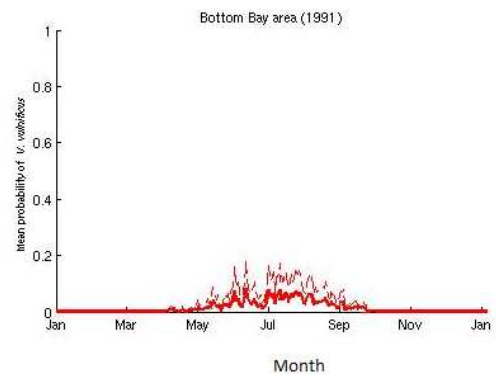
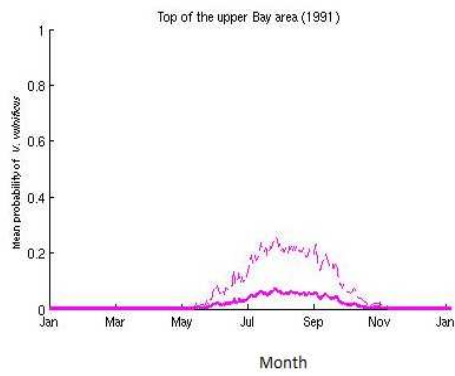
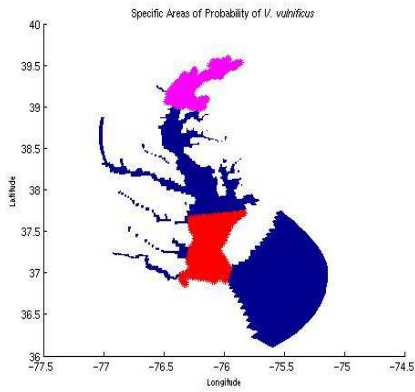
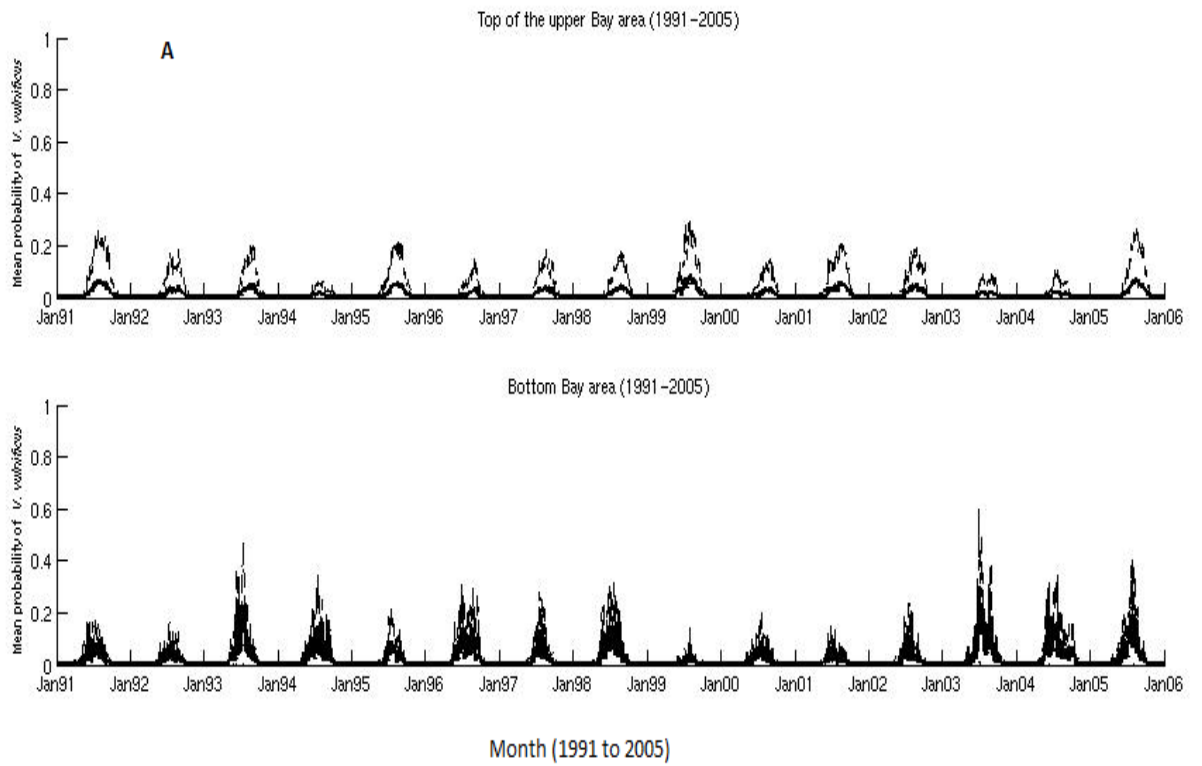


Figure 18: Annual mean probabilities of *V. vulnificus* (1991) for the “Alternate Areas” i.e. Top of the Upper Bay and Bottom Bay area (lower panel).



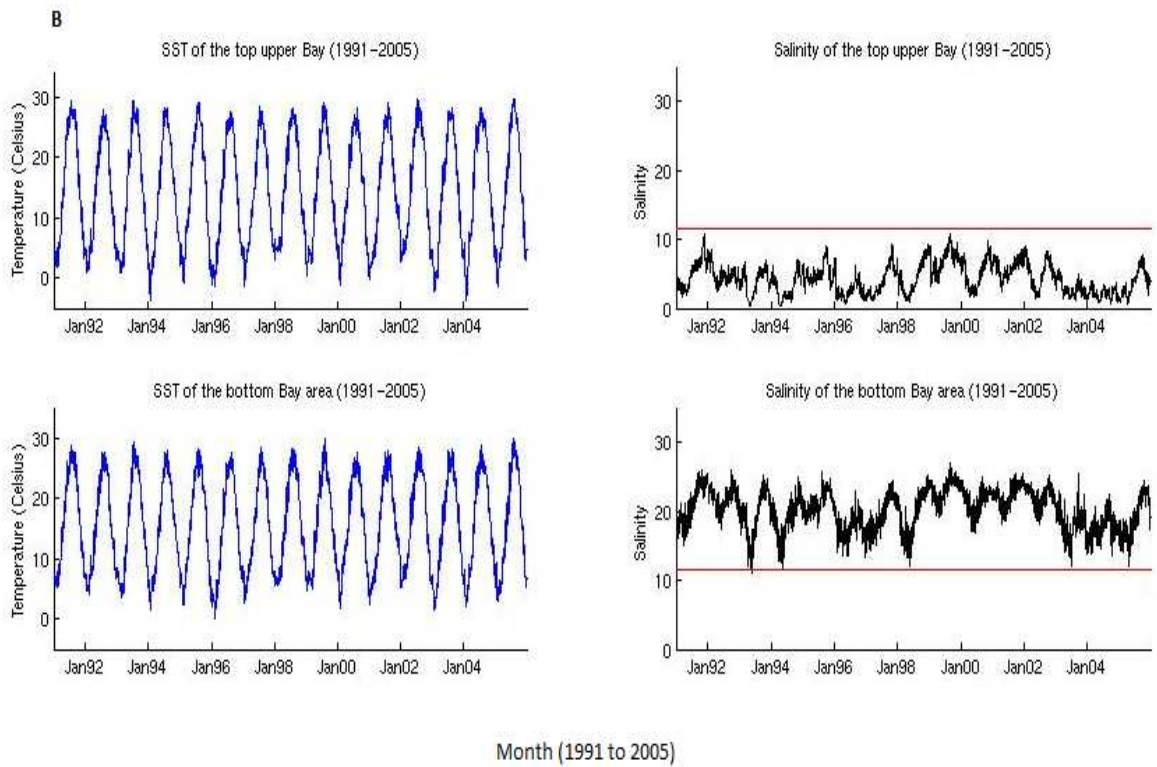


Figure 19: A) Inter-annual variability in the daily mean (solid line) and (+) standard deviation (line) of predicted *V. vulnificus* presence in the “Alternate Areas” from 1991 to 2005, i.e., top of the upper Bay (top panel) and bottom Bay (lower panel).

B) Inter-annual variability in the simulated sea surface temperature and salinity by the hydrodynamic model (ROMS) for the Top of the Upper Bay and Bottom Bay from 1991 to 2005. The red horizontal line represents the optimal salinity (11.5 ppt) as recorded by Jacobs *et al.*

Appendix

Script 1

```
% Vulnificusmodel.m
% calculate the Vibrio vulnificus probability based on John Jacobs model
% Guillaume and Vinita
yr=input('please input the year you want (1991-2005):');
inputfile=['HABdata_new' num2str(yr) '.mat'];
%---load the input file ---
load(inputfile);
[Nt, Ny, Nx]=size(saltall); %obtain the dimensions in time and space
vvulnifall=nan*zeros([Nt,Ny, Nx]); %make up empty array to store final results

%calculate the Vibrio vulnificus using the John Jacob's model
for it=1:Nt
%S and T at one day
    salt =squeeze(saltall(it,:,:));
    temp =squeeze(tempall(it,:,:));
%vulnificus model
%according to John Jacobs Documents
% the probability of Vibrio vulnificus being positive can be modeled by:
%
% 
$$P = \frac{1}{1 + \exp[-(a + b_1 T + b_2 S)]}$$

% where a is called intercept, b1, b2 are coefficients for significant
% explanatory variable T and S respectively
% the odds=P/(1-P), and log(odds)=a+b1*T+b2*S, here we use logV to store
log(odds)
%
% 
$$\text{Hence } P = \frac{1}{1 + \exp[-\log(\text{odds})]}$$

%
    a=-7.867; %according to Jacobs,
    b1=0.316;
    b2=-0.342;

    for j=1:Ny
    for i=1:Nx

        S1=abs(11.5-salt(j,i)); % determined the SALopt as defined in the
report
        T1=temp(j,i);

        logV= a+b1*T1+b2*S1;
        P=1/(1+exp(-logV));
        vvulnifall(it,j,i)=P;
    end
    end
    clear temp, salt;
end

%save the final results in the matlab file

save(['HABdata_VcholVvulni' num2str(yr) '.mat'],'tempall',
'saltall','kmicall','snpball', 'vvulnifall', 'vchoall5','dateall','lat',
'lon','mask_rho','-mat');%'vchoall',
%make some plots
mask=mask_rho(1:end-1,1:end-1);
inan=find(mask<0.5);
v5=squeeze(mean(vvulnifall,1));
v5(inan)=nan;
```

```

figure; pcolor(lon(1:end-1,1:end-1),lat(1:end-1,1:end-1), v5); shading flat;
caxis([0 0.25]); colorbar;
title(['\itVibrio vulnificus\rm model mean probability for ' num2str(yr) ]);
xlabel('longitude');
ylabel('latitude');
%v3=squeeze(mean(vchoall,1));
%v3(inan)=nan;
%figure; pcolor(lon(1:end-1,1:end-1),lat(1:end-1,1:end-1), v3);shading flat;
colorbar;
%title('model 3 probability');
%xlabel('longitude');
%ylabel('latitude');
%figure; pcolor(lon(1:end-1,1:end-1),lat(1:end-1,1:end-1),v5-v3);shading flat;
colorbar;
%title('model 5 probability-model 3 probability');
%xlabel('longitude');
%ylabel('latitude');

```

Script 2.

```

% VulnificusMeanPlot.m
% Generate the plot of the yearly mean of the Vibrio vulnificus probability
based on John Jacobs model
%
% Guillaume and Vinita
%
yr=input('please input the year you want (1991-2005):');

inputfile=['HABdata_VcholVvulni' num2str(yr) '.mat'];
%---load the input file ---
load(inputfile);
%---make the plot ---

mask=mask_rho(1:end-1,1:end-1); %Create a mask for land pixels
inan=find(mask<0.5);
v5=squeeze(mean(vvulnifall,1)); %Calculate the yearly mean
v5(inan)=nan; %Put not a number for the land pixels

hfig2=figure('Visible','on','Position',[1 1 600 600]);
clf;

pcolor(lon(1:end-1,1:end-1),lat(1:end-1,1:end-1), v5); shading flat; caxis([0
0.25]); colorbar;
title(['\itVibrio vulnificus\rm model mean probability for ' num2str(yr) ]);
xlabel('longitude');
ylabel('latitude');

%finally save the plot

saveas(gcf,['.\Figures\VvulnifMean-' num2str(yr_choose) '.fig'], 'fig');
saveas(gcf,['.\Figures\VvulnifMean-' num2str(yr_choose) '.eps'],
'eps');
saveas(gcf,['.\Figures\VvulnifMean-' num2str(yr_choose) '.emf'], 'emf');
saveas(gcf,['.\Figures\VvulnifMean-' num2str(yr_choose) '.png'], 'png');

% --- End of the script ---

```

Script 3


```

%----program plot_area_average_multi_year.m ----Whole Bay.
%
% This programs tries open a chosen series of years matlab files that
% contain the Vibrio vulnificus
% probability of surface water of CBay, then the data is processed
%
% I: for each year
%
% 1) take area average of 3 most apparent locations where V.vulnificus
% probability is high to produce a time series of that area. And the difference
% between individual cells within the area and the area average is saved as a set
% of random variables to calculate
% variance/standard deviation as a measure of the variability within that
% area
%
% Hence, two time series for each area
% will be obtained and plotted against time: a) time series of area
% average
% b) time series of standard deviation
%
% 2) a plot is made that contain the curve of average time series, with
% standard deviation as upper and lower bound envelop sitting in the average time
% series
%
% 3) a separate plot is made to show the areas that are concerned.
%
% II: the area average and standard deviation of V.vulnificus probability,
% SST and Salinity for each year will be put together into a long time series.
% Plots of them are also made to show the interannual variability of them.
%
% find model data file and year of it
%
% modeloutputdir=input('please input the model output directory: (e.g.
% '..../old_data/') ');
%
% find the model data files
%
% modelfilenames=dir([modeloutputdir '/HABdata_V*.mat']);
%
% Nfile=length(modelfilenames); % number of files found
%
% if(Nfile<=0)
% error(['Not able to find files with ' modeloutputdir '/HAB*.mat']);
% end
% display('The following are the model files you have:');
%
% for ifile=1:Nfile
% display(['file number ', num2str(ifile), ': '
% modelfilenames(ifile).name]);
% end
%
% y_start=input(['Please give the starting file number you want (1-'
% num2str(Nfile) '): ']);
% y_end =input(['Please give the ending file number you want ('
% num2str(y_start) '-' num2str(Nfile) '): ']);
%
% if(y_end<y_start)
% error('Oops, you can not have ending year earlier than starting
% year');

```

```

end

%      modelname=input('Please give the name of the model ('model3'' or
%'model5'') :');

      yesno_individual_year=input('Please indicate yes or no for plotting
individual years (1=yes,0=no): ');

% processs the data year by year

display('Searching for data of Vibrio vulnificus ...');

for y_choose= y_start: y_end

      modeloutputfile=[modeloutputdir      '/'      modelfilenames(y_choose).name];
%find file name of that particular year

      display(['Processing file :' modeloutputfile ' ...']);

% load the data

      load(modeloutputfile);

% list what is in the data file

% whos

      clear kmicall, snpball;      %free memory for these are not used in this
program

      %find the dimensions

      [nt,ny,nx]=size(vvulnifall);

      %make sure the grid information all have the same dimensions
      mask=mask_rho(1:ny,1:nx);
      lat=lat(1:ny,1:nx);
      lon=lon(1:ny,1:nx);

%find beginning and ending year

      if(y_choose==y_start)
          yr_start=dateall(1,1);
      end

      if(y_choose==y_end)
          yr_end=dateall(1,1);
      end

%find the sum of the year for all cells

      indexland=find(mask<0.5);
      vvulnif_sum=squeeze(sum(vvulnifall,1));
      vvulnif_sum(indexland)=nan;      %make sure the land points are excluded

%end

display('Processing data year by year (file by file)');

```

```

%for y_choose= y_start: y_end

    %find file name of that particular year

%   modeloutputfile=[modeloutputdir '/' modelfilenames(y_choose).name];

%   display(['Processing file :' modeloutputfile ' ...']);

% load the data

%   load(modeloutputfile);

% list what is in the data file

%   whos

%   clear kmicall, snpball;   %free memory for these are not used in this
program

    %find the dimensions

%   [nt,ny,nx]=size(vchoall5);

%make sure the grid information all have the same dimensions
%   mask=mask_rho(1:ny,1:nx);
%   lat=lat(1:ny,1:nx);
%   lon=lon(1:ny,1:nx);

% find area that are interested, basically we want to separate Susquehanna flat
area, Choptank estuary area
% and the rest of west estuaries (Patuxent, Potomac, Rappahannoc, York and
James river estuaries)
%
% this is done by a) find all points where the sum of the year of vulnificus
probability is > 5%
%                               b) separate the found points/cells into 3 areas as described
above
%
%

% select the values of the vvulnificus for the whole Bay

    %values in the box
    VvulB_select=vvulnifall(1:nt, :, :);

    clear vvulnifall;   %free memory for not used after this

    %values of the indexd portion set in the box

%       chop_select_final=chop_select(1:nt,index_chop_max);
%       susq_select_final=susq_select(1:nt,index_susq_max);
%       west_select_final=west_select(1:nt,index_west_max);

% calculate the area mean and also standard deviation

VvulB_mean=zeros([nt,1]); VvulB_std=zeros([nt,1]);

for it=1:nt
    VvulB_mean(it)=mean(squeeze(VvulB_select(it,:)));
    VvulB_std(it) = std(squeeze(VvulB_select(it,:)));
end

```

```

% find time axis for making time series plots

time=datetime(dateall); %this converts the dates in dateall array into a
time axis series in days from 0001-01-01 0 0 0 AD

yr_choose=dateall(1,1); %get the year of the data

% Concatenate the mean and standard deviation data to a grand array

if(y_choose==y_start)
    VvulB_mean_all=VvulB_mean; VvulB_std_all=VvulB_std;
    time_all=time;
else
    VvulB_mean_all=[VvulB_mean_all; VvulB_mean];
VvulB_std_all=[VvulB_std_all; VvulB_std];
    time_all=[time_all;time];
end

if (yesno_individual_year==1)

% make plot

hfig2=figure('Visible','on','Position',[1 1 1000 500]);
clf;

subplot(1,2,1); hold on;

pcolor(lon, lat, vvulnif_sum); axis([-77.5,-74.5,36,40]);
legend([hchop, hsusq, hwest], 'Choptank area', ...
        'Susquehanna flat area', ...
        'West estuaries area');
legend('boxoff');
caxis([0, 100000]);
colorbar; shading interp; % large caxis to make background blue for
nonselected area
xlabel('Longitude', 'FontSize',9);ylabel('Latitude', 'FontSize',9);
title('Sum of probability of \itV. vulnificus\rm ');

subplot(1,2,2); hold on;

hwholeB_mean=plot(time,VvulB_mean,'r-','LineWidth',2);
hwholeB_up =plot(time,VvulB_mean+VvulB_std,'r--','LineWidth',1);
hwholeB_down=plot(time,VvulB_mean-VvulB_std,'r--','LineWidth',1);
datetick('x','mmyy');
title(['The Chesapeake Bay (' num2str(yr_choose) ')']);
ylabel(['Mean probability of \it V. vulnificus\rm ', 'FontSize',9);
xlabel('Month')
set(gca,'XLim',[time(1) time(end)]);
set(gca,'XTick',[time(1):60:time(end)]);
set(gca,'XTickLabel',{'Jan','Mar','May','Jul','Sep','Nov','Jan'})
% set(gca,'YLim',[0 1]);

saveas(gcf,['.\Figures\VvulnifiAreaTS-' num2str(yr_choose) '.fig'],
'fig');
saveas(gcf,['.\Figures\VvulnificusAreaTS-' num2str(yr_choose) '.eps'],
'eps');
saveas(gcf,['.\Figures\VvulnificusAreaTS-' num2str(yr_choose) '.emf'],
'emf');
saveas(gcf,['.\Figures\VvulnificusAreaTS-' num2str(yr_choose) '.png'],
'png');

```

```

%         delete(hfig2);

% in order to make a prettier figure about the area
% we need to save the data of chosen places
%

end %end of plotting individual years

%%%%%%%%%%
%
% STOP HERE EDITING THE SCRIPT FOR VULNIFICUS
%
%%%%%%%%%%

%Light seasonal study.

% select the values of the SST and Salinity for each of the point in
% areas

% SST values in the box
CB_temp_select=tempall(1:nt, :, :);
clear tempall; %free memory for not used after this

% Salinity values in the box
CB_salt_select=saltall(1:nt, :, :);
clear saltall; %free memory for not used after this

% calculate the SST area mean and also standard deviation
% and also calculate the Salinity area mean and also standard
deviation

CB_temp_area_mean=zeros([nt,1]); CB_temp_area_std=zeros([nt,1]);
%define arrays to store mean and standard deviation
CB_salt_area_mean=zeros([nt,1]); CB_salt_area_std=zeros([nt,1]);

for it=1:nt
    CB_temp_area_mean(it)= mean(squeeze(CB_temp_select(it,:))); %SST
    CB_temp_area_std(it) = std(squeeze(CB_temp_select(it,:)));

    CB_salt_area_mean(it)=mean(squeeze(CB_salt_select(it,:))); %Salinity
    CB_salt_area_std(it) = std(squeeze(CB_salt_select(it,:)));
end

% find time axis for plots (days)

time=datetime(dateall); %this converts the dates in dateall array into a
time axis series in days from 0001-01-01 0 0 0 AD

%concatenate data into a grand array for keeping all years

if(y_choose==y_start)
    CB_temp_area_mean_all=CB_temp_area_mean;
CB_temp_area_std_all=CB_temp_area_std;
    CB_salt_area_mean_all=CB_salt_area_mean;
CB_salt_area_std_all=CB_salt_area_std;
else
    CB_temp_area_mean_all=[CB_temp_area_mean_all; CB_temp_area_mean];
CB_temp_area_std_all=[CB_temp_area_std_all; CB_temp_area_std];

```

```

        CB_salt_area_mean_all=[CB_salt_area_mean_all;          CB_salt_area_mean];
CB_salt_area_std_all=[CB_salt_area_std_all; CB_salt_area_std];
    end

    if(yesno_individual_year==1)

% make new plot of V vulnificus probability and SST and Salinity
%
[haxes,hline1,hline2]=plotyy(time,chop_temp_area_mean,time,chop_salt_area_mean)
;

    hfig3=figure('Visible','on','Position',[1 1 1200 1500]); clf;

    subplot(3,1,1); hold on;

    hwholeB_mean=plot(time,VvulB_mean,'r-','LineWidth',2);
    hwholeB_up   =plot(time,VvulB_mean+VvulB_std,'r--','LineWidth',1);
    hwholeB_down=plot(time,VvulB_mean-VvulB_std,'r--','LineWidth',1);
    datetick('x','mmyy');
    title(['The Chesapeake Bay (' num2str(yr_choose) ')']);
    ylabel(['Mean probability of \it V. vulnificus\rm ', 'FontSize',9]);
    xlabel('Month')
    set(gca,'XLim',[time(1) time(end)]);
    set(gca,'XTick',[time(1):60:time(end)]);
    set(gca,'XTickLabel',{'Jan','Mar','May','Jul','Sep','Nov','Jan'})
%
    subplot(3,1,2); hold on;

    hCB_temp_mean =plot(time, CB_temp_area_mean,'b-');%,'LineWidth',2);
    hCB_temp_up   =plot(time, CB_temp_area_mean+CB_temp_area_std,'b--
');%,'LineWidth',1);
    hCB_temp_down =plot(time, CB_temp_area_mean-CB_temp_area_std,'b--
');%,'LineWidth',1);
    datetick('x','mmyy');
    ylabel('Temperature (Celsius)', 'FontSize',9);
    set(gca,'XLim',[time_all(1) time_all(end)]);
    set(gca,'Ylim',[-5 30]);
    set(gca,'YTick',[0 10:10:30]);
%
    set(gca,'XTick',[time_all(1):365:time_all(end)]);
    title(['SST of the Chesapeake Bay (' num2str(yr_start) '-'
num2str(yr_end) ')']);

    subplot(3,1,3); hold on;

    hCB_salt_mean =plot(time, CB_salt_area_mean,'k-');%,'LineWidth',2);
    hCB_salt_up   =plot(time, CB_salt_area_mean+CB_salt_area_std,'k--
');%,'LineWidth',1);
    hCB_salt_down =plot(time, CB_salt_area_mean-CB_salt_area_std,'k--
');%,'LineWidth',1);
    ylabel('Salinity', 'FontSize',9);
    datetick('x','mmyy');
    set(gca,'Ylim',[0 20]);
    set(gca,'XLim',[time_all(1) time_all(end)]);
%
    set(gca,'YTick',[0:2:12]);
%
    set(gca,'XTick',[time_all(1):365:time_all(end)]);
    title(['Salinity of the Chesapeake Bay (' num2str(yr_start) '-'
num2str(yr_end) ')']);

```

```

        % Save plot hfig3

        saveas(gcf,['.\Figures\VulniTempSaltAreaTS-' num2str(yr_choose) '.fig'],
'fig');
        saveas(gcf,['.\Figures\VulniTempSaltAreaTS-' num2str(yr_choose) '.eps'],
'epsc');
        saveas(gcf,['.\Figures\VulniTempSaltAreaTS-' num2str(yr_choose) '.emf'],
'emf');
        saveas(gcf,['.\Figures\VulniTempSaltAreaTS-' num2str(yr_choose) '.png'],
'png');

    end %end of the plotting of individual year T and S

%end %end of the y_choose loop
end %end of plotting individual years

%finally plot all the years together

%A_bis: plot TS of V vulnificus for max area in the CB
    yr_seq=[yr_start:yr_end];

    hfigall2Bis=figure('Visible','on','Position',[1 1 1200 1500]);
    clf;
    subplot(3,1,1); hold on;

    hwholeB_mean=plot(time_all,VvulB_mean_all,'k-','LineWidth',2);
    hwholeB_up      =plot(time_all,VvulB_mean_all+VvulB_std_all,'k--
','LineWidth',1);
    hwholeB_down=plot(time_all,VvulB_mean_all-VvulB_std_all,'k--
','LineWidth',1);
    title(['Mean probability of \it V. vulnificus\rm in the Chesapeake Bay
(' num2str(yr_start) '-' num2str(yr_end) ')']);
    %; n max=' num2str(npnts_chop_max)', year max='
num2str(yr_seq(npnts_chop_max_year) ')'];
    ylabel(['Mean probability of \it V. vulnificus\rm '], 'FontSize',9);
    set(gca,'YLim',[0 0.5]);
    datetick('x','mmyy');
%    set(gca,'XTick',[time_all(1):365:time_all(end)]);
    set(gca,'XLim',[time_all(1) time_all(end)]);

    subplot(3,1,2); hold on;

    hCB_temp_mean      =plot(time_all,CB_temp_area_mean_all,'b-
');%; 'LineWidth',1);
    hCB_temp_up      =plot(time_all,CB_temp_area_mean_all+CB_temp_area_std_all,'b--
');%; 'LineWidth',1);
    hCB_temp_down      =plot(time_all,CB_temp_area_mean_all-
CB_temp_area_std_all,'b--');%; 'LineWidth',1);
    datetick('x','mmyy');
    ylabel('Temperature (Celsius)', 'FontSize',9);
    set(gca,'XLim',[time_all(1) time_all(end)]);
    set(gca,'Ylim',[-5 30]);
    set(gca,'YTick',[0 10:10:30]);
%    set(gca,'XTick',[time_all(1):365:time_all(end)]);
    title(['SST of the Chesapeake Bay (' num2str(yr_start) '-'
num2str(yr_end) ')']);

    subplot(3,1,3); hold on;

```

```

        hCB_salt_mean =plot(time_all, CB_salt_area_mean_all, 'k-');%, 'LineWidth', 1);
        hCB_salt_up =plot(time_all, CB_salt_area_mean_all+CB_salt_area_std_all, 'k--');%, 'LineWidth', 1);
        hCB_salt_down =plot(time_all, CB_salt_area_mean_all-CB_salt_area_std_all, 'k--');%, 'LineWidth', 1);
        ylabel('Salinity', 'FontSize', 9);
        datetick('x', 'mmmyy');
        set(gca, 'Ylim', [0 20]);
        set(gca, 'Xlim', [time_all(1) time_all(end)]);
%       set(gca, 'YTick', [0:2:12]);
%       set(gca, 'XTick', [time_all(1):365:time_all(end)]);
        title(['Salinity of the Chesapeake Bay (' num2str(yr_start) '-' num2str(yr_end) ')']);

%finally save the plot

        saveas(gcf, ['. \Figures \VvulniSSTSalAreaTS-all-' num2str(yr_start) '-' num2str(yr_end) '.fig'], 'fig');
        saveas(gcf, ['. \Figures \VvulniSSTSalAreaTS-all-' num2str(yr_start) '-' num2str(yr_end) '.emf'], 'emf');
        saveas(gcf, ['. \Figures \VvulniSSTSalAreaTS-all-' num2str(yr_start) '-' num2str(yr_end) '.eps'], 'eps');
        saveas(gcf, ['. \Figures \VvulniSSTSalAreaTS-all-' num2str(yr_start) '-' num2str(yr_end) '.png'], 'png');

```

Script 4

```

%----program plot_area_average_multi_year.m ----- 3 zones.
%
% This programs tries open a chosen series of years matlab files that
% contain the Vibrio vulnificus
% probability of surface water of CBay, then the data is processed
%
% I: for each year
%
% 1) take area average of 3 most apparent locations where V vulnificus
% proability is high
% to produce a time series of that area. And the difference between
% individual cells within
% the area and the area average is saved as a set of random variables to
% calculate
% variance/standard deviation as a measure of the variability within that
% area
%
% Hence, two time series for each area
% will be obtained and plotted against time: a) time series of area
% average
% b) time series of standard
% deviation
%
% 2) a plot is made that contain the curve of average time series, with
% standard deviation as upper and
% lower bound envelop sitting in the average time series
%
% 3) a separate plot is made to show the areas that are concerned.
%

```



```

%      II: the area average and standard deviation of vvulnificus probability,
SST and Salinity for each year
%      will be put together into a long time series. Plots of them are also
made to show
%      the interannual variability of them.
%
% find model data file and year of it

    modeloutputdir=input('please input the model output directory: (e.g.
'../old_data/') ');

% find the model data files

    modelfilenames=dir([modeloutputdir '/HABdata_V*.mat']);

    Nfile=length(modelfilenames); % number of files found

    if(Nfile<=0)
        error(['Not able to find files with ' modeloutputdir '/HAB*.mat']);
    end
    display('The following are the model files you have:');

    for ifile=1:Nfile
        display(['file      number      ',      num2str(ifile),      ':      '
modelfilenames(ifile).name]);
    end

    y_start=input(['Please give the starting file number you want (1-'
num2str(Nfile) '): ']);
    y_end      =input(['Please give the ending file number you want ('
num2str(y_start) '-' num2str(Nfile) '): ']);

    if(y_end<y_start)
        error('Oops, you can not have ending year earlier than starting
year');
    end

    yesno_individual_year=input('Please indicate yes or no for plotting
individual years (1=yes,0=no): ');

% processes the data year by year

display('Searching for data of Vibrio vulnificus ...');

for y_choose= y_start: y_end

    modeloutputfile=[modeloutputdir      '/'      modelfilenames(y_choose).name];
%find file name of that particular year

    display(['Processing file :' modeloutputfile ' ...']);

% load the data

    load(modeloutputfile);

% list what is in the data file

```

```

% whos

clear kmicall snpball %free memory for these are not used in this program

%find the dimensions

[nt,ny,nx]=size(vvulnifall);

%make sure the grid information all have the same dimensions
mask=mask_rho(1:ny,1:nx);
lat=lat(1:ny,1:nx);
lon=lon(1:ny,1:nx);

%find beginning and ending year

if(y_choose==y_start)
    yr_start=dateall(1,1);
end

if(y_choose==y_end)
    yr_end=dateall(1,1);
end

%find the sum of the year for all cells

indexland=find(mask<0.5);
vvulnif_sum=squeeze(sum(vvulnifall,1));
vvulnif_sum(indexland)=nan; %make sure the land points are excluded
% vvulnifall(indexland)=nan; %make sure the land points are excluded

%end

if(y_choose==y_start) %find the boxes
    midB_iy=38:70; midB_ix=39:99;
    lon_midB=lon(midB_iy,midB_ix); lat_midB=lat(midB_iy,midB_ix);
mask_midB=mask(midB_iy,midB_ix);

    uppB_iy=71:101; uppB_ix=27:99;
    lon_uppB=lon(uppB_iy,uppB_ix); lat_uppB=lat(uppB_iy,uppB_ix);
mask_uppB=mask(uppB_iy,uppB_ix);

    west_iy=1:70; west_ix=1:38;
    lon_west=lon(west_iy,west_ix); lat_west=lat(west_iy,west_ix);
mask_west=mask(west_iy,west_ix);
end

index_midB=find(vvulnif_sum(midB_iy,midB_ix)>0);
index_uppB=find(vvulnif_sum(uppB_iy,uppB_ix)>0);
index_west=find(vvulnif_sum(west_iy,west_ix)>0);

display('Processing data year by year (file by file)');

%%%%%%%%%%%%%%%%%%%%%%%%%%%%%%%%%%%%%%%%%%%%%%%%%%%%%%%%%%%%%%%%%%%%%%%%
%%%%%%%%%%%%%%%%%%%%%%%%%%%%%%%%%%%%%%%%%%%%%%%%%%%%%%%%%%%%%%%%%%%%%%%%
%values in the box
midB_select=vvulnifall(1:nt,midB_iy,midB_ix);
uppB_select=vvulnifall(1:nt,uppB_iy,uppB_ix);
west_select=vvulnifall(1:nt,west_iy,west_ix);

```

```

clear vvulnifall; %free memory for not used after this

%values of the indexd portion set in the box

midB_select_final=midB_select;
uppB_select_final=uppB_select;
west_select_final=west_select;

% calculate the area mean and also standard deviation

midB_area_mean=zeros([nt,1]); midB_area_std=zeros([nt,1]);
uppB_area_mean=zeros([nt,1]); uppB_area_std=zeros([nt,1]);
west_area_mean=zeros([nt,1]); west_area_std=zeros([nt,1]);

for it=1:nt
    midB_area_mean(it)=mean(squeeze(midB_select_final(it,:))); %midBtank
    midB_area_std(it) = std(squeeze(midB_select_final(it,:)));
%    midB_area_mean(indexland)=nan;
%    midB_area_std(indexland)=nan;

    uppB_area_mean(it)=mean(squeeze(uppB_select_final(it,:))); %uppbay
    uppB_area_std(it) = std(squeeze(uppB_select_final(it,:)));
%    uppB_area_mean(indexland)=nan;
%    uppB_area_std(indexland)=nan;

    west_area_mean(it)=mean(squeeze(west_select_final(it,:)));
%westestuaries
    west_area_std(it) = std(squeeze(west_select_final(it,:)));
%    west_area_mean(indexland)=nan;
%    west_area_std(indexland)=nan;
end

%    midB_area_mean(indexland)=nan;
%    midB_area_std(indexland)=nan;
%    uppB_area_mean(indexland)=nan;
%    uppB_area_std(indexland)=nan;
%    west_area_mean(indexland)=nan;
%    west_area_std(indexland)=nan;

% find time axis for making time series plots

time=datenum(dateall); %this converts the dates in dateall array into a
time axis series in days from 0001-01-01 0 0 0 AD

yr_choose=dateall(1,1); %get the year of the data

% Concatenate the mean and standard deviation data to a grand array

if(y_choose==y_start)
    midB_area_mean_all=midB_area_mean; midB_area_std_all=midB_area_std;
    uppB_area_mean_all=uppB_area_mean; uppB_area_std_all=uppB_area_std;
    west_area_mean_all=west_area_mean; west_area_std_all=west_area_std;
    time_all=time;
else
    midB_area_mean_all=[midB_area_mean_all; midB_area_mean];
midB_area_std_all=[midB_area_std_all; midB_area_std];
    uppB_area_mean_all=[uppB_area_mean_all; uppB_area_mean];
uppB_area_std_all=[uppB_area_std_all; uppB_area_std];
    west_area_mean_all=[west_area_mean_all; west_area_mean];
west_area_std_all=[west_area_std_all; west_area_std];
    time_all=[time_all;time];
end

```

```

%%%%%%%%%%%%%%%%%%%%%%%%%%%%%%%%%%%%%%%%%%%%%%%%%%%%%%%%%%%%%%%%%%%%%%%%
%%%%%%%%%%%%%%%%%%%%%%%%%%%%%%%%%%%%%%%%%%%%%%%%%%%%%%%%%%%%%%%%%%%%%%%%

        if (yesno_individual_year==1)

% make plot

%%%%%%%%%%%%%%%%%%%%%%%%%%%%%%%%%%%%%%%%%%%%%%%%%%%%%%%%%%%%%%%%%%%%%%%%
%%%%%%%%%%%%%%%%%%%%%%%%%%%%%%%%%%%%%%%%%%%%%%%%%%%%%%%%%%%%%%%%%%%%%%%%

        hfig2=figure('Visible','on','Position',[1 1 1200 1500]);
        clf;

        subplot(2,2,1); hold on;

        pcolor(lon, lat, vvulnif_sum); axis([-77.5,-74.5,36,40]);
        hmidB=plot(lon_midB(index_midB),lat_midB(index_midB),'r*');      % plot
stars with color red
        huppB=plot(lon_uppB(index_uppB),lat_uppB(index_uppB),'m*'); % meganta
        hwest=plot(lon_west(index_west),lat_west(index_west),'g*'); % yellow
%       legend([hmidB, huppB, hwest], 'midBtank area', ...
%               'uppBuehannaflat area', ...
%               'West estuaries area');
%       legend('boxoff');
        caxis([0, 100000]); shading interp; % large caxis to make background blue
for nonselected area
        xlabel('Longitude', 'FontSize',9); ylabel('Latitude', 'FontSize',9);
        title('Specific Areas of Probability of \itV. vulnificus\rm');

        subplot(2,2,2); hold on;

        huppB_mean=plot(time,uppB_area_mean,'m-','LineWidth',2);
        huppB_up   =plot(time,uppB_area_mean+uppB_area_std,'m--','LineWidth',1);
        huppB_down=plot(time,uppB_area_mean-uppB_area_std,'m--','LineWidth',1);
        datetick('x','mmyy');
        title(['Upper Bay area (' num2str(yr_choose) ')']);
        ylabel('Mean probability of \it V. vulnificus\rm ', 'FontSize',9);
        set(gca,'XLim',[time(1) time(end)]);
        set(gca,'XTick',time(1):60:time(end));
        set(gca,'XTickLabel',{'Jan','Mar','May','Jul','Sep','Nov','Jan'})
        set(gca,'YLim',[0 1]);

        subplot(2,2,3); hold on;

        hmidB_mean=plot(time,midB_area_mean,'r-','LineWidth',2);
        hmidB_up   =plot(time,midB_area_mean+midB_area_std,'r--','LineWidth',1);
        hmidB_down=plot(time,midB_area_mean-midB_area_std,'r--','LineWidth',1);
        datetick('x','mmyy');
        title(['Mid-Bay area (' num2str(yr_choose) ')']);
        ylabel('Mean probability of \it V. vulnificus\rm ', 'FontSize',9);
        set(gca,'XLim',[time(1) time(end)]);
        set(gca,'XTick',time(1):60:time(end));
        set(gca,'XTickLabel',{'Jan','Mar','May','Jul','Sep','Nov','Jan'})
        set(gca,'YLim',[0 1]);

        subplot(2,2,4); hold on;

        hwest_mean=plot(time,west_area_mean,'g-','LineWidth',2);
        hwest_up   =plot(time,west_area_mean+west_area_std,'g--','LineWidth',1);
        hwest_down=plot(time,west_area_mean-west_area_std,'g--','LineWidth',1);
        datetick('x','mmyy');

```

```

title(['West estuaries area of the bay (' num2str(yr_choose) ')']);
ylabel('Mean probability of \it V. vulnificus\rm ', 'FontSize',9);
set(gca,'XLim',[time(1) time(end)]);
set(gca,'XTick',time(1):60:time(end));
set(gca,'XTickLabel',{'Jan','Mar','May','Jul','Sep','Nov','Jan'})
set(gca,'YLim',[0 1]);

    saveas(gcf,['.\Figures\VvulnifiZonesTS-' num2str(yr_choose) '.fig'],
'fig');
    saveas(gcf,['.\Figures\VvulnifiZonesTS-' num2str(yr_choose) '.eps'],
'eps');
    saveas(gcf,['.\Figures\VvulnifiZonesTS-' num2str(yr_choose) '.emf'],
'emf');
    saveas(gcf,['.\Figures\VvulnifiZonesTS-' num2str(yr_choose) '.png'],
'png');

%    delete(hfig2);

% in order to make a prettier figure about the area
% we need to save the data of chosen places
%

    end
%end of plotting individual years

%Light seasonal study.
%%%%%%%%%%%%%%%%%%%%%%%%%%%%%%%%%%%%%%%%%%%%%%%%%%%%%%%%%%%%%%%%%%%%%%%%
% select the values of the SST and Salinity for each of the point in
% areas

    % SST values in the box
    midB_temp_select=tempall(1:nt,midB_iy,midB_ix);
    uppB_temp_select=tempall(1:nt,uppB_iy,uppB_ix);
    west_temp_select=tempall(1:nt,west_iy,west_ix);
    clear tempall; %free memory for not used after this

    % Salinity values in the box
    midB_salt_select=saltall(1:nt,midB_iy,midB_ix);
    uppB_salt_select=saltall(1:nt,uppB_iy,uppB_ix);
    west_salt_select=saltall(1:nt,west_iy,west_ix);

    clear saltall; %free memory for not used after this

    % SST values of the indexd portion set in the box

    midB_temp_select_final=midB_temp_select(1:nt,index_midB);
    uppB_temp_select_final=uppB_temp_select(1:nt,index_uppB);
    west_temp_select_final=west_temp_select(1:nt,index_west);

    % Salinity values of the indexd portion set in the box
    midB_salt_select_final=midB_salt_select(1:nt,index_midB);
    uppB_salt_select_final=uppB_salt_select(1:nt,index_uppB);
    west_salt_select_final=west_salt_select(1:nt,index_west);

    %define arrays to store mean and standard deviation
    midB_temp_area_mean=zeros([nt,1]);
    midB_temp_area_std=zeros([nt,1]);
    uppB_temp_area_mean=zeros([nt,1]);
    uppB_temp_area_std=zeros([nt,1]);

```

```

        west_temp_area_mean=zeros([nt,1]);
west_temp_area_std=zeros([nt,1]);

        midB_salt_area_mean=zeros([nt,1]);
midB_salt_area_std=zeros([nt,1]);
        uppB_salt_area_mean=zeros([nt,1]);
uppB_salt_area_std=zeros([nt,1]);
        west_salt_area_mean=zeros([nt,1]);
west_salt_area_std=zeros([nt,1]);

        for it=1:nt
            midB_temp_area_mean(it)=mean(squeeze(midB_temp_select_final(it,:)));
%SST midBtank
            midB_temp_area_std(it) = std(squeeze(midB_temp_select_final(it,:)));

            midB_salt_area_mean(it)=mean(squeeze(midB_salt_select_final(it,:)));
%Salinity midBtank
            midB_salt_area_std(it) = std(squeeze(midB_salt_select_final(it,:)));

            uppB_temp_area_mean(it)=mean(squeeze(uppB_temp_select_final(it,:)));
%SST uppBuehanna
            uppB_temp_area_std(it) = std(squeeze(uppB_temp_select_final(it,:)));

            uppB_salt_area_mean(it)=mean(squeeze(uppB_salt_select_final(it,:)));
%Salinity uppBuehanna
            uppB_salt_area_std(it) = std(squeeze(uppB_salt_select_final(it,:)));

            west_temp_area_mean(it)=mean(squeeze(west_temp_select_final(it,:)));
%SST West estuaries
            west_temp_area_std(it) = std(squeeze(west_temp_select_final(it,:)));

            west_salt_area_mean(it)=mean(squeeze(west_salt_select_final(it,:)));
%Salinity West estuaries
            west_salt_area_std(it) = std(squeeze(west_salt_select_final(it,:)));

        end

        % find time axis for plots (days)

        time=datetime(dateall); %this converts the dates in dateall array into a
time axis series in days from 0001-01-01 0 0 0 AD

        %concatenate data into a grand array for keeping all years

        if(y_choose==y_start)
            midB_temp_area_mean_all=midB_temp_area_mean;
midB_temp_area_std_all=midB_temp_area_std;
            uppB_temp_area_mean_all=uppB_temp_area_mean;
uppB_temp_area_std_all=uppB_temp_area_std;
            west_temp_area_mean_all=west_temp_area_mean;
west_temp_area_std_all=west_temp_area_std;

            midB_salt_area_mean_all=midB_salt_area_mean;
midB_salt_area_std_all=midB_salt_area_std;
            uppB_salt_area_mean_all=uppB_salt_area_mean;
uppB_salt_area_std_all=uppB_salt_area_std;
            west_salt_area_mean_all=west_salt_area_mean;
west_salt_area_std_all=west_salt_area_std;

        else
            midB_temp_area_mean_all=[midB_temp_area_mean_all; midB_temp_area_mean];
midB_temp_area_std_all=[midB_temp_area_std_all; midB_temp_area_std];

```

```

        uppB_temp_area_mean_all=[uppB_temp_area_mean_all; uppB_temp_area_mean];
uppB_temp_area_std_all=[uppB_temp_area_std_all; uppB_temp_area_std];
        west_temp_area_mean_all=[west_temp_area_mean_all; west_temp_area_mean];
west_temp_area_std_all=[west_temp_area_std_all; west_temp_area_std];

        midB_salt_area_mean_all=[midB_salt_area_mean_all; midB_salt_area_mean];
midB_salt_area_std_all=[midB_salt_area_std_all; midB_salt_area_std];
        uppB_salt_area_mean_all=[uppB_salt_area_mean_all; uppB_salt_area_mean];
uppB_salt_area_std_all=[uppB_salt_area_std_all; uppB_salt_area_std];
        west_salt_area_mean_all=[west_salt_area_mean_all; west_salt_area_mean];
west_salt_area_std_all=[west_salt_area_std_all; west_salt_area_std];

end

if(yesno_individual_year==1)

% make new plot of V vulnificus probability and SST and Salinity

        hfig3=figure('Visible','on','Position',[1 1 1200 1500]); clf;

        subplot(3,2,1); hold on;

        huppB_temp_mean =plot(time,uppB_temp_area_mean,'b-');%,'LineWidth',2);
        huppB_temp_up      =plot(time,uppB_temp_area_mean+uppB_temp_area_std,'b--
');%,'LineWidth',1);
        huppB_temp_down    =plot(time,uppB_temp_area_mean-uppB_temp_area_std,'b--
');%,'LineWidth',1);
        datetick('x','mmm');
        ylabel('Temperature (Celsius)');
        set(gca,'XLim',[time(1) time(end)]);
        set(gca,'Ylim',[-5 35]);
        set(gca,'YTick',[0 10:10:30]);
        title(['SST Upper Bay area (' num2str(yr_choose) ')']);

        subplot(3,2,2); hold on;

        huppB_salt_mean =plot(time,uppB_salt_area_mean,'k-');%,'LineWidth',2);
        huppB_salt_up      =plot(time,uppB_salt_area_mean+uppB_salt_area_std,'k--
');%,'LineWidth',1);
        huppB_salt_down    =plot(time,uppB_salt_area_mean-uppB_salt_area_std,'k--
');%,'LineWidth',1);
        line([time_all(1) time_all(end)],[11.5
11.5],'Color','r','LineWidth',1.5);
        ylabel('Salinity');
        datetick('x','mmm');
        set(gca,'XLim',[time(1) time(end)]);
        set(gca,'Ylim',[0 25]);
        set(gca,'YTick', 0:5:25);
        title(['Salinity Upper Bay area (' num2str(yr_choose) ')']);

        subplot(3,2,3); hold on;

        hmidB_temp_mean =plot(time,midB_temp_area_mean,'b-');%,'LineWidth',2);
        hmidB_temp_up      =plot(time,midB_temp_area_mean+midB_temp_area_std,'b--
');%,'LineWidth',1);
        hmidB_temp_down    =plot(time,midB_temp_area_mean-midB_temp_area_std,'b--
');%,'LineWidth',1);
        datetick('x','mmm');
        ylabel('Temperature (Celsius)');
        set(gca,'XLim',[time(1) time(end)]);

```

```

set(gca,'Ylim',[-5 35]);
set(gca,'YTick',[0 10:10:30]);
title(['SST Mid-Bay area (' num2str(yr_choose) ')']);

subplot(3,2,4); hold on;
hmidB_salt_mean =plot(time,midB_salt_area_mean,'k-');%,'LineWidth',2);
hmidB_salt_up   =plot(time,midB_salt_area_mean+midB_salt_area_std,'k--');%,'LineWidth',1);
hmidB_salt_down =plot(time,midB_salt_area_mean-midB_salt_area_std,'k--');%,'LineWidth',1);
line([time_all(1) time_all(end)], [11.5 11.5], 'Color','r','LineWidth',1.5);
ylabel('Salinity');
datetick('x','mmm');
set(gca,'Ylim',[0 25]);
set(gca,'YTick', 0:5:25 );
set(gca,'XLim',[time(1) time(end)]);
title(['Salinity Mid-Bay area (' num2str(yr_choose) ')']);

subplot(3,2,5); hold on;

hwest_temp_mean =plot(time,west_temp_area_mean,'b-');%,'LineWidth',2);
hwest_temp_up   =plot(time,west_temp_area_mean+west_temp_area_std,'b--');%,'LineWidth',1);
hwest_temp_down =plot(time,west_temp_area_mean-west_temp_area_std,'b--');%,'LineWidth',1);
datetick('x','mmm');
ylabel('Temperature (Celsius)');
set(gca,'Ylim',[-5 35]);
set(gca,'XLim',[time(1) time(end)]);
set(gca,'YTick',[0 10:10:30]);
title(['SST West estuaries area of the bay (' num2str(yr_choose) ')']);

subplot(3,2,6); hold on;

hwest_salt_mean =plot(time,west_salt_area_mean,'k-');%,'LineWidth',5);
hwest_salt_up   =plot(time,west_salt_area_mean+west_salt_area_std,'k--');%,'LineWidth',1);
hwest_salt_down =plot(time,west_salt_area_mean-west_salt_area_std,'k--');%,'LineWidth',1);
line([time_all(1) time_all(end)], [11.5 11.5], 'Color','r','LineWidth',1.5);
ylabel('Salinity');
datetick('x','mmm');
set(gca,'Ylim',[0 25]);
set(gca,'YTick', 0:5:25);
set(gca,'XLim',[time(1) time(end)]);
title(['Salinity West estuaries area of the bay (' num2str(yr_choose) ')']);

% Save plot hfig3

saveas(gcf,['.\Figures\TempSaltAreaTS-' num2str(yr_choose) '.fig'],
'fig');
saveas(gcf,['.\Figures\TempSaltAreaTS-' num2str(yr_choose) '.eps'],
'eps');
saveas(gcf,['.\Figures\TempSaltAreaTS-' num2str(yr_choose) '.emf'],
'emf');
saveas(gcf,['.\Figures\TempSaltAreaTS-' num2str(yr_choose) '.png'],
'png');

```



```

end %end of the plotting of individual year T and S

%end %end of the y_choose loop
end %end of plotting individual years

%finally plot all the years together

%A: plot TS of V vulnificus for max area in the CB

hfigall2=figure('Visible','on');%,'Position',[1 1 1200 1500]);
clf;

% subplot(2,2,1);
hold on;

pcolor(lon, lat, vvulnif_sum); axis([-77.5,-74.5,36,40]);
hmidB=plot(lon_midB(index_midB),lat_midB(index_midB),'r*'); % plot
stars with color red
huppB=plot(lon_uppB(index_uppB),lat_uppB(index_uppB),'m*'); % meganta
hwest=plot(lon_west(index_west),lat_west(index_west),'g*'); % yellow
% legend([hmidB, huppB, hwest],'midBtank area', ...
% 'uppBuehannaflat area', ...
% 'West estuaries area');
% legend('boxoff');
caxis([0, 100000]);shading interp; % large caxis to make background blue
for nonselected area
xlabel('Longitude', 'FontSize',9);ylabel('Latitude', 'FontSize',9);
title('Specific Areas of Probability of \itV. vulnificus\rm');

%finally save the plot

saveas(gcf,['.\Figures\Vvulnifzones-all-' num2str(yr_start) '-'
num2str(yr_end) '.fig'], 'fig');
saveas(gcf,['.\Figures\Vvulnifzones-all-' num2str(yr_start) '-'
num2str(yr_end) '.eps'], 'epsc');
saveas(gcf,['.\Figures\Vvulnifzones-all-' num2str(yr_start) '-'
num2str(yr_end) '.emf'], 'emf');
saveas(gcf,['.\Figures\Vvulnifzones-all-' num2str(yr_start) '-'
num2str(yr_end) '.png'], 'png');

%A_bis: plot TS of V vulnificus for max area in the CB

yr_seq= yr_start:yr_end;

hfigall2Bis=figure('Visible','on','Position',[1 1 1200 1500]);
clf;
subplot(3,1,1); hold on;

huppB_mean=plot(time_all,uppB_area_mean_all,'k-', 'LineWidth',2);
huppB_up =plot(time_all,uppB_area_mean_all+uppB_area_std_all,'k--
','LineWidth',1);
huppB_down=plot(time_all,uppB_area_mean_all-uppB_area_std_all,'k--
','LineWidth',1);
datetick('x','mmyy');
title(['Upper Bay area (' num2str(yr_start) '-' num2str(yr_end) ')']);
% n max=' num2str(npnts_midB_max)', year max='
num2str(yr_seq(npnts_midB_max_year)) ');
ylabel('Mean probability of \it V. vulnificus\rm ', 'FontSize',9);
set(gca,'YLim',[0 1]);
% set(gca,'XTick',[time_all(1):365:time_all(end)]);
set(gca,'XLim',[time_all(1) time_all(end)]);

```

```

    datetick('x','mmyy');

subplot(3,1,2); hold on;

    hmidB_mean=plot(time_all,midB_area_mean_all,'k-','LineWidth',2);
    hmidB_up      =plot(time_all,midB_area_mean_all+midB_area_std_all,'k--',
'LineWidth',1);
    hmidB_down=plot(time_all,midB_area_mean_all-midB_area_std_all,'k--',
'LineWidth',1);
    title(['Mid-Bay area (' num2str(yr_start) '-' num2str(yr_end) ')']);
    %;      n      max='      num2str(npnts_uppB_max)',      year      max='
num2str(yr_seq(npnts_uppB_max_year)) ');
    ylabel('Mean probability of \it V. vulnificus\rm ', 'FontSize',9);
%      set(gca,'XTick',[time_all(1):365:time_all(end)]);
    set(gca,'YLim',[0 1]);
    set(gca,'XLim',[time_all(1) time_all(end)]);
    datetick('x','mmyy');

subplot(3,1,3); hold on;

    hwest_mean=plot(time_all,west_area_mean_all,'k-','LineWidth',2);
    hwest_up      =plot(time_all,west_area_mean_all+west_area_std_all,'k--',
'LineWidth',1);
    hwest_down=plot(time_all,west_area_mean_all-west_area_std_all,'k--',
'LineWidth',1);
    title(['West estuaries area of the Bay (' num2str(yr_start) '-'
num2str(yr_end) ')']);
    %;      n      max='      num2str(npnts_west_max)',      year      max='
num2str(yr_seq(npnts_west_max_year)) ');
    ylabel('Mean probability of \it V. vulnificus\rm ', 'FontSize',9);
%      set(gca,'XTick',[time_all(1):365:time_all(end)]);
    set(gca,'YLim',[0 1]);
    set(gca,'XLim',[time_all(1) time_all(end)]);
    datetick('x','mmyy');

%finally save the plot

    saveas(gcf,['.\Figures\VvulnificusAreaTS-all-' num2str(yr_start) '-'
num2str(yr_end) '.fig'], 'fig');
    saveas(gcf,['.\Figures\VvulnificusAreaTS-all-' num2str(yr_start) '-'
num2str(yr_end) '.emf'], 'emf');
    saveas(gcf,['.\Figures\VvulnificusAreaTS-all-' num2str(yr_start) '-'
num2str(yr_end) '.eps'], 'eps');
    saveas(gcf,['.\Figures\VvulnificusAreaTS-all-' num2str(yr_start) '-'
num2str(yr_end) '.png'], 'png');

%B: plot SST, and salinity for each area with red line as the
%optimal salinity defined by Oxford study at 11.5

hfigall3=figure('Visible','on','Position',[1 1 1200 1500]); clf;

    subplot(3,2,1); hold on;

    huppB_temp_mean      =plot(time_all,uppB_temp_area_mean_all,'b-
');%;'LineWidth',1);
%      huppB_temp_up
=plot(time_all,uppB_temp_area_mean_all+uppB_temp_area_std_all,'b--
');%;'LineWidth',1);
%      huppB_temp_down      =plot(time_all,uppB_temp_area_mean_all-
uppB_temp_area_std_all,'b--');%;'LineWidth',1);

```

```

    datetick('x','mmyy');
    ylabel('Temperature (Celsius)');
    set(gca,'XLim',[time_all(1) time_all(end)]);
    set(gca,'Ylim',[-5 35]);
    set(gca,'YTick',[0 10:10:30]);
%    set(gca,'XTick',[time_all(1):365:time_all(end)]);
    title(['SST of the upper Bay (' num2str(yr_start) '-' num2str(yr_end)
    ')']);

    subplot(3,2,2); hold on;

    huppB_salt_mean =plot(time_all,uppB_salt_area_mean_all,'k-
    ');%; 'LineWidth',1);
    line([time_all(1) time_all(end)], [11.5
    11.5], 'Color', 'r', 'LineWidth', 1.5);
%    huppB_salt_up
=plot(time_all,uppB_salt_area_mean_all+uppB_salt_area_std_all,'k--
    ');%; 'LineWidth',1);
%    huppB_salt_down =plot(time_all,uppB_salt_area_mean_all-
    uppB_salt_area_std_all,'k--');%; 'LineWidth',1);
    ylabel('Salinity');
    datetick('x','mmyy');
    set(gca,'Ylim',[0 25]);
    set(gca,'YTick', 0:5:25);
    set(gca,'XLim',[time_all(1) time_all(end)]);
%    set(gca,'XTick',[time_all(1):365:time_all(end)]);
    title(['Salinity of the upper Bay (' num2str(yr_start) '-'
    num2str(yr_end) ')']);

    subplot(3,2,3); hold on;

    hmidB_temp_mean =plot(time_all,midB_temp_area_mean_all,'b-
    ');%; 'LineWidth',1);
%    hmidB_temp_up
=plot(time_all,midB_temp_area_mean_all+midB_temp_area_std_all,'b--
    ');%; 'LineWidth',1);
%    hmidB_temp_down =plot(time_all,midB_temp_area_mean_all-
    midB_temp_area_std_all,'b--');%; 'LineWidth',1);
    datetick('x','mmyy');
    ylabel('Temperature (Celsius)');
    set(gca,'XLim',[time_all(1) time_all(end)]);
    set(gca,'Ylim',[-5 35]);
    set(gca,'YTick',[0 10:10:30]);
%    set(gca,'XTick',[time_all(1):365:time_all(end)]);
    title(['SST of the mid Bay area (' num2str(yr_start) '-' num2str(yr_end)
    ')']);

    subplot(3,2,4); hold on;

    hmidB_salt_mean =plot(time_all,midB_salt_area_mean_all,'k-
    ');%; 'LineWidth',1);
    line([time_all(1) time_all(end)], [11.5
    11.5], 'Color', 'r', 'LineWidth', 1.5);
%    hmidB_salt_up
=plot(time_all,midB_salt_area_mean_all+midB_salt_area_std_all,'k--
    ');%; 'LineWidth',1);
%    hmidB_salt_down =plot(time_all,midB_salt_area_mean_all-
    midB_salt_area_std_all,'k--');%; 'LineWidth',1);
    ylabel('Salinity');
    datetick('x','mmyy');
    set(gca,'Ylim',[0 25]);
    set(gca,'XLim',[time_all(1) time_all(end)]);
    set(gca,'YTick', 0:5:25);

```

```

%       set(gca,'XTick',[time_all(1):365:time_all(end)]);
       title(['Salinity of the mid Bay area (' num2str(yr_start) '-'
num2str(yr_end) ')']);

       subplot(3,2,5); hold on;

       hwest_temp_mean           =plot(time_all,west_temp_area_mean_all,'b-
');;%,'LineWidth',1);
%
%                               hwest_temp_up
=plot(time_all,west_temp_area_mean_all+west_temp_area_std_all,'b--
');;%,'LineWidth',1);
%
%                               hwest_temp_down   =plot(time_all,west_temp_area_mean_all-
west_temp_area_std_all,'b--');;%,'LineWidth',1);

       datetick('x','mmyy');
       ylabel('Temperature (Celsius)');
       set(gca,'Ylim',[-5 35]);
       set(gca,'XLim',[time_all(1) time_all(end)]);
       set(gca,'YTick',[0 10:10:30]);
%       set(gca,'XTick',[time_all(1):365:time_all(end)]);
       title(['SST of West estuaries area of the bay (' num2str(yr_start) '-'
num2str(yr_end) ')']);

       subplot(3,2,6); hold on;

       hwest_salt_mean           =plot(time_all,west_salt_area_mean_all,'k-
');;%,'LineWidth',1);
       line([time_all(1)                               time_all(end)], [11.5
11.5], 'Color', 'r', 'LineWidth', 1.5);
%
%                               hwest_salt_up
=plot(time_all,west_salt_area_mean_all+west_salt_area_std_all,'k--
');;%,'LineWidth',1);
%
%                               hwest_salt_down   =plot(time_all,west_salt_area_mean_all-
west_salt_area_std_all,'k--');;%,'LineWidth',1);
       ylabel('Salinity');

       datetick('x','mmyy');
       axis([time_all(1),time_all(end),0,12]);
       set(gca,'Ylim',[0 25]);
       set(gca,'YTick', 0:5:25);
       set(gca,'XLim',[time_all(1) time_all(end)]);
       title(['Salinity of West estuaries area of the bay (' num2str(yr_start)
-' num2str(yr_end) ')']);

% Save plot hfigall3

       saveas(gcf,['.\Figures\TempSaltAreaTS-all-' num2str(yr_start) '-'
num2str(yr_end) '.fig'], 'fig');
       saveas(gcf,['.\Figures\TempSaltAreaTS-all-' num2str(yr_start) '-'
num2str(yr_end) '.eps'], 'epsc');
       saveas(gcf,['.\Figures\TempSaltAreaTS-all-' num2str(yr_start) '-'
num2str(yr_end) '.emf'], 'emf');
       saveas(gcf,['.\Figures\TempSaltAreaTS-all-' num2str(yr_start) '-'
num2str(yr_end) '.png'], 'png');

```

Script 5

```

%----program plot_Vulnificus_average_multi_year_bis.m ----
% This programs tries open a chosen series of years matlab files that
% contain the Vibrio vulnificus
% probability of surface water of CBay, then the data is processed
% I: for each year
% 1) take area average of 3 most aparent locations where V vulnificus
% probability is high
% to produce a time sereis of that area. And the difference between
% individual cells within
% the area and the area average is saved as a set of random variables to
% calculate
% varaince/standard deviation as a mesure of the variability within that
% area
% Hence, two time series for each area
% will be obtained and plotted against time: a) time series of area
% average
% b) time series of standard deviation
%
% 2) a plot is made that contain the curve of average time series, with
% standard deviation as upper and
% lower bound envelop sitting in the average time series
%
% 3) a separate plot is made to show the areas that are concerned.
%
% II: the area average and standard deviation of vvulnificus probability,
% SST and Salinity for each year
% will be put together into a long time series. Plots of them are also
% made to show
% the interannual variability of them.
%
% find model data file and year of it

modeloutputdir=input('please input the model output directory: (e.g.
'../old_data/') ');

% find the model data files

modelfilenames=dir([modeloutputdir '/HABdata_V*.mat']);

Nfile=length(modelfilenames); % number of files found

if(Nfile<=0)
    error(['Not able to find files with ' modeloutputdir '/HAB*.mat']);
end
display('The following are the model files you have:');

for ifile=1:Nfile
    display(['file number ', num2str(ifile), ': '
modelfilenames(ifile).name]); end

y_start=input(['Please give the starting file number you want (1-'
num2str(Nfile) '): ']);
y_end =input(['Please give the ending file number you want ('
num2str(y_start) '-' num2str(Nfile) '): ']);
if(y_end<y_start)
    error('Oops, you can not have ending year earlier than starting
year');
end

% modelname=input('Please give the name of the model ('model13' or
'model15') :');

```

```

    yesno_individual_year=input('Please indicate yes or no for plotting
individual years (1=yes,0=no): ');
% processs the data year by year

display('Searching for data of Vibrio vulnificus ...');

for y_choose= y_start: y_end

    modeloutputfile=[modeloutputdir      '/'      modelfilenames(y_choose).name];
%find file name of that particular year

    display(['Processing file :' modeloutputfile ' ...']);
% load the data
    load(modeloutputfile);

% list what is in the data file
% whos
    clear kmicall snpball %free memory for these are not used in this program

%find the dimensions
    [nt,ny,nx]=size(vvulnifall);
%make sure the grid information all have the same dimensions
    mask=mask_rho(1:ny,1:nx);
    lat=lat(1:ny,1:nx);
    lon=lon(1:ny,1:nx);

%find beginning and ending year
    if(y_choose==y_start)
        yr_start=dateall(1,1);
    end

    if(y_choose==y_end)
        yr_end=dateall(1,1);
    end

%find the sum of the year for all cells

    indexland=find(mask<0.5);
    vvulnif_sum=squeeze(sum(vvulnifall,1));
    vvulnif_sum(indexland)=nan; %make sure the land points are excluded
% vvulnifall(indexland)=nan; %make sure the land points are excluded

%end

    if(y_choose==y_start) %find the boxes
%
        midB_iy=1:37; midB_ix=39:75;
        midB_iy=28:37; midB_ix=39:75;
        lon_midB=lon(midB_iy,midB_ix); lat_midB=lat(midB_iy,midB_ix);
    mask_midB=mask(midB_iy,midB_ix);
        midB2_iy=1:27; midB2_ix=39:60;
        lon_midB2=lon(midB2_iy,midB2_ix); lat_midB2=lat(midB2_iy,midB2_ix);
    mask_midB2=mask(midB2_iy,midB2_ix);

        uppB_iy=102:149; uppB_ix=27:99;
        lon_uppB=lon(uppB_iy,uppB_ix); lat_uppB=lat(uppB_iy,uppB_ix);
    mask_uppB=mask(uppB_iy,uppB_ix);

        west_iy=1:37; west_ix=76:99;
        lon_west=lon(west_iy,west_ix); lat_west=lat(west_iy,west_ix);
    mask_west=mask(west_iy,west_ix);
    end
    index_midB=find(vvulnif_sum(midB_iy,midB_ix)>0);

```

```

index_midB2=find(vvulnif_sum(midB2_iy,midB2_ix)>0);
index_uppB=find(vvulnif_sum(uppB_iy,uppB_ix)>0);
index_west=find(vvulnif_sum(west_iy,west_ix)>0);

display('Processing data year by year (file by file)');

%%%%%%%%%%%%%%%%%%%%%%%%%%%%%%%%%%%%%%%%%%%%%%%%%%%%%%%%%%%%%%%%%%%%%%%%
%%%%%%%%%%%%%%%%%%%%%%%%%%%%%%%%%%%%%%%%%%%%%%%%%%%%%%%%%%%%%%%%%%%%%%%%
%values in the box
midB_select=vvulnifall(1:nt,midB_iy,midB_ix);
midB2_select=vvulnifall(1:nt,midB2_iy,midB2_ix);
uppB_select=vvulnifall(1:nt,uppB_iy,uppB_ix);
west_select=vvulnifall(1:nt,west_iy,west_ix);

clear vvulnifall; %free memory for not used after this

%values of the indexd portion set in the box

midB_select_final=midB_select;
midB2_select_final=midB2_select;
uppB_select_final=uppB_select;
west_select_final=west_select;

% calculate the area mean and also standard deviation

midB_area_mean=zeros([nt,1]); midB_area_std=zeros([nt,1]);
midB2_area_mean=zeros([nt,1]); midB2_area_std=zeros([nt,1]);
uppB_area_mean=zeros([nt,1]); uppB_area_std=zeros([nt,1]);
west_area_mean=zeros([nt,1]); west_area_std=zeros([nt,1]);

for it=1:nt
midB_area_mean(it)=mean([squeeze(midB_select_final(it,:))
squeeze(midB2_select_final(it,:))]); %midBtank
midB_area_std(it) = std([squeeze(midB_select_final(it,:))
squeeze(midB2_select_final(it,:))]);
% midB_area_mean(indexland)=nan;
% midB_area_std(indexland)=nan;

uppB_area_mean(it)=mean(squeeze(uppB_select_final(it,:)));
%uppBuehanna
uppB_area_std(it) = std(squeeze(uppB_select_final(it,:)));
% uppB_area_mean(indexland)=nan;
% uppB_area_std(indexland)=nan;

west_area_mean(it)=mean(squeeze(west_select_final(it,:))); %standard
deviation
west_area_std(it) = std(squeeze(west_select_final(it,:)));
% west_area_mean(indexland)=nan;
% west_area_std(indexland)=nan;
end

% midB_area_mean(indexland)=nan;
% midB_area_std(indexland)=nan;
% uppB_area_mean(indexland)=nan;
% uppB_area_std(indexland)=nan;
% west_area_mean(indexland)=nan;
% west_area_std(indexland)=nan;

% find time axis for making time series plots
time=datenum(dateall); %this converts the dates in dateall array into a
time axis series in days from 0001-01-01 0 0 0 AD

```

```

yr_choose=dateall(1,1); %get the year of the data

% Concatenate the mean and standard deviation data to a grand array

if(y_choose==y_start)
    midB_area_mean_all=midB_area_mean; midB_area_std_all=midB_area_std;
    uppB_area_mean_all=uppB_area_mean; uppB_area_std_all=uppB_area_std;
    west_area_mean_all=west_area_mean; west_area_std_all=west_area_std;
    time_all=time;
else
    midB_area_mean_all=[midB_area_mean_all; midB_area_mean];
midB_area_std_all=[midB_area_std_all; midB_area_std];
    uppB_area_mean_all=[uppB_area_mean_all; uppB_area_mean];
uppB_area_std_all=[uppB_area_std_all; uppB_area_std];
    west_area_mean_all=[west_area_mean_all; west_area_mean];
west_area_std_all=[west_area_std_all; west_area_std];
    time_all=[time_all;time];
end

%%%%%%%%%%%%%%%%%%%%%%%%%%%%%%%%%%%%%%%%%%%%%%%%%%%%%%%%%%%%%%%%%%%%%%%%
%%%%%%%%%%%%%%%%%%%%%%%%%%%%%%%%%%%%%%%%%%%%%%%%%%%%%%%%%%%%%%%%%%%%%%%%

    if (yesno_individual_year==1)
% make plot

%%%%%%%%%%%%%%%%%%%%%%%%%%%%%%%%%%%%%%%%%%%%%%%%%%%%%%%%%%%%%%%%%%%%%%%%
%%%%%%%%%%%%%%%%%%%%%%%%%%%%%%%%%%%%%%%%%%%%%%%%%%%%%%%%%%%%%%%%%%%%%%%%

    hfig2=figure('Visible','on','Position',[1 1 1200 1500]);
    clf;

    subplot(2,2,1); hold on;

    pcolor(lon, lat, vvulnif_sum); axis([-77.5,-74.5,36,40]);
    hmidB=plot(lon_midB(index_midB),lat_midB(index_midB),'r*'); % plot
stars with color red
    hmidB2=plot(lon_midB2(index_midB2),lat_midB2(index_midB2),'r*'); % plot
stars with color red
%    huppB=plot(lon_uppB(index_uppB),lat_uppB(index_uppB),'m*'); % meganta
    hwest=plot(lon_west(index_west),lat_west(index_west),'g*'); % yellow
%    legend([hmidB, huppB, hwest],'midBtank area', ...
%           'uppBuehanna flat area', ...
%           'West estuaries area');
%    legend('boxoff');
    caxis([0, 100000]);shading interp; % large caxis to make background blue
for nonselected area
    xlabel('Longitude', 'FontSize',9);ylabel('Latitude', 'FontSize',9);
    title('Specific Areas of Probability of \itV. vulnificus\rm');

    subplot(2,2,2); hold on;

    huppB_mean=plot(time,uppB_area_mean,'m-', 'LineWidth',2);
    huppB_up =plot(time,uppB_area_mean+uppB_area_std,'m--', 'LineWidth',1);
    huppB_down=plot(time,uppB_area_mean-uppB_area_std,'m--', 'LineWidth',1);
    datetick('x','mmyy');
    title(['Top of the upper Bay area (' num2str(yr_choose) ')']);
    ylabel('Mean probability of \it V. vulnificus\rm ', 'FontSize',9);

    set(gca,'XLim',[time(1) time(end)]);
    set(gca,'XTick',time(1):60:time(end));
    set(gca,'XTickLabel',{'Jan','Mar','May','Jul','Sep','Nov','Jan'})
    set(gca,'YLim',[0 1]);

```



```

subplot(2,2,3); hold on;

hmidB_mean=plot(time,midB_area_mean,'r-','LineWidth',2);
hmidB_up =plot(time,midB_area_mean+midB_area_std,'r--','LineWidth',1);
hmidB_down=plot(time,midB_area_mean-midB_area_std,'r--','LineWidth',1);
datetick('x','mmyy');
title(['Bottom Bay area (' num2str(yr_choose) ')']);
ylabel('Mean probability of \it V. vulnificus\rm ', 'FontSize',9);
set(gca,'XLim',[time(1) time(end)]);
set(gca,'XTick',time(1):60:time(end));
set(gca,'XTickLabel',{'Jan','Mar','May','Jul','Sep','Nov','Jan'})
set(gca,'YLim',[0 1]);

% subplot(2,2,4); hold on;

% hwest_mean=plot(time,west_area_mean,'g-','LineWidth',2);
% hwest_up =plot(time,west_area_mean+west_area_std,'g--','LineWidth',1);
% hwest_down=plot(time,west_area_mean-west_area_std,'g--','LineWidth',1);
% datetick('x','mmyy');
% title(['West estuaries area of the bay (' num2str(yr_choose) ')']);
% ylabel('Mean probability of \it V. vulnificus\rm ', 'FontSize',9);
% set(gca,'XLim',[time(1) time(end)]);
% set(gca,'XTick',time(1):60:time(end));
% set(gca,'XTickLabel',{'Jan','Mar','May','Jul','Sep','Nov','Jan'})
% set(gca,'YLim',[0 1]);

saveas(gcf,['.\Figures\VvulnifiZonesTS_bis-' num2str(yr_choose) '.fig'],
'fig');
saveas(gcf,['.\Figures\VvulnifiZonesTS_bis-' num2str(yr_choose) '.eps'],
'eps');
saveas(gcf,['.\Figures\VvulnifiZonesTS_bis-' num2str(yr_choose) '.emf'],
'emf');
saveas(gcf,['.\Figures\VvulnifiZonesTS_bis-' num2str(yr_choose) '.png'],
'png');

% delete(hfig2);

% in order to make a prettier figure about the area
% we need to save the data of chosen places
%

end
%end of plotting individual years
%Light seasonal study.
%%%%%%%%%%%%%%%%%%%%%%%%%%%%%%%%%%%%%%%%%%%%%%%%%%%%%%%%%%%%%%%%%%%%%%%%
%%%%%%%%%%%%%%%%%%%%%%%%%%%%%%%%%%%%%%%%%%%%%%%%%%%%%%%%%%%%%%%%%%%%%%%%
% select the values of the SST and Salinity for each of the point in
% areas
% SST values in the box
midB_temp_select=tempall(1:nt,midB_iy,midB_ix);
midB2_temp_select=tempall(1:nt,midB2_iy,midB2_ix);
uppB_temp_select=tempall(1:nt,uppB_iy,uppB_ix);
west_temp_select=tempall(1:nt,west_iy,west_ix);
clear tempall; %free memory for not used after this

% Salinity values in the box
midB_salt_select=saltall(1:nt,midB_iy,midB_ix);
midB2_salt_select=saltall(1:nt,midB2_iy,midB2_ix);
uppB_salt_select=saltall(1:nt,uppB_iy,uppB_ix);
west_salt_select=saltall(1:nt,west_iy,west_ix);

clear saltall; %free memory for not used after this

```

```

% SST values of the indexd portion set in the box

midB_temp_select_final=midB_temp_select(1:nt,index_midB);
midB2_temp_select_final=midB2_temp_select(1:nt,index_midB2);
uppB_temp_select_final=uppB_temp_select(1:nt,index_uppB);
west_temp_select_final=west_temp_select(1:nt,index_west);

% Salinity values of the indexd portion set in the box
midB_salt_select_final=midB_salt_select(1:nt,index_midB);
midB2_salt_select_final=midB2_salt_select(1:nt,index_midB2);
uppB_salt_select_final=uppB_salt_select(1:nt,index_uppB);
west_salt_select_final=west_salt_select(1:nt,index_west);

%define arrays to store mean and standard deviation
midB_temp_area_mean=zeros([nt,1]);
midB_temp_area_std=zeros([nt,1]);
uppB_temp_area_mean=zeros([nt,1]);
uppB_temp_area_std=zeros([nt,1]);
west_temp_area_mean=zeros([nt,1]);
west_temp_area_std=zeros([nt,1]);

midB_salt_area_mean=zeros([nt,1]);
midB_salt_area_std=zeros([nt,1]);
uppB_salt_area_mean=zeros([nt,1]);
uppB_salt_area_std=zeros([nt,1]);
west_salt_area_mean=zeros([nt,1]);
west_salt_area_std=zeros([nt,1]);

for it=1:nt
midB_temp_area_mean(it)=mean([squeeze(midB_temp_select_final(it,:))
squeeze(midB2_temp_select_final(it,:))]); %SST midBtank
midB_temp_area_std(it) = std([squeeze(midB_temp_select_final(it,:))
squeeze(midB2_temp_select_final(it,:))]);

midB_salt_area_mean(it)=mean([squeeze(midB_salt_select_final(it,:))
squeeze(midB2_salt_select_final(it,:))]); %Salinity midBtank
midB_salt_area_std(it) = std([squeeze(midB_salt_select_final(it,:))
squeeze(midB2_salt_select_final(it,:))]);

uppB_temp_area_mean(it)=mean(squeeze(uppB_temp_select_final(it,:)));
%SST uppBuehanna
uppB_temp_area_std(it) = std(squeeze(uppB_temp_select_final(it,:)));

uppB_salt_area_mean(it)=mean(squeeze(uppB_salt_select_final(it,:)));
%Salinity uppBuehanna
uppB_salt_area_std(it) = std(squeeze(uppB_salt_select_final(it,:)));

west_temp_area_mean(it)=mean(squeeze(west_temp_select_final(it,:)));
%SST West estuaries
west_temp_area_std(it) = std(squeeze(west_temp_select_final(it,:)));

west_salt_area_mean(it)=mean(squeeze(west_salt_select_final(it,:)));
%Salinity West estuaries
west_salt_area_std(it) = std(squeeze(west_salt_select_final(it,:)));

end

% find time axis for plots (days)

time=datetime(dateall); %this converts the dates in dateall array into a
time axis series in days from 0001-01-01 0 0 0 AD

%concatenate data into a grand array for keeping all years

```

```

        if(y_choose==y_start)
            midB_temp_area_mean_all=midB_temp_area_mean;
midB_temp_area_std_all=midB_temp_area_std;
            uppB_temp_area_mean_all=uppB_temp_area_mean;
uppB_temp_area_std_all=uppB_temp_area_std;
            west_temp_area_mean_all=west_temp_area_mean;
west_temp_area_std_all=west_temp_area_std;

            midB_salt_area_mean_all=midB_salt_area_mean;
midB_salt_area_std_all=midB_salt_area_std;
            uppB_salt_area_mean_all=uppB_salt_area_mean;
uppB_salt_area_std_all=uppB_salt_area_std;
            west_salt_area_mean_all=west_salt_area_mean;
west_salt_area_std_all=west_salt_area_std;

        else
            midB_temp_area_mean_all=[midB_temp_area_mean_all; midB_temp_area_mean];
midB_temp_area_std_all=[midB_temp_area_std_all; midB_temp_area_std];
            uppB_temp_area_mean_all=[uppB_temp_area_mean_all; uppB_temp_area_mean];
uppB_temp_area_std_all=[uppB_temp_area_std_all; uppB_temp_area_std];
            west_temp_area_mean_all=[west_temp_area_mean_all; west_temp_area_mean];
west_temp_area_std_all=[west_temp_area_std_all; west_temp_area_std];

            midB_salt_area_mean_all=[midB_salt_area_mean_all; midB_salt_area_mean];
midB_salt_area_std_all=[midB_salt_area_std_all; midB_salt_area_std];
            uppB_salt_area_mean_all=[uppB_salt_area_mean_all; uppB_salt_area_mean];
uppB_salt_area_std_all=[uppB_salt_area_std_all; uppB_salt_area_std];
            west_salt_area_mean_all=[west_salt_area_mean_all; west_salt_area_mean];
west_salt_area_std_all=[west_salt_area_std_all; west_salt_area_std];

        end

        if(yesno_individual_year==1)

% make new plot of V vulnificus probability and SST and Salinity

            hfig3=figure('Visible','on','Position',[1 1 1200 1500]); clf;

            subplot(3,2,1); hold on;

            huppB_temp_mean =plot(time,uppB_temp_area_mean,'b-');%,'LineWidth',2);
huppB_temp_up      =plot(time,uppB_temp_area_mean+uppB_temp_area_std,'b--
');%,'LineWidth',1);
            huppB_temp_down      =plot(time,uppB_temp_area_mean-uppB_temp_area_std,'b--
');%,'LineWidth',1);
            set(gca,'XTick',time(1):60:time(end));
            datetick('x','mmm');
            ylabel('Temperature (Celsius)');
            set(gca,'XLim',[time(1) time(end)]);
            set(gca,'Ylim',[-5 35]);
            set(gca,'YTick',[0 10:10:30]);
            title(['SST Top of the upper Bay area (' num2str(yr_choose) ')']);

            subplot(3,2,2); hold on;

            huppB_salt_mean =plot(time,uppB_salt_area_mean,'k-');%,'LineWidth',2);
huppB_salt_up      =plot(time,uppB_salt_area_mean+uppB_salt_area_std,'k--
');%,'LineWidth',1);
            huppB_salt_down      =plot(time,uppB_salt_area_mean-uppB_salt_area_std,'k--
');%,'LineWidth',1);
            line([time_all(1)                                time_all(end)], [11.5
11.5], 'Color', 'r', 'LineWidth', 1.5);

```

```

ylabel('Salinity');
datetick('x','mmm');
set(gca,'XLim',[time(1) time(end)]);
set(gca,'Ylim',[0 35]);
set(gca,'YTick', 0:10:35);
title(['Salinity Top of the upper Bay area (' num2str(yr_choose) ')']);

subplot(3,2,3); hold on;

hmidB_temp_mean =plot(time,midB_temp_area_mean,'b-');%,'LineWidth',2);
hmidB_temp_up   =plot(time,midB_temp_area_mean+midB_temp_area_std,'b--');%,'LineWidth',1);
hmidB_temp_down =plot(time,midB_temp_area_mean-midB_temp_area_std,'b--');%,'LineWidth',1);
set(gca,'XTick', time(1):60:time(end));
datetick('x','mmm');
ylabel('Temperature (Celsius)');
set(gca,'XLim', [time(1) time(end)]);
set(gca,'Ylim', [-5 35]);
set(gca,'YTick', [0 10:10:30]);
title(['SST bottom Bay area (' num2str(yr_choose) ')']);
subplot(3,2,4); hold on;
hmidB_salt_mean =plot(time,midB_salt_area_mean,'k-');%,'LineWidth',2);
hmidB_salt_up   =plot(time,midB_salt_area_mean+midB_salt_area_std,'k--');%,'LineWidth',1);
hmidB_salt_down =plot(time,midB_salt_area_mean-midB_salt_area_std,'k--');%,'LineWidth',1);
line([time_all(1) time_all(end)], [11.5 11.5], 'Color', 'r', 'LineWidth', 1.5);
ylabel('Salinity');
datetick('x','mmm');
set(gca,'Ylim',[0 35]);
set(gca,'YTick', 0:10:35);
set(gca,'XLim',[time(1) time(end)]);
title(['Salinity bottom Bay area (' num2str(yr_choose) ')']);
% subplot(3,2,5); hold on;

% hwest_temp_mean =plot(time,west_temp_area_mean,'b-');%,'LineWidth',2);
% hwest_temp_up   =plot(time,west_temp_area_mean+west_temp_area_std,'b--');%,'LineWidth',1);
% hwest_temp_down =plot(time,west_temp_area_mean-west_temp_area_std,'b--');%,'LineWidth',1);
% set(gca,'XTick', time(1):60:time(end));
% datetick('x','mmm');
% ylabel('Temperature (Celsius)');
% set(gca,'Ylim', [-5 35]);
% set(gca,'XLim', [time(1) time(end)]);
% set(gca,'YTick', [0 10:10:30]);
% title(['SST open ocean of the bay (' num2str(yr_choose) ')']);

% subplot(3,2,6); hold on;

% hwest_salt_mean =plot(time,west_salt_area_mean,'k-');%,'LineWidth',5);
% hwest_salt_up   =plot(time,west_salt_area_mean+west_salt_area_std,'k--');%,'LineWidth',1);
% hwest_salt_down =plot(time,west_salt_area_mean-west_salt_area_std,'k--');%,'LineWidth',1);
% line([time_all(1) time_all(end)], [11.5 11.5], 'Color', 'r', 'LineWidth', 1.5);
% ylabel('Salinity');
% datetick('x','mmm');
% set(gca,'Ylim',[0 35]);
% set(gca,'YTick', 0:10:35);

```

```

%       set(gca,'XLim',[time(1) time(end)]);
%       title(['Salinity open ocean of the bay (' num2str(yr_choose) ')']);

% Save plot hfig3

saveas(gcf,['.\Figures\TempSaltAreaTS_bis-' num2str(yr_choose) '.fig'],
'fig');
saveas(gcf,['.\Figures\TempSaltAreaTS_bis-' num2str(yr_choose) '.eps'],
'eps');
saveas(gcf,['.\Figures\TempSaltAreaTS_bis-' num2str(yr_choose) '.emf'],
'emf');
saveas(gcf,['.\Figures\TempSaltAreaTS_bis-' num2str(yr_choose) '.png'],
'png');

end %end of the plotting of individual year T and S

%end %end of the y_choose loop
end %end of plotting individual years

%finally plot all the years together

%A: plot TS of V vulnificus for max area in the CB

hfigall2=figure('Visible','on');%,'Position',[1 1 1200 1500]);
clf;

%       subplot(2,2,1);
%       hold on;

pcolor(lon, lat, vvulnif_sum); axis([-77.5,-74.5,36,40]);
hmidB=plot(lon_midB(index_midB),lat_midB(index_midB),'r*'); % plot
stars with color red
hmidB2=plot(lon_midB2(index_midB2),lat_midB2(index_midB2),'r*'); % plot
stars with color red
huppB=plot(lon_uppB(index_uppB),lat_uppB(index_uppB),'m*'); % meganta
%       hwest=plot(lon_west(index_west),lat_west(index_west),'g*'); % yellow
%       legend([hmidB, huppB, hwest],'midBtank area', ...
%               'uppBuehanna flat area', ...
%               'West estuaries area');
%       legend('boxoff');
%       caxis([0, 100000]);shading interp; % large caxis to make background blue
for nonselected area
xlabel('Longitude', 'FontSize',9);ylabel('Latitude', 'FontSize',9);
title('Specific Areas of Probability of \itV. vulnificus\rm');

%finally save the plot

saveas(gcf,['.\Figures\Vvulnifzones-all_bis-' num2str(yr_start) '-'
num2str(yr_end) '.fig'], 'fig');
saveas(gcf,['.\Figures\Vvulnifzones-all_bis-' num2str(yr_start) '-'
num2str(yr_end) '.eps'], 'eps');
saveas(gcf,['.\Figures\Vvulnifzones-all_bis-' num2str(yr_start) '-'
num2str(yr_end) '.emf'], 'emf');
saveas(gcf,['.\Figures\Vvulnifzones-all_bis-' num2str(yr_start) '-'
num2str(yr_end) '.png'], 'png');

%A_bis: plot TS of V vulnificus for max area in the CB

yr_seq= yr_start:yr_end;

hfigall2Bis=figure('Visible','on','Position',[1 1 1200 1500]);
clf;

```

```

subplot(3,1,1); hold on;

huppB_mean=plot(time_all,uppB_area_mean_all,'k-','LineWidth',2);
huppB_up      =plot(time_all,uppB_area_mean_all+uppB_area_std_all,'k--',
'LineWidth',1);
huppB_down=plot(time_all,uppB_area_mean_all-uppB_area_std_all,'k--',
'LineWidth',1);
datetick('x','mmyy');
title(['Top of the upper Bay area (' num2str(yr_start) '-'
num2str(yr_end) ')']);
%      n      max='      num2str(npnts_midB_max)',      year      max='
num2str(yr_seq(npnts_midB_max_year)) ');
ylabel('Mean probability of \it V. vulnificus\rm ', 'FontSize',9);
set(gca,'YLim',[0 1]);
%      set(gca,'XTick',[time_all(1):365:time_all(end)]);
set(gca,'XLim',[time_all(1) time_all(end)]);
datetick('x','mmyy');
subplot(3,1,2); hold on;

hmidB_mean=plot(time_all,midB_area_mean_all,'k-','LineWidth',2);
hmidB_up      =plot(time_all,midB_area_mean_all+midB_area_std_all,'k--',
'LineWidth',1);
hmidB_down=plot(time_all,midB_area_mean_all-midB_area_std_all,'k--',
'LineWidth',1);
title(['Bottom Bay area (' num2str(yr_start) '-' num2str(yr_end) ')']);
%      n      max='      num2str(npnts_uppB_max)',      year      max='
num2str(yr_seq(npnts_uppB_max_year)) ');
ylabel('Mean probability of \it V. vulnificus\rm ', 'FontSize',9);
%      set(gca,'XTick',[time_all(1):365:time_all(end)]);
set(gca,'YLim',[0 1]);
set(gca,'XLim',[time_all(1) time_all(end)]);
datetick('x','mmyy');

%      subplot(3,1,3); hold on;

%      hwest_mean=plot(time_all,west_area_mean_all,'k-','LineWidth',2);
%      hwest_up      =plot(time_all,west_area_mean_all+west_area_std_all,'k--',
%      'LineWidth',1);
%      hwest_down=plot(time_all,west_area_mean_all-west_area_std_all,'k--',
%      'LineWidth',1);
%      title(['Open ocean of the Bay (' num2str(yr_start) '-' num2str(yr_end)
%      ')']);
%      %';      n      max='      num2str(npnts_west_max)      ',      year      max='
num2str(yr_seq(npnts_west_max_year)) ');
%      ylabel('Mean probability of \it V. vulnificus\rm ', 'FontSize',9);
%      set(gca,'XTick',[time_all(1):365:time_all(end)]);
%      set(gca,'YLim',[0 1]);
%      set(gca,'XLim',[time_all(1) time_all(end)]);
%      datetick('x','mmyy');
%      %finally save the plot

saveas(gcf,['.\Figures\VvulnificusAreaTS-all_bis-' num2str(yr_start) '-'
num2str(yr_end) '.fig'], 'fig');
saveas(gcf,['.\Figures\VvulnificusAreaTS-all_bis-' num2str(yr_start) '-'
num2str(yr_end) '.emf'], 'emf');
saveas(gcf,['.\Figures\VvulnificusAreaTS-all_bis-' num2str(yr_start) '-'
num2str(yr_end) '.eps'], 'eps');
saveas(gcf,['.\Figures\VvulnificusAreaTS-all_bis-' num2str(yr_start) '-'
num2str(yr_end) '.png'], 'png');

%B: plot SST, and salinity for each area with red line as the
%optimal salinity defined by Oxford study at 11.5

```

```

hfigall3=figure('Visible','on','Position',[1 1 1200 1500]); clf;

subplot(3,2,1); hold on;
huppB_temp_mean =plot(time_all,huppB_temp_area_mean_all,'b-');%,'LineWidth',1);
%
% huppB_temp_up
=plot(time_all,huppB_temp_area_mean_all+huppB_temp_area_std_all,'b--');%,'LineWidth',1);
%
% huppB_temp_down =plot(time_all,huppB_temp_area_mean_all-huppB_temp_area_std_all,'b--');%,'LineWidth',1);
datetick('x','mmyy');
ylabel('Temperature (Celsius)');
set(gca,'XLim',[time_all(1) time_all(end)]);
set(gca,'Ylim',[-5 35]);
set(gca,'YTick',[0 10:10:30]);
%
set(gca,'XTick',[time_all(1):365:time_all(end)]);
title(['SST of the top upper Bay (' num2str(yr_start) '-' num2str(yr_end) ')']);
subplot(3,2,2); hold on;

huppB_salt_mean =plot(time_all,huppB_salt_area_mean_all,'k-');%,'LineWidth',1);
line([time_all(1) time_all(end)], [11.5 11.5], 'Color', 'r', 'LineWidth', 1.5);
%
% huppB_salt_up
=plot(time_all,huppB_salt_area_mean_all+huppB_salt_area_std_all,'k--');%,'LineWidth',1);
%
% huppB_salt_down =plot(time_all,huppB_salt_area_mean_all-huppB_salt_area_std_all,'k--');%,'LineWidth',1);
ylabel('Salinity');
datetick('x','mmyy');
set(gca,'Ylim',[0 35]);
set(gca,'XLim',[time_all(1) time_all(end)]);
set(gca,'YTick', 0:10:35);
%
set(gca,'XTick',[time_all(1):365:time_all(end)]);
title(['Salinity of the top upper Bay (' num2str(yr_start) '-' num2str(yr_end) ')']);

subplot(3,2,3); hold on;

hmidB_temp_mean =plot(time_all,hmidB_temp_area_mean_all,'b-');%,'LineWidth',1);
%
% hmidB_temp_up
=plot(time_all,hmidB_temp_area_mean_all+hmidB_temp_area_std_all,'b--');%,'LineWidth',1);
%
% hmidB_temp_down =plot(time_all,hmidB_temp_area_mean_all-hmidB_temp_area_std_all,'b--');%,'LineWidth',1);
datetick('x','mmyy');
ylabel('Temperature (Celsius)');
set(gca,'XLim',[time_all(1) time_all(end)]);
set(gca,'Ylim',[-5 35]);
set(gca,'YTick',[0 10:10:30]);
%
set(gca,'XTick',[time_all(1):365:time_all(end)]);
title(['SST of the bottom Bay area (' num2str(yr_start) '-' num2str(yr_end) ')']);
subplot(3,2,4); hold on;

hmidB_salt_mean =plot(time_all,hmidB_salt_area_mean_all,'k-');%,'LineWidth',1);
line([time_all(1) time_all(end)], [11.5 11.5], 'Color', 'r', 'LineWidth', 1.5);

```

```

%
% hmidB_salt_up
=plot(time_all,midB_salt_area_mean_all+midB_salt_area_std_all,'k--
');%,'LineWidth',1);
% hmidB_salt_down =plot(time_all,midB_salt_area_mean_all-
midB_salt_area_std_all,'k--');%,'LineWidth',1);
ylabel('Salinity');
datetick('x','mmyy');
set(gca,'Ylim',[0 35]);
set(gca,'XLim',[time_all(1) time_all(end)]);
set(gca,'YTick', 0:10:35);
% set(gca,'XTick',[time_all(1):365:time_all(end)]);
title(['Salinity of the bottom Bay area (' num2str(yr_start) '-'
num2str(yr_end) ')']);
% subplot(3,2,5); hold on;
% hwest_temp_mean =plot(time_all,west_temp_area_mean_all,'b-
');%,'LineWidth',1);
% hwest_temp_up
=plot(time_all,west_temp_area_mean_all+west_temp_area_std_all,'b--
');%,'LineWidth',1);
% hwest_temp_down =plot(time_all,west_temp_area_mean_all-
west_temp_area_std_all,'b--');%,'LineWidth',1);
% datetick('x','mmyy');
% ylabel('Temperature (Celsius)');
% set(gca,'Ylim',[-5 35]);
% set(gca,'XLim',[time_all(1) time_all(end)]);
% set(gca,'YTick',[0 10:10:30]);
% set(gca,'XTick',[time_all(1):365:time_all(end)]);
% title(['SST of open ocean of the bay (' num2str(yr_start) '-'
num2str(yr_end) ')']);
% subplot(3,2,6); hold on;
% hwest_salt_mean =plot(time_all,west_salt_area_mean_all,'k-
');%,'LineWidth',1);
% line([time_all(1) time_all(end)],[11.5
11.5],'Color','r','LineWidth',1.5);
% hwest_salt_up
=plot(time_all,west_salt_area_mean_all+west_salt_area_std_all,'k--
');%,'LineWidth',1);
% hwest_salt_down =plot(time_all,west_salt_area_mean_all-
west_salt_area_std_all,'k--');%,'LineWidth',1);
% ylabel('Salinity');
% datetick('x','mmyy');
% axis([time_all(1),time_all(end),0,12]);
% set(gca,'Ylim',[0 35]);
% set(gca,'XLim',[time_all(1) time_all(end)]);
% set(gca,'YTick', 0:10:35);
% title(['Salinity of open ocean of the bay (' num2str(yr_start) '-'
num2str(yr_end) ')']);

% Save plot hfigall3

saveas(gcf,['.\Figures\TempSaltAreaTS-all_bis-' num2str(yr_start) '-'
num2str(yr_end) '.fig'],'fig');
saveas(gcf,['.\Figures\TempSaltAreaTS-all_bis-' num2str(yr_start) '-'
num2str(yr_end) '.eps'],'epsc');
saveas(gcf,['.\Figures\TempSaltAreaTS-all_bis-' num2str(yr_start) '-'
num2str(yr_end) '.emf'],'emf');
saveas(gcf,['.\Figures\TempSaltAreaTS-all_bis-' num2str(yr_start) '-'
num2str(yr_end) '.png'],'png');

```


References

1. **Amaro, C., and E. G. Biosca.** 1996. *Vibrio vulnificus* biotype 2, pathogenic for eels, is also an opportunistic pathogen for humans. *Appl Environ Microbiol* **62**:1454-7.
2. **Biosca, E. G., J. D. Oliver, and C. Amaro.** 1996. Phenotypic characterization of *Vibrio vulnificus* biotype 2, a lipopolysaccharide-based homogeneous O serogroup within *Vibrio vulnificus*. *Appl Environ Microbiol* **62**:918-927.
3. **Bisharat, N., V. Agmon, R. Finkelstein, R. Raz, G. Ben-Dror, L. Lerner, S. Soboh, R. Colodner, D. N. Cameron, D. L. Wykstra, D. L. Swerdlow, and J. J. Farmer, 3rd.** 1999. Clinical, epidemiological, and microbiological features of *Vibrio vulnificus* biogroup 3 causing outbreaks of wound infection and bacteraemia in Israel. Israel Vibrio Study Group. *Lancet* **354**:1421-4.
4. **Boesch, D.** 2008. Global warming and the free state: comprehensive assessment of climate change impacts in Maryland. University of Maryland Center for Environmental Science.
5. **Chatzidaki-Livanis, M., M. A. Hubbard, K. Gordon, V. J. Harwood, and A. C. Wright.** 2006. Genetic distinctions among clinical and environmental strains of *Vibrio vulnificus*. *Appl Environ Microbiol* **72**:6136-41.
6. **Clark, J. S., S. R. Carpenter, M. Barber, S. Collins, A. Dobson, J. A. Foley, D. M. Lodge, M. Pascual, R. Pielke, Jr., W. Pizer, C. Pringle, W. V. Reid, K. A. Rose, O. Sala, W. H. Schlesinger, D. H. Wall, and D. Wear.** 2001. Ecological forecasts: an emerging imperative. *Science* **293**:657-60.
7. **Colwell, R. R.** 1996. Global climate and infectious disease: the cholera paradigm. *Science* **274**:2025-31.
8. **Constantin de Magny, G., W. Long, C. W. Brown, R. R. Hood, A. Huq, R. Murtugudde, and R. R. Colwell.** 2009. Predicting the distribution of *Vibrio spp.* in the Chesapeake Bay: a *Vibrio cholerae* case study. *Ecohealth* **6**:378-89.
9. **Constantin de Magny, G., R. Murtugudde, M. R. Sapiano, A. Nizam, C. W. Brown, A. J. Busalacchi, M. Yunus, G. B. Nair, A. I. Gil, C. F. Lanata, J. Calkins, B. Manna, K. Rajendran, M. K. Bhattacharya, A. Huq, R. B. Sack, and R. R. Colwell.** 2008. Environmental signatures associated with cholera epidemics. *Proc Natl Acad Sci U S A* **105**:17676-81.

10. **Cook, D. W.** 1994. Effect of time and temperature on multiplication of *Vibrio vulnificus* in postharvest Gulf Coast shellstock oysters. *Appl Environ Microbiol* **60**:3483-4.
11. **Cook, D. W., P. Oleary, J. C. Hunsucker, E. M. Sloan, J. C. Bowers, R. J. Blodgett, and A. DePaola.** 2002. *Vibrio vulnificus* and *Vibrio parahaemolyticus* in U.S. retail shell oysters: a national survey from June 1998 to July 1999. *J Food Prot* **65**:79-87.
12. **DePaola, A., G. M. Capers, and D. Alexander.** 1994. Densities of *Vibrio vulnificus* in the intestines of fish from the U.S. Gulf Coast. *Appl Environ Microbiol* **60**:984-8.
13. **DePaola, A., S. McLeroy, and G. McManus.** 1997. Distribution of *Vibrio vulnificus* phage in oyster tissues and other estuarine habitats. *Appl Environ Microbiol* **63**:2464-7.
14. **DePaola, A., M. L. Motes, A. M. Chan, and C. A. Suttle.** 1998. Phages infecting *Vibrio vulnificus* are abundant and diverse in oysters (*Crassostrea virginica*) collected from the Gulf of Mexico. *Appl Environ Microbiol* **64**:346-51.
15. **Drake, S. L.** 2009. The Ecology *Vibrio vulnificus* and *Vibrio parahaemolyticus* from Oyster Harvest Sites in the Gulf of Mexico. North Carolina State University, Raleigh, NC.
16. **Dziuban, E. J., J. L. Liang, G. F. Craun, V. Hill, P. A. Yu, J. Painter, M. R. Moore, R. L. Calderon, S. L. Roy, and M. J. Beach.** 2006. Surveillance for waterborne disease and outbreaks associated with recreational water--United States, 2003-2004. *MMWR Surveill Summ* **55**:1-30.
17. **Feldhusen, F.** 2000. The role of seafood in bacterial foodborne diseases. *Microbes Infect* **2**:1651-60.
18. **Fukushima, H., and R. Seki.** 2004. Ecology of *Vibrio vulnificus* and *Vibrio parahaemolyticus* in brackish environments of the Sada River in Shimane Prefecture, Japan. *FEMS Microbiol Ecol* **48**:221-9.
19. **Gibson, J. R., and R. G. Najjar.** 2000. The response of Chesapeake Bay salinity to climate-induced changes in streamflow. *Limnol. Oceanogr.* **45**:1764-1772.
20. **Gonzalez-Escalona, N., L. A. Jaykus, and A. DePaola.** 2007. Typing of *Vibrio vulnificus* strains by variability in their 16S-23S rRNA intergenic spacer regions. *Foodborne Pathog Dis* **4**:327-37.
21. **Goo, S. Y., H. J. Lee, W. H. Kim, K. L. Han, D. K. Park, S. M. Kim, K. S. Kim, K. H. Lee, and S. J. Park.** 2006. Identification of OmpU of *Vibrio*

- vulnificus* as a fibronectin-binding protein and its role in bacterial pathogenesis. Infect Immun **74**:5586-94.
22. **Grau, B. L., M. C. Henk, and G. S. Pettis.** 2005. High-frequency phase variation of *Vibrio vulnificus* 1003: isolation and characterization of a rugose phenotypic variant. J Bacteriol **187**:2519-25.
 23. **Gray, L. D., and A. S. Kreger.** 1987. Mouse skin damage caused by cytotoxin from *Vibrio vulnificus* and by *V. vulnificus* infection. J Infect Dis **155**:236-41.
 24. **Gulig, P. A., K. L. Bourdage, and A. M. Starks.** 2005. Molecular Pathogenesis of *Vibrio vulnificus*. J. Microbiol. **43**:118-131.
 25. **Heidelberg, J. F., K. B. Heidelberg, and R. R. Colwell.** 2002. Bacteria of the gamma-subclass Proteobacteria associated with zooplankton in Chesapeake Bay. Appl Environ Microbiol **68**:5498-507.
 26. **Hervio-Heath, D., R. R. Colwell, A. Derrien, A. Robert-Pillot, J. M. Fournier, and M. Pommepuy.** 2002. Occurrence of pathogenic vibrios in coastal areas of France. J Appl Microbiol **92**:1123-35.
 27. **Hilton, T., T. Rosche, B. Froelich, B. Smith, and J. Oliver.** 2006. Capsular polysaccharide phase variation in *Vibrio vulnificus*. Appl Environ Microbiol **72**:6986-93.
 28. **Hilton, T. W., R. G. Najjar, L. Zhong, and M. Li.** 2008. Is there a signal of sea-level rise in Chesapeake Bay salinity? Journal of Geophysical Research **113**:C09002 1-12.
 29. **Hlady, W. G., and K. C. Klontz.** 1996. The epidemiology of *Vibrio* infections in Florida, 1981-1993. J Infect Dis **173**:1176-83.
 30. **Hoge, C. W., D. Watsky, R. N. Peeler, J. P. Libonati, E. Israel, and J. G. Morris, Jr.** 1989. Epidemiology and spectrum of *Vibrio* infections in a Chesapeake Bay community. J Infect Dis **160**:985-93.
 31. **Hollis, D. J., R. E. Weaver, C. N. Baker, and C. Thornsberry.** 1976. Halophilic *Vibrio* species isolated from blood cultures. J Clin Microbiol **3**:425-431.
 32. **Hsieh, J. L., J. S. Fries, and R. T. Noble.** 2007. *Vibrio* and phytoplankton dynamics during the summer of 2004 in a eutrophying estuary. Ecol Appl **17**:S102-S109.
 33. **Huq, A., E. B. Small, P. A. West, M. I. Huq, R. Rahman, and R. R. Colwell.** 1983. Ecological relationships between *Vibrio cholerae* and planktonic crustacean copepods. Appl Environ Microbiol **45**:275-83.

34. **Jacobs, J. M., M. Rhodes, C. W. Brown, R. R. Hood, A. Leight, W. Long, and R. Wood.** 2010. Predicting the Distribution of *Vibrio vulnificus* in the Chesapeake Bay. NOAA Technical Memorandum NOS NCCOS 112:1-16.
35. **Jones, M. K., and J. D. Oliver.** 2009. *Vibrio vulnificus*: disease and pathogenesis. Infect Immun **77**:1723-33.
36. **Kaspar, C. W., and M. L. Tamplin.** 1993. Effects of temperature and salinity on the survival of *Vibrio vulnificus* in seawater and shellfish. Appl Environ Microbiol **59**:2425-9.
37. **Kaysner, C. A., C. Abeyta, Jr., M. M. Wekell, A. DePaola, Jr., R. F. Stott, and J. M. Leitch.** 1987. Virulent strains of *Vibrio vulnificus* isolated from estuaries of the United States West Coast. Appl Environ Microbiol **53**:1349-51.
38. **Kelly, M. T.** 1982. Effect of temperature and salinity on *Vibrio (Beneckeia) vulnificus* occurrence in a Gulf Coast environment. Appl Environ Microbiol **44**:820-824.
39. **Kimmel, D. G., M. R. Roman, and X. Zhang.** 2006. Spatial and temporal variability in factors affecting mesozooplankton dynamics in Chesapeake Bay: Evidence from biomass size spectra. Limnol. Oceanogr. **51**:131-141.
40. **Linder, K., and J. D. Oliver.** 1989. Membrane fatty acid and virulence changes in the viable but nonculturable state of *Vibrio vulnificus*. Appl Environ Microbiol **55**:2837-42.
41. **Lipp, E., C. R. Rodriguez, and J. B. Rose.** 2001. Occurrence and distribution of the human pathogen *Vibrio vulnificus* in a subtropical Gulf of Mexico estuary. Hydrobiologia **460**:165-173.
42. **Lipp, E. K., A. Huq, and R. R. Colwell.** 2002. Effects of global climate on infectious disease: the cholera model. Clin Microbiol Rev **15**:757-70.
43. **Lobitz, B., L. Beck, A. Huq, B. Wood, G. Fuchs, A. S. Faruque, and R. Colwell.** 2000. Climate and infectious disease: use of remote sensing for detection of *Vibrio cholerae* by indirect measurement. Proc Natl Acad Sci U S A **97**:1438-43.
44. **Martinez-Urtaza, J., B. Huapaya, R. G. Gavilan, V. Blanco-Abad, J. Ansedo-Bermejo, C. Cadarso-Suarez, A. Figueiras, and J. Trinanes.** 2008. Emergence of Asiatic *Vibrio* diseases in South America in phase with El Nino. Epidemiology **19**:829-37.

45. **McLaughlin, J. B., A. DePaola, C. A. Bopp, K. A. Martinek, N. P. Napolilli, C. G. Allison, S. L. Murray, E. C. Thompson, M. M. Bird, and J. P. Middaugh.** 2005. Outbreak of *Vibrio parahaemolyticus* gastroenteritis associated with Alaskan oysters. *N Engl J Med* **353**:1463-70.
46. **Merkel, S. M., S. Alexander, E. Zufall, J. D. Oliver, and Y. M. Huet-Hudson.** 2001. Essential role for estrogen in protection against *Vibrio vulnificus*-induced endotoxic shock. *Infect Immun* **69**:6119-22.
47. **Moebus, K., and H. Nattkemper.** 1983. Taxonomic investigations of bacteriophages sensitive bacteria isolated from marine waters. *Helgo Meeresunters* **36**:357-373.
48. **Motes, M. L., A. DePaola, D. W. Cook, J. E. Veazey, J. C. Hunsucker, W. E. Garthright, R. J. Blodgett, and S. J. Chirtel.** 1998. Influence of water temperature and salinity on *Vibrio vulnificus* in Northern Gulf and Atlantic Coast oysters (*Crassostrea virginica*). *Appl Environ Microbiol* **64**:1459-65.
49. **Murtugudde, R.** 2009. Regional Earth System prediction: a decision-making tool for sustainability? *Current Opinion in Environmental Sustainability* **1**:37-45.
50. **Najjar, R. G., C. R. Pyke, M. B. Adams, D. Brietberg, C. Hershner, M. Kemp, R. Howarth, M. R. Mulholland, M. Paolisso, D. Secor, K. Sellner, D. Wardrop, and R. Wood.** 2010. Potential climate-change impacts on the Chesapeake Bay. *Estuarine, Coastal and Shelf Science* **86**:1-20.
51. **O'Neill, K. R., S. H. Jones, and D. J. Grimes.** 1992. Seasonal incidence of *Vibrio vulnificus* in the Great Bay estuary of New Hampshire and Maine. *Appl Environ Microbiol* **58**:3257-62.
52. **Oliver, J. D.** 2005. Wound infections caused by *Vibrio vulnificus* and other marine bacteria. *Epidemiol Infect* **133**:383-91.
53. **Oliver, J. D., R. A. Warner, and D. R. Cleland.** 1982. Distribution and ecology of *Vibrio vulnificus* and other lactose-fermenting marine vibrios in coastal waters of the southeastern United States. *Appl Environ Microbiol* **44**:1404-14.
54. **Paranjpye, R. N., and M. S. Strom.** 2005. A *Vibrio vulnificus* type IV pilin contributes to biofilm formation, adherence to epithelial cells, and virulence. *Infect Immun* **73**:1411-22.
55. **Parvathi, A., H. S. Kumar, and I. Karunasagar.** 2004. Detection and enumeration of *Vibrio vulnificus* in oysters from two estuaries along the southwest coast of India, using molecular methods. *Appl Environ Microbiol* **70**:6909-13.

56. **Paz, S., N. Bisharat, E. Paz, O. Kidar, and D. Cohen.** 2007. Climate change and the emergence of *Vibrio vulnificus* disease in Israel. *Environ Res* **103**:390-6.
57. **Pelon, W., R. J. Siebeling, J. Simonson, and R. B. Luftig.** 1995. Isolation of bacteriophage infectious for *Vibrio vulnificus*. *Curr Microbiol* **30**:331-6.
58. **Pfeffer, C. S., M. F. Hite, and J. D. Oliver.** 2003. Ecology of *Vibrio vulnificus* in estuarine waters of eastern North Carolina. *Appl Environ Microbiol* **69**:3526-31.
59. **Phillips, A. M., A. Depaola, J. Bowers, S. Ladner, and D. J. Grimes.** 2007. An evaluation of the use of remotely sensed parameters for prediction of incidence and risk associated with *Vibrio parahaemolyticus* in Gulf Coast oysters (*Crassostrea virginica*). *J Food Prot* **70**:879-84.
60. **Randa, M. A., M. F. Polz, and E. Lim.** 2004. Effects of temperature and salinity on *Vibrio vulnificus* population dynamics as assessed by quantitative PCR. *Appl Environ Microbiol* **70**:5469-76.
61. **Rosche, T. M., Y. Yano, and J. D. Oliver.** 2005. A rapid and simple PCR analysis indicates there are two subgroups of *Vibrio vulnificus* which correlate with clinical or environmental isolation. *Microbiol Immunol* **49**:381-9.
62. **Shapiro, R. L., S. Altekruse, L. Hutwagner, R. Bishop, R. Hammond, S. Wilson, B. Ray, S. Thompson, R. V. Tauxe, and P. M. Griffin.** 1998. The role of Gulf Coast oysters harvested in warmer months in *Vibrio vulnificus* infections in the United States, 1988-1996. *Vibrio Working Group. J Infect Dis* **178**:752-9.
63. **Strom, M. S., and R. N. Paranjpye.** 2000. Epidemiology and pathogenesis of *Vibrio vulnificus*. *Microbes Infect* **2**:177-88.
64. **Tamplin, M. L., and G. M. Capers.** 1992. Persistence of *Vibrio vulnificus* in tissues of Gulf Coast oysters, *Crassostrea virginica*, exposed to seawater disinfected with UV light. *Appl Environ Microbiol* **58**:1506-10.
65. **Warner, E., and J. D. Oliver.** 2008. Population structures of two genotypes of *Vibrio vulnificus* in oysters (*Crassostrea virginica*) and seawater. *Appl Environ Microbiol* **74**:80-5.
66. **Warner, J. M., and J. D. Oliver.** 1998. Randomly amplified polymorphic DNA analysis of starved and viable but nonculturable *Vibrio vulnificus* cells. *Appl Environ Microbiol* **64**:3025-8.

67. **Wetz, J. J., A. D. Blackwood, J. S. Fries, Z. F. Williams, and R. T. Noble.** 2008. Trends in total *Vibrio spp.* and *Vibrio vulnificus* concentrations in the eutrophic Neuse River Estuary, North Carolina, during storm events. *Aquat Microb Ecol* **53**:141-149.
68. **Whitesides, M. D., and J. D. Oliver.** 1997. Resuscitation of *Vibrio vulnificus* from the Viable but Nonculturable State. *Appl Environ Microbiol* **63**:1002-5.
69. **Wright, A. C., R. T. Hill, J. A. Johnson, M. C. Roghman, R. R. Colwell, and J. G. Morris, Jr.** 1996. Distribution of *Vibrio vulnificus* in the Chesapeake Bay. *Appl Environ Microbiol* **62**:717-24.
70. **Wright, A. C., and J. G. Morris, Jr.** 1991. The extracellular cytolysin of *Vibrio vulnificus*: inactivation and relationship to virulence in mice. *Infect Immun* **59**:192-7.
71. **Morbidity and Mortality Weekly Report (MMWR)**, Centers for Disease Control and Prevention (CDC). 2005, 2006, 2010.
72. **Under the Weather: Climate, Ecosystems, Infectious Disease, and Human Health.** Board on Atmospheric Sciences and Climate, Division of Earth and Life Studies, National Research Council. National Academy Press, Washington DC, 1-146.